AN ABSTRACT OF THE DISSERTATION OF

Nicole M. Czarnomski for the degree of Doctor of Philosophy in Water Resources Engineering presented on June 3, 2010.

Title: Influence of Vegetation on Streambank Hydraulics.

Abstract approved: _____.

Desireé Tullos

Proper use of vegetation in streambank bioengineering practices requires a comprehensive understanding of the influence of vegetation density on streambank hydraulics. A series of studies were conducted to investigate the relationship between independent variables vegetation density, bank angle, and discharge and dependent variables channel velocity, resistance, turbulence, and shear stress. Flume experiments were conducted varying vegetation stem density (number of plants/horizontal area) and frontal area (number of leaves/vertical area) on 30° and 15° vegetated bank-toes at three discharge rates. Three sets of 3D velocity measures were collected using an ADV at: 1) 0.6 x depth, 2) near-boundary, and 3) velocity profiles. Resistance parameters for drag coefficient (C_d) and Manning's n were estimated. Turbulent stress measures based on turbulent kinetic energy and Reynolds stress were used to evaluate boundary shear stress. Tensor fields were visualized to explore vorticity and near-boundary hydraulics. Results demonstrated that as vegetation density increased, water was increasingly redirected from the bank-toe to the main channel, decreasing downstream velocity along the bank-toe by 35-95% and increasing downstream velocity in the main channel by 80-240%. As vegetation density increased and water velocity decreased along the bank-toe, depths increased, surface slope flattened, and an eddy formed downstream of the vegetated patch. C_d increased with increasing vegetation density, and decreasing stem Reynolds number. Estimates of C_d and n were high relative to commonly published values,

especially when vegetation density was high. Increasing vegetation density also increased turbulence and shear stress, creating greater opportunity for erosion at sensitive locations along the bottom of the bank-toe and in the main channel. Reynolds stresses also increased under the canopy, resulting in higher shearing forces along the bank-toe, especially on the 30° bank-toe. Differences in results between bank-toe angles were minimal, dominated by the influence of vegetation. Magnitude of results decreased with decreasing discharge, but patterns were similar. Findings suggest planting at higher densities may protect the bank from erosion, but may increase the potential for erosion along the interface between the bank and main channel if unprotected, though further research with natural plant communities is encouraged to confirm findings.

INFLUENCE OF VEGETATION ON STREAMBANK HYDRAULICS

by

Nicole M. Czarnomski

A DISSERTATION

Submitted to

Oregon State University

in partial fulfillment of
the requirements for the
degree of

Doctor of Philosophy

Presented June 3, 2010
Commencement June 2010

Doctor of Philosophy dissertation of <u>Nicole M. Czarnomski</u> presented on <u>June 3, 2010</u>.

APPROVED:

_____

Major Professor, representing Water Resources Engineering

_____

Director of the Water Resources Engineering Graduate Program

_____

Dean of the Graduate School

I understand that my dissertation will become part of the permanent collection of Oregon State University libraries. My signature below authorizes release of my dissertation to any reader upon request.

_____

Nicole M. Czarnomski, Author

ACKNOWLEDGEMENTS

I also want to thank the entire visualization team for sharing their knowledge and efforts. Jonathan Palacios took the time to run datasets through the visualizations and explaining the results to me. Eugene Zhang and Harry Yeh provided valuable interpretations of methods and results. Darrel Palke aided by setting up the streamlines program so I could explore the data.

The PhD trip was long and arduous, and the support of friends and family helped me stay on the path. I want to thank my PhD colleagues for countless conversations about exams, deadlines, funding, careers, and all the other things that we have to worry about! Thanks to Harold, Alan, Biniam, Terry, and Liz – as well as so many others at OSU! Also, thanks go to all my non-graduate school friends and the family, who put up with all my complaints over the years and encouraged me to stick with it.

Last, but certainly not least, I'd like to acknowledge my husband, Cameron Bergen, for support and understanding during my entire graduate experience. I don't think there are enough words to explain all that he has done for me over these last 5 years. He was patient and encouraging through all the trials that graduate school sent my way. He lived for years with a woman who spent evenings and weekends on research or studying for exams, and even left him alone at home for nearly 6 months to conduct research across the country. Finishing this dissertation is for him as much as it is for me.

CONTRIBUTION OF AUTHORS

My advisor, Dr. Tullos, helped me with all chapters by assisting with the experimental design, aiding in the interpretation of data and contributing helpful advice and edits throughout the project. Assistance was provided by Dr. Thomas and Dr. Simon on Chapters 2 and 4. Dr. Thomas oversaw the construction of the flume, assisted with experimental design, aided in the interpretation of data and contributed helpful advice and edits throughout the project. Dr. Simon made it possible to conduct the flume experiments by inviting me to the National Sedimentation Laboratory and giving me access to the flume, providing financial assistance, and supporting staff to assist with the research project. Additionally, he provided insight and advice for the experimental design and valuable feedback through the data collection process. Additionally, assistance was provided by Jonathan Palacios and Dr. Zhang on Chapter 4. Palacios conducted the tensor field visualizations and shared the results for this paper. Dr. Zhang provided support for the tensor field analysis, including software, discussion of methods and results, and feedback on text.

TABLE OF CONTENTS

TABLE OF CONTENTS (Continued)

LIST OF FIGURES

LIST OF FIGURES (Continued)

LIST OF TABLES

INFLUENCE OF VEGETATION ON STREAMBANK HYDRAULICS

CHAPTER 1. INTRODUCTION

Streambank erosion is a challenging problem for landowners, land managers, and practitioners. Bioengineering techniques are being used to alleviate problems at a lower cost and lower impact than protecting the bank with structures (Allen and Leech 1997; Bentrup and Hoag 1998). Structures need continual maintenance and tend to fail over time (Thompson 2005). In using bioengineering techniques, ecological benefits are provided by the vegetation and some of the natural hydraulic processes are maintained, creating a more sustainable solution to streambank erosion problems.

One streambank bioengineering technique is to use plantings as roughness elements to protect streambanks from erosion. Several studies have shown that increases in vegetation reduces velocity (Bertram 1984; Fathi-Moghadam and Kouwen 1997; Freeman et al. 2000; Järvelä 2002a, 2004; Wilson et al. 2003; McBride et al. 2007; Yang et al. 2007; White and Nepf 2008; Hopkinson and Nepf 2009), reduces shear stress within the vegetation (Thornton et al. 2000; Bennett et al. 2002; Thompson et al. 2004; Hopkinson and Wynn 2009), and encourages sediment deposition (López and García 1998; Corenblit et al. 2009; Zong and Nepf 2010). Most of these studies have been performed on floodplains, for in-channel vegetation, or for submerged vegetation. Though we might expect similar results on an inclined streambank, there are also unique situations related to the streambank that must be considered.

Unlike a floodplain, the streambank is continuously affected by the force of water. Most banks are compound and consist of the top of bank, the bank face, and a bank-toe. Flow forces on the bank-toe are acting at both low and high flow conditions, making it vulnerable to erosive forces. Furthermore, there is often a slope break between the bank-toe and the open channel, making flow dynamics more complex. Depending on cross-sectional geometry, secondary circulation currents may meet at the bottom of the bank-toe (Tominaga et al. 1989; Knight et al. 2007). Due to forces on the streambank, the bank-toe is often the first to erode, leaving 1) cut-face banks that are more susceptible to erosion and lack critical habitat features, and 2) over-hanging banks that eventually fail and widen the channel.

Vegetation in fluid hydraulics is challenging to study because of the variability in plant biomechanics and morphology. Vegetation influences flow patterns depending on stem density (Li and Shen 1973; Pasche and Rouvé 1985; Lopez and Garcia 1998, 2001; Nepf 1999; Bennett et al. 2002; Stone and Shen 2002; Järvelä 2002a; White and Nepf 2008), frontal area (Petryk and Bosmajian 1975; Fathi-Moghadam and Kouwen 1997; Järvelä 2002a, 2004; Wilson et al. 2003, 2006a, 2006b), pattern of stem placement (Li and Shen 1973), depth of submergence (Fathi-Moghadam and Kouwen 1997; Stone and Shen 2002; Wilson 2006a) and flexibility of the stem (Fathi-Moghadam and Kouwen 1997; Freeman et al. 2000).

In this study, I used a series of flume experiments to explore how vegetation can influence flow patterns and hydraulics on a bank-toe. Inserts were consecutively installed in the flume to represent a bank-toe for two commonly observed bank angles (15° and 30°) in a prototype channel. Artificial vegetation was built to mimic the flexibility, frontal area, and relative size (stem diameter and height) of small woody vegetation that is common on streambanks. The vegetation was installed on the bank-toe in four patterns to represent plants without leaves and plants with leaves at two different stem densities. Three-dimensional velocity measurements were collected near the boundary and within the water column, and surface water elevations were collected throughout the flume.

The purpose of this research was to observe, over a range of discharges: 1) how varying densities of vegetation influence flow patterns through and around the vegetation, 2) the resistance provided by the vegetation and 3) the forces on a bank-toe of two angles. Results of this study were expected to provide insight on how hydraulics are altered based on vegetation densities that may be expected on streambanks; and by the presence or absence of leaves. Equipped with an understanding of how density influences streambank hydraulics, practitioners can make better decisions on where and how dense to plant vegetation to reduce erosion on streambanks.

CHAPTER 2. STREAMBANK VELOCITY AND FLOW PATTERNS WHEN INFLUENCED BY VEGETATION DENSITY

Nicole M. Czarnomski, Desireé Tullos, Robert E. Thomas, and Andrew Simon

Abstract

Vegetation along the toe of a streambank can reduce near bank velocities and deflect water away from banks, leading to greater protection against erosion. In this study, we investigate the relationships between vegetation densities (frontal and stem) and channel velocity (along the bank-toe) and the energy gradient (along the bank). Five flume experiments were conducted varying vegetation stem density (number of plants/horizontal area) and frontal area (number of leaves/vertical area) on 30° and 15° vegetated bank-toes at three discharge rates. For each experiment, vegetation was characterized by overall blockage ratio and 3D time-averaged velocities were measured upstream, within, and downstream of the vegetation. Our experiments indicate that water was increasingly redirected from the bank to the main channel as blockage increased, decreasing downstream velocity along the bank by 35 to 95%, increasing downstream velocity in the main channel by 80 to 240%, and altering flow patterns downstream of the vegetated patch. An eddy formed downstream of the vegetated patch when blockage was high. As water velocity decreased along the bank-toe, depths increased and surface slope decreased, depending on downstream distance through the vegetated patch. Results indicate that increases in vegetation density enlarge differences between streambank and channel velocities, altering patterns in channel depth and flow directionality. Based on these results, it appears that planting at higher densities may protect the bank from erosion, but may increase the potential for erosion along the interface between the bank and main channel if unprotected.

Introduction

Riparian vegetation is increasingly used to protect streambanks against erosion and to promote channel stability in areas where it has been previously removed. Riparian vegetation promotes channel stability by acting as resistance to water flowing through a channel, redirecting flows, acting as root reinforcement, altering channel velocities, and influencing erosional and depositional patterns. Understanding the features of the vegetation that most influence these effects on flow may lead to more effective use of vegetation in restoration activities.

Studies have shown that vegetation reduces velocity in vegetated areas and routes flow to the open channel (Bertram 1984; McBride et al. 2007; Yang et al. 2007; White and Nepf 2008). Vegetation influences these flow patterns depending on stem density (Li and Shen 1973; Pasche and Rouvé 1985; Lopez and Garcia 1998, 2001; Nepf 1999; Bennett et al. 2002; Stone and Shen 2002; Järvelä 2002a; White and Nepf 2008), frontal area (Petryk and Bosmajian 1975; Fathi-Moghadam and Kouwen 1997; Järvelä 2002a, 2004; Wilson et al. 2003, 2006a, 2006b), pattern of stem placement (Li and Shen 1973), depth of submergence (Fathi-Moghadam and Kouwen 1997; Stone and Shen 2002; Wilson 2006a) and flexibility of the stem (Fathi-Moghadam and Kouwen 1997; Freeman et al. 2000).

Frontal area and stem density are two parameters used in estimating the total obstruction, or resistance, of the plant community to the flow volume. Increases in frontal area (the cross-sectional area over which the plant obstructs flow) are related to reductions in flow velocity (Fathi-Moghadam and Kouwen 1997; Freeman et al. 2000; Järvelä 2002a, 2004; Wilson et al. 2003). The density of stems influences flow velocity by increasing or decreasing the frontal area of the cross-section (Petryk and Bosmajian 1975; Järvelä 2004). As a stem flexes and bends, the frontal area of the plant may decrease, reducing the influence that plant has on flow (Fathi-Mogohadam and Kouwen 1997; Freeman et al. 2000; Järvelä 2002a; Wilson et al. 2006b). While frontal area differs by plant species and individual plant characteristics (Freeman et al. 2000), one of the

most significant sources of variability in frontal area is associated with the seasonal presence and absence of leaves (Fischenich and Dudley 1999; Järvelä 2004).

Variability in plant morphology and biomechanics makes it challenging to accurately represent vegetation in experimental and modeling studies. Most flume experiments of channel floodplains and banks represent woody vegetation as wooden dowels or similarly rigid structures, though some studies have used both artificial and natural flexible woody vegetation (Fathi-Moghadam and Kouwen 1997; Freeman et al. 2000; Järvelä 2002a; Wilson et al. 2006a). Accounting for flexibility of woody vegetation is important in accurately estimating vegetative resistance to flow (Fathi-Moghadam and Kouwen 1997), especially when modeling a streambank where much of the woody vegetation is young and small in diameter, and therefore more flexible.

Several models have been proposed to estimate the effects of vegetation as resistance features on the floodplain (Pasche and Rouvé 1985; Bennett et al. 2002; McBride et al. 2007; Yang et al. 2007; White and Nepf 2008), but fewer studies have examined the impact of vegetation on the streambank (Bertram 1984; Wilkerson 2007; Hopkinson et al. 2009). Though many of the relationships between vegetation and flow may be similar on banks as for floodplains (Wilkerson 2007; Hopkinson et al. 2009), bank angle may influence channel hydraulics (Wilkerson 2007; McBride et al. 2007). Most sensitive to erosion is the bank-toe – the interface between the bank and open channel. Experimental studies of streambanks have indicated that velocity along the bank-toe decreases when vegetation is present (Wilkerson 2007, Hopkinson et al. 2009); however, the effects of differing bank-toe angles and changes in plant and plant community frontal area are not well understood.

In this study, we used a scaled flume experiment to analyze the relative magnitude of difference in channel velocity and energy gradient at locations along the streambank due to changes in vegetation stem density, frontal area, and bank-toe angle. The flume was configured to represent a bank-toe of a compound bank (Figure 2.1). Our primary objective was to evaluate how densities of streambank vegetation influence velocity along the bank-toe at locations most sensitive to erosion. More specifically, we asked: 1)

What are the resulting magnitude and patterns of channel velocity when vegetation is present on an inclined bank-toe? 2) How do changes in vegetation stem density and frontal area alter this pattern? 3) How do changes of bank-toe angle alter this pattern?

Methods

Experimental design

Experiments were conducted in a $6.0 \times 0.6 \times 0.6$ m recirculating flume set at a fixed slope of 0.01 m m^{-1} (Figure 2.2). At the inlet, water passed through a rock-filled baffle box and then a baffle box composed of 0.30 m long, 0.02 m diameter tubes (flow straighteners), in order to dampen turbulence and provide uniform flow. To simulate a bank-toe, an insert was installed along one side of the flume immediately downstream of the flow straighteners. Two 4.88 m long inclined inserts were used alternately to simulate a 30° and 15° toe of a compound streambank, scaled by average Froude scaling factors of 4.35 and 4.88, respectively, from an average prototype stream of a 3rd-4th order channel. The downstream end of the flume was controlled by a weir, backwatering the entire length of the flume; therefore, depth at the end of the measured reach was greater than depth on the upstream end of the reach.

Artificial plants were used to represent natural plants, with scaled flexibility and "leaved" and "leafless" conditions. The vegetation array was 3 m long, beginning immediately downstream of the flow straighteners (Figure 2.2). Vegetation was installed in two patterns: low stem density (D_{lo}) of 202 stems per m^2 and high stem density (D_{hi}) of 615 stems per m^2, which scale to 8 and 24 stems per m^2, respectively (Figure 2.3). Eight stems per square meter can be considered a fairly normal stand of mature willow or cottonwood saplings, whereas twenty-four stems per square meter can be considered a very dense stand. Plants were made of 450 mm long, 4.54 mm diameter acrylic rods, scaled down from 2 m tall, 20 mm diameter woody vegetation. Artificial plants represent small riparian trees and shrubs with a similar range of flexibility, such as willow and ash. Plants were in two forms: leaves (designated with an "L" – LD_{lo}, LD_{hi}) and no leaves (D_{lo}, D_{hi}). Leaved plants consisted of the same acrylic rods affixed with ten 28-gauge

wire "branches" and ten 25 × 35 mm "leaves" made of contact paper (875 mm^2 total) spaced to reflect a pattern of frontal area found by Wilson et al. (2006a).

To determine flexibility of artificial vegetation, an appropriate range of values of modulus of elasticity (E) for riparian woody plants were obtained from previous studies (Niklas 1992, Freeman et al. 2000) and scaled for the physical model. The relationship J = EI was used, where J is flexural stiffness (N m^2), I is the second moment of inertia (I= πD^4/64, in m^4) and E is Young's modulus of elasticity (N m^{-2}):

$$E = \frac{Fa^2}{2\delta I}(3L - a) \tag{1}$$

where F is applied force (N), L is length of the beam (m), δ is deflection (m), a is the length at the end of which the force is applied (m), and D is stem diameter (m). If x is defined as an appropriate length scale, it can be seen that I scales by x^4 and E scales by x, thus J scales by x^5 according to Cauchy similitude (Wilson et al. 2003). E for the acrylic rod was tested using a one-point beam test (Gartner 1991, Freeman et al. 2000) and resulted in J = 0.04 N m^2.

Table 2.1 illustrates the experimental design for the four vegetated cases and one non-vegetated case. The three different discharges (0.015, 0.030, and 0.050 m^{3}s^{-1}) correspond to 0.6, 1.2, and 2.0 m^{3}s^{-1} in the prototype stream. Blockage ratio (frontal area/flow area) was determined for a cross-section 2.95 m from the beginning of the vegetated patch for each of the 30 experiments (Figure 2.3, Table 2.2). It was computed separately for the bank-toe and for the bank-toe-main channel margin (henceforth referred to as "margin"). Blockage ratio for the plants with leaves was 5.5-6.5 times the blockage ratio for the plants without leaves, holding stem density constant (Table 2.2).

In order to characterize the depth-averaged velocity without vegetation present, it was assumed that the variation of the streamwise velocity (u) in the vertical direction could be adequately described throughout the flow depth by the von Kàrmàn-Prandtl law of the wall:

$$\bar{u} = \frac{u_*}{\kappa} \ln\left(\frac{d-z}{z_0}\right) \tag{2}$$

Where $\overline{u}$ = time-averaged streamwise velocity (m/s[1]), u_* = shear velocity (m/s), κ = von Kàrmàn constant ($\approx$ 0.33 in suspended sediment-laden flows (Bennett et al. 1998)), d = flow depth measured from the water surface (m), z = elevation within the water column measured from the bed (m) and z_0 = roughness height (m). Depth-averaging equation 2 yields the result that the depth-averaged velocity occurs at 0.632 d. Velocity was therefore measured at ~0.6 × the flow depth (0.6d) at 7 cross-stream locations within 9 cross-sections (Figure 2.2). Velocities within vegetation have been demonstrated to be nearly uniform with depth (White and Nepf 2008), hence measures within vegetation also were made at 0.6D. The assumption that the $\overline{u}$-velocity profile approximated the law of the wall was tested by measuring several vertical profiles of the $\overline{u}$-velocity in the unobstructed channel, and it was found that the u-velocity at 0.6d was within 10% of the depth-averaged velocity. Within and downstream of the vegetation, velocities were very low and 0.6d estimates were generally within an order of magnitude of the depth-averaged velocity. Additionally, near-boundary velocities were measured at nine locations along a cross-section at 2.0 m. Velocities were measured for 300 seconds at 25 Hz with a 10 MHz Nortek acoustic Doppler velocimeter (ADV). Data were filtered and processed using the WinADV software Version 2.027 (Wahl 2009).

Analysis

Measurement locations were classified according to channel location – bank-toe ("bank") from 0 to 0.35 m across the channel, bank-toe-main channel margin ("margin") from 0.35 to 0.44 m, and main channel ("main") from 0.44 to 0.62 m. Location classes of bank, margin, and main were compared to confirm independence between classes (Czarnomski in prep, Appendix A). For each location class (bank, margin or main), average velocity was calculated using the discharge and cross-sectional area of the location of interest. Discharge for the channel location was determined by summing the discharge for each subsection within the location. Average velocity for a channel location was normalized using the average velocity for the entire cross-section.

Two-way interactions were plotted for combinations of stem density, frontal area, the interaction between stem density and frontal area (i.e. noveg, D_{lo}, D_{hi}, LD_{lo}, LD_{hi}), bank-toe angle and discharge. Data for this analysis were taken from the cross-sectional transect 0.05 m upstream of the end of the vegetated bank-toe (i.e. cross-section 2.95 m). The cross-section at 2.95 m was chosen because there was less variation in velocity between it and the upstream and downstream transects, and because ADV measures along this transect had the least noise (Czarnomski in prep, Appendix B).

Results

Influence of vegetation blockage

Blockage due to vegetation was a dominant influence on streamwise velocity. Despite differences in discharge and bank-toe angle, an increase in blockage ratio corresponded with a non-linear decrease in normalized streamwise velocity on the bank-toe (Figure 2.4). Velocity is uniformly reduced after a blockage ratio of approximately 0.3, possibly indicating a minimum amount of vegetation necessary for a reduction in velocity. This relationship is not as strong at the margin, where there is a larger range of potential normalized velocities for a given blockage ratio. Closer examination of each case at a single cross-sectional location helps to demonstrate the relationship between blockage ratio and velocity. As blockage ratio increased, streamwise velocity decreased 35-95% over the unvegetated case on the bank-toe and increased 80-240% in the main channel (Figure 2.5, Figure 2.6a,b).

Along the margin, a greater difference was observed between cases with leaves and without leaves than blockage ratio can explain. For example, for the high discharge case on the 30° bank-toe, blockage ratios for the cases without leaves were $D_{lo} = 0.027$ and $D_{hi} = 0.052$, and for those with leaves they were $LD_{lo} = 0.094$ and $LD_{hi} = 0.282$ (Table 2.2). At the margin, when plants had leaves velocity decreased 20-75% compared to the unvegetated case and without leaves velocity marginally increased (Figure 2.5), despite the small difference between blockage ratio of LD_{lo} and D_{hi}. If blockage ratio was

the dominant factor, one would expect the results for LD_{lo} to be more similar to the results for D_{hi} than LD_{hi}.

This difference in velocity along the margin between cases with and without leaves may be a result of the local hydraulics at the sampling location. Plant stems were located on the bank-toe and, when leaves were present, they extended towards the sampling location at the margin, providing a wider area of influence. An increase in turbulent conditions may also create error in the measurement, biasing it to be up to 20% lower than actual (Muller et al. 2007). Also, the wide variability in normalized velocities by blockage ratio (Figure 2.4) suggests sampling locations along the margin are influenced by small eddies and the flux of water from the main channel. In upstream cross-sections, differences in velocity along the margin between leaves/no-leaves cases were not as distinct, also suggesting sampling location may have been a reason for observed differences.

Effects of bank-toe angle on velocity were not strongly evident in this study, often obscured by the strong influence of vegetation (Figure 2.7a,b,c). The only evidence that bank-toe angle influenced streamwise velocity on the bank-toe was when blockage ratio was ≤ 0.1 (i.e. no leaves were present), when blockage ratios were fairly similar for both angles. In both these cases, velocity on the 30° bank-toe was significantly lower than on the 15° bank-toe, possibly due to greater flow deflection into the open channel. Changing the angle of the bank-toe was observed to cause differences in the streamwise velocity in both the main channel and along the margin, but our ability to quantitatively describe these trends has been hampered by concurrent changes of blocking ratio. In the main channel, differences in velocity by bank-toe angle were observed for the LD_{hi} case, where the 30° bank-toe had a higher blockage ratio than the 15° bank-toe. Along the margin, the arrangement of plants created a situation where the 15° blockage ratio was considerably less than the 30° blockage ratio. The 30° bank-toe was wider, thus an additional row of vegetation was installed that fell within the margin. This was likely the cause of the significantly lower velocity for the 30° margin over the 15° margin.

Flow energy

Velocity decreased sharply at the upstream end of the vegetated bank-toe when blockage ratio was high, suggesting that a large portion of the flow energy was reduced at the upstream-most end of the vegetated patch. For example, when discharge was high and leaves were present, streamwise velocity was reduced to less than 50% of the no vegetation case at the first measurement location 0.25 m down from the beginning of the vegetated patch (Figure 2.6a,b). In this part of the channel, flow was rapidly redirected into the main channel, where velocity increased by 1.5-2.5 times the no vegetation condition by the first meter of the start of vegetation (e.g. Figure 2.6c,d). Over the remaining 2.75 m of the vegetated patch, velocity continued to decrease, totaling an 80-100% reduction by the downstream end of the vegetated patch. This within-patch reduction of velocity in the streamwise direction was observed at all discharges, although the magnitude of the reduction varied. On the bank-toe, the LD_{hi} case resulted in a further drop in velocity and evidence of secondary circulation (described further below).

Low blockage ratios resulted in a smaller reduction in both the rate and magnitude of energy dissipation, as measured by reductions in velocity. With low blockage ratios, the transfer of energy to the plants was more gradual throughout the vegetated patch. During the experiments conducted at high discharge, for example, by the first measurement location velocity had decreased by less than 30% with a low blockage ratio, but it had decreased by more than 50% with a high blockage ratio. Velocity continued to decrease through the vegetation, reducing by a total of 40-70% by the downstream end of the vegetated patch. Velocities continued to be suppressed for up to 1.0 m downstream of the vegetated patch.

Backwatering occurred as blockage ratio increased, flattening the water surface slope within the vegetation, steepening the water surface slope at the downstream end of the vegetation, and increasing channel depths within the vegetation (Figure 2.8a). Water surface elevations within the vegetation were higher than the no vegetation condition, though the difference decreased over the length of the vegetated patch. The greatest

increase in depth normalized by maximum depth was on the upstream-most end of the vegetated bank-toe, where, in agreement with continuity theory, the largest incremental decrease in velocity also occurred (e.g. Figure 2.8b). Non-uniform increases in depth resulted in a slope break, where the slope of the upstream 1.0 m of the vegetated patch was flatter than the slope of the following 2.0 m (e.g. Figure 2.8a,c). Upon exiting the vegetated patch on the 30° bank-toe when LD_{hi}, the slope steepened to drop the water surface elevation to that of the unvegetated condition, possibly due to secondary flow development downstream of the patch. Recovery to the no vegetation slope occurred within 0.1 m after the vegetation (3% of the length of vegetated patch). A similar pattern was observed for the 15° bank-toe, though when blockage ratio was high, the slope steepened before the end of the vegetated patch.

Flow patterns

When no vegetation was present, flow was directed predominantly downstream with little influence from the walls or inclined bank-toe (Figure 2.9a). Conversely, when vegetation was present, flow was deflected away from the bank-toe and into the main channel at the upstream end of the vegetated patch, altering flow patterns in the main channel (Figure 2.9b,c). Flow in the main channel was then diverted off the opposite wall of the flume and redirected back towards the bank-toe. This occurred irrespective of the discharge though the magnitude of the effect was lessened at lower discharges.

Flow within the vegetation was influenced by the presence or absence of leaves. Without leaves, flow along the bank-toe continued to be directed predominantly downstream (e.g. Figure 2.9b). When leaves were present, flow within the vegetation was more likely to be redirected around the nearest obstructions (e.g. Figure 2.9c).

When blockage ratio was highest, secondary flow developed downstream of the vegetated patch (Figure 2.9a). Development of a large-scale eddy corresponded with an increase in velocity immediately downstream of the vegetated patch (Figure 2.6a,b). Large-scale eddy structures were observed for all discharges and both bank-toe angles for the LD_{hi} case, but were not present in the other vegetated cases. Some indication of large-

scale eddy development was observed downstream of the vegetated patch for the LD_{lo} case, though only for the 30° bank-toe.

In the absence of vegetation, cross-sectional flow circulation was fairly uniform for both bank-toe angles. Flow circulated from the main channel into the bank-toe along the bed (Figure 2.10a,b). Within the flow cross-section (velocity measures at 0.6D), flow was directed out towards the main channel for the 30° bank-toe and in toward the bank-toe for the 15° bank-toe. Differences in 0.6D flow direction based on bank-toe angle may be an indication of the scale of flow circulation through the varied cross-sectional flow areas.

With vegetation, flow patterns are more nuanced. For example, at the 2.0 m cross-section, with high discharge, flow through the canopy became more turbulent when leaves were present (Czarnomski et al. in prep), as indicated by the multi-directional vectors within the bank-toe cross-section (Figure 2.10g,h,i,j). Near-boundary velocity along the vegetated 30° bank-toe decreased 21% on average over the unvegetated case. However, on the 15 ° bank-toe, near-boundary velocity increased by 60% on average when the bank-toe was vegetated, likely because of low near-boundary velocity when no vegetation was present.

Despite decreases in near-boundary velocity along the bank-toe with increases in vegetation density, near-boundary velocity at the margin and in the main channel increased with increasing vegetation density and blockage by leaves (Figure 2.10). Along the margin, as vegetation density increased, the magnitude of near-boundary velocity increased 2 to 5.5 times on the 30° bank-toe and 1.5 to 3.5 times on the 15° bank-toe. In the main channel, velocity increased as it did along the margin and was directed back towards the bank-toe.

Results were similar at lower discharge rates, though overall velocities were lower. The magnitude of differences was similar regardless of discharge. The one exception was when discharge decreased on the 15° bank-toe, near-boundary velocities when vegetated decreased 15% on average over the unvegetated bank-toe.

Discussion

Fluvial processes

The experiments presented have shown that vegetation has a substantial effect on in-channel fluvial processes by changing flow patterns, altering bank-toe and main channel velocities, creating a backwater effect, and changing flow energy dynamics, confirming previous findings (e.g. Pasche and Rouvé 1985). Of the independent variables evaluated in the present research, it was found that changing the vegetation blockage ratio had a larger effect on flow dynamics than changing bank-toe angle.

Redirection of flow from the bank-toe to the main channel was likely a result of the plants decreasing velocities on the bank-toe (Figure 2.4, Figure 2.5, Figure 2.6). Past studies of emergent vegetation describe similar patterns of increases in main channel velocities and considerable decreases in velocity along vegetated floodplains and streambanks (Bertram 1984; Pasche and Rouvé 1985; Bennett et al. 2002; McBride et al. 2007; Yang et al. 2007; Hopkinson et al. 2009). The magnitude of difference between vegetated and unobstructed channels is related to the volumetric density of vegetation (Bennett et al. 2002), likely due to drag.

Continuity of flow dictates that reduced velocity within the vegetated patches resulted in a rise in water surface elevation and flattening of water surface slope (Figure 2.8). Vegetation can cause substantial increases in water depth over extended channel lengths (Lopez and Garcia 1998; Thomas and Nisbet 2006). The higher the blockage ratio, the greater the backwatering effect in the upstream end of the vegetated patch. In our study, the upstream end of the vegetated patch was also the section of the vegetated patch responsible for a substantial amount of velocity reduction and energy transfer (Figure 2.6), especially for cases where plants had leaves.

The elevated main channel velocities observed in this study have important implications for channel stability because high velocities in the main channel signal increase sediment transport capacity, which could lead to incision and erosion of the opposite bank. Increases in main channel velocity are expected where flow is unobstructed, though the magnitude of elevated velocities in the main channel of our

experiments may also be a result of the narrow main channel width. A wider channel with greater conveyance capacity could dampen velocity differences between the bank and main channel, especially further from the vegetated bank (McBride et al. 2007). If the main channel is narrow, unconstrained, and no vegetation is present on the opposite bank, it is possible that erosion could occur on the opposite bank, widening the channel. If the opposing bank is also vegetated, flow redirection and constriction caused by dense stands of vegetation may promote vertical incision.

When vegetation is present, the abrupt contrast between bank-toe velocity and main channel velocity suggests that most of the work in slowing the velocity and redirecting flow is being accomplished by plants along the interface. In our experiments, vegetation on the upstream-most end of the vegetated patch bent and oscillated with the force of water, but the movement of individual plants was undetectable further downstream where velocities on the bank-toe had decreased. Vegetation was also observed bending and oscillating along the longitudinal margin of the patch. Small vortices formed and collapsed, applying pressure on the vegetation over short time spans. Development of vortices along the interface could be a result of a velocity differential between the vegetation and unobstructed flow (Shiono and Knight 1991; Wormleaton 1996), forming a shear layer (Tritton 1988; Smith 1996). Vortices were frequently observed on the downstream end of the vegetated patch, with the most continuous force on the downstream corner of the vegetated patch that was adjacent to the main channel. Plants without leaves primarily oscillated, whereas plants with leaves experienced some oscillation, but were more prone to bending than those without leaves.

Eddy formation on the bank-toe downstream of the vegetated patch is likely due to the velocity difference between the main channel and bank-toe. The magnitude of the cross-stream velocity gradient controls the strength of shearing at the margin and hence the strength of the eddy, so that an eddy was only observed at the highest vegetation densities and blockage ratios. While water reflecting off the opposite wall may have contributed to eddy development, it is likely not the main cause of eddy formation. Instead, the difference in velocity due to vegetation density is likely the cause of eddy

formation, similar to other observations that eddy formation is vegetation density-dependent (Bennett et al. 2002).

Formation of an eddy downstream of the vegetated patch could result in sediment deposition or erosion. Strong secondary flows may promote the transportation of sediment to the downstream end of the vegetated patch resulting in deposition. Conversely, encroachment of high energy secondary flows into previously deposited material may result in erosion. Preliminary particle tracking experiments conducted as part of this study, using sediment in the silt range, indicate that deposition occurs downstream of a vegetated patch, resulting in the formation of an isosceles triangle-shaped deposit with the apex pointing downstream. Continued deposition downstream of a vegetated patch could lead to additional sedimentation and establishment of vegetation, further changing channel hydraulics and erosional and depositional patterns (Gurnell and Petts 2006).

Circulation patterns on banks of trapezoidal channels may be expected to have two major circulating flow cells, one at the water surface circulating towards the top of the bank and a second lower down rotating in the opposite direction (Tominaga et al. 1989; Knight et al. 2007; Hopkinson and Wynn 2009). In half of a simple trapezoidal channel, a third cell is present, rotating from the free surface towards the bank, then downward toward the bottom of the bank. This circulation pattern may be true for the unvegetated bank-toes and possibly when blockage ratio was low. However, when blockage was higher, the canopy introduced turbulence and circulation patterns which likely disrupted this third cell. The flow direction along the bank-toe boundary was fairly similar across blockage ratios, suggesting that, despite the disruption of the surface water flows over the bank-toe, some remnant of the original secondary circulation pattern remained. Further, with overall decreases in velocity on the bank-toe, notable increases in velocity occurred at the margin and main channel boundary. Increased velocities may be a sign of increased forces at the margin and main channel boundaries, locations that are susceptible to erosion. Regardless, stress associated with secondary circulation is likely low in magnitude compared to Reynolds stress (van Prooijen et al. 2005; White and Nepf

2008; Hopkinson and Wynn 2009); therefore, may not be an important component when considering erosion on the boundary.

Characterizing vegetation for hydraulic analyses

Correlations between blockage ratio, density, and leafiness make it difficult to determine which of these parameters is most important in describing vegetation resistance in the channel. Of the three parameters, blockage ratio may be one of the best methods for estimating resistance (Freeman et al. 2000, Nikora et al. 2006) because it represents both the density of stems and the density of plant biomass over a volume. Our results confirm findings (Järvelä 2004) that the presence of leaves greatly influences the resistance from vegetation. The magnitude of the effect of leaves on velocity may be best quantified by comparing blockage ratio of plants rather than by comparing overall density of plants with and without leaves.

Although previous studies have developed species-specific parameters for describing resistance (e.g. Fathi-Moghadam and Kouwen 1997), there is some evidence that species-specific parameters are not as important as site-averaged physical parameters (Nikora et al. 2008). Using the blockage ratio as a key parameter for bulk calculations of resistance may reduce the need to rely on species-specific information. Additionally, the blockage parameter can account for variations in plant morphology that exist between or within species.

The difference in blockage ratio for the same stem density but differing leaf conditions stresses the importance of considering seasonal differences in backwatering, velocity reduction along the bank, and fill and scour in the channel. Hydrologic seasonality, specifically the likelihood and duration of flood events, should be examined by managers considering planting vegetation as resistance elements along a streambank. If high flow events are likely to occur during the winter period when deciduous plants have shed their leaves, the effectiveness of those plants as resistance elements is likely to be reduced. In this situation, it may be necessary to install a higher density of plants to achieve the desired result. In addition, in a mixed herbaceous-woody vegetation

community, managers should also consider the role of vegetation community dynamics. For example, woody vegetation may provide a large proportion of overall resistance when those plants are leaved but herbaceous plants may be dominant when deciduous woody species are dormant (Järvelä 2004). Furthermore, if blockage ratio is a driving factor to the formation of eddies downstream of vegetated patches on banks, then both depositional and erosional patterns along the bank may also be influenced by the presence or absence of leaves.

Bending was only observed when plants had leaves, suggesting that issues such as stem flexibility are more important when leaves are present or when the total frontal area of the individual plant is high (i.e. individual plant blockage ratio is high therefore drag increases). The force of flow on plants with leaves is likely to be greater, thus the stems and roots of plants along the upstream end of the vegetated patch streamwise margin experience greater stress when plants have leaves and may suffer from partial or full uprooting if the stem strength or total root resistance is exceeded. In an experimental study of willows, Järvelä (2002a) also observed that the plants with leaves were more likely to bend and those without leaves more likely to oscillate.

Conclusions

An understanding of how vegetation influences streambank hydraulics is important in modeling flow dynamics, flood conditions, and the influence of restoration activities. Results of this study indicate that blockage of flow plays a more important role than bank angle in characterizing resistance on streambanks. The importance of accurately estimating vegetation density and frontal area is evident in: 1) the blockage-dependent decrease in magnitude of channel velocities on the vegetated bank-toe, 2) the formation of eddies downstream of vegetation when blockage is high, 3) redirecting of flow from the bank-toe to the main channel, and 4) differences in surface water slope based on blockage and location within the vegetated patch.

Acknowledgements

References

Bennett, S. J., Bridge, J. S., and Best, J. L. (1998). "The fluid and sediment dynamics of upper-stage plane beds." *Journal of Geophysical Research*, 103(C1), 1239-1274.

Bennett, S. J., Pirim, T., and Barkdoll, B. D. (2002). "Using simulated emergent vegetation to alter stream flow direction within a straight experimental channel." *Geomorphology*, 44, 115-126.

Bertram, V. H.-U. (1984). "Uber die hydraulische Berechnung von Gerinnen mit Uferbewuchs." *Z.f. Kulturtechnik und Flurbereinigung*, 25, 77-86.

Czarnomski, N.M. (in prep). Influence of Vegetation on Streambank Hydraulics. PhD dissertation, Oregon State University, Corvallis.

Czarnomski, N.M., Tullos, D., Thomas, R.E., Simon A., Palacios, J. and Zhang E. (in prep). "Shear stress and turbulence along a streambank due to changes in vegetation canopy density and bank angle."

Fathi-Moghadam, M., and Kouwen, N. (1997). "Nonrigid, nonsubmerged, vegetative roughness on floodplains." *J. Hydr. Engr.*, 123(1), 51-57.

Fischenich, J. C., and Dudley, S. (1999). "Determining drag coefficients and area for vegetation." U.S. Army Engineer Research and Development Center, Vicksburg, MS.

Freeman, G. E., Rahmeyer, W. H., and Copeland, R. R. (2000). "Determination of resistance due to shrubs and woody vegetation." ERDC/CHL TR-00-25, U.S.ACE.

Gartner, B. L. (1991). "Structural staability and architecture of vines vs. shrubs of poison oak, Toxicodendron diversilobum." *Ecology*, 72(6), 2005-2015.

Gurnell, A. M., and Petts, G. (2006). "Trees as riparian engineers: The Tagliamento River, Italy." *Earth Surface Processes and Landforms*, 31, 1558-1574.

Hopkinson, L., and Wynn, T. (2009). "Vegetation impacts on near bank flow." *Ecohydrology*, online, 1-15.

Järvelä, J. (2002a). "Flow resistance of flexible and stiff vegetation: a flume study with natural plants." *J. Hydr.*, 269, 44-54.

Järvelä, J. (2004). "Determination of flow resistance caused by non-submerged woody vegetation." *Int. J. River Basin Mgmt.*, 2(1), 61-70.

Knight, D. W., Omran, M., and Tang, X. (2007). "Modeling depth-averaged velocity and boundary shear in trapezoidal channels with secondary flows." *Journal of Hydraulic Engineering*, 133(1), 39-47.

Li, R. M., and Shen, H. W. (1973). "Effect of tall vegetations on flow and sediment." *J. Hydr. Div., Proc., ASCE*, 99(HY5), 793-814.

Lopez, F., and Garcia, M. H. (1998). "Open-channel flow through simulated vegetation: suspended sediment transport modeling." *Water Resources Research*, 34(9), 2341-2352.

Lopez, F., and Garcia, M. H. (2001). "Mean flow and turbulence structure of open-channel flow through non-emergent vegetation." *Journal of Hydraulic Engineering*, 127(5), 392-402.

McBride, M., Hession, W. C., Rizzo, D. M., and Thompson, D. M. (2007). "The influence of riparian vegetation on near-bank turbulence: a flume experiment." *Earth Surf. Proc. Landf.,* 32(13), 2019-2037.

Mueller, D. S., Abad, J. D., Garcia, C. M., Gartner, J. W., Garcia, M. H., and Oberg, K. A. (2007). "Errors in acoustic doppler profiler velocity measurements caused by flow disturbance." *Journal of Hydraulic Engineering*, 133(12), 1411-1420.

Nepf, H. M. (1999). "Drag, turbulence, and diffusion in flow through emergent vegetation." *Water Res. Research.*, 35(2), 479-489.

Niklas, K.J. (1992). *Plant Biomechanics*. University of Chicago Press, Chicago, 607.

Nikora,V., Larned, S., Debnath, K., Cooper, G., Reid, M., Nikora, N. (2006). "Effects of aquatic and bank-side vegetation on hydraulic performance of small streams." *Proceedings of the International Conference on Fluvial Hydraulics River Flow 2006*, v. 1, Taylor and Francis, London, pp. 639-646.

Nikora, V., Larned, S., Nikora, N., Debnath, K., Cooper, G., and Reid, M. (2008). "Hydraulic resistance due to aquatic vegetation in small streams: field study." *Journal of Hydraulic Engineering*, 134(9), 1326-1332.

Pasche, E., and Rouvé, G. (1985). "Overbank flow with vegetatively roughened flood plains." *J. Hydr. Engr.*, 111(9), 1262-1278.

Petryk, S., and Bosmajian, G. (1975). "Analysis of flow through vegetation." *J. Hydr. Div., Proc., ASCE*, 101(HY7), 871-884.

Shiono, K., and Knight, D.W. (1991). "Turbulent open-channel flows with variable depth across the cross-section." *J. Fluid Mech.*, 222, 617-646.

Smith C.R. (1996). "Coherent flow structures in smooth-wall turbulent boundary layers: facts, mechanisms, and speculation." Coherent Flow Structures in Open Channels, P.J. Ashworth, S.J. Bennett, J.L. Best, and S.J. McClelland, eds., Wiley, Chichester, 1–39.

Stone, B. M., and Shen, H. T. (2002). "Hydraulic resistance of flow in channels with cylindrical roughness." *Journal of Hydraulic Engineering*, 128(5), 500-506.

Thomas, H., and Nisbet, T. R. (2006). "An assessment of the impact of floodplain woodland on flood flows." *Water and Environment Journal*, Journal compilation, 1-13.

Tominaga A., Nezu I., Ezaki K., Nakagawa H. (1989). "Turbulent structure in straight open channel flows." *Journal of Hydraulic Research,* 27(1), 149–173.

Tritton DJ. 1988. Physical Fluid Dynamics. Clarendon, Oxford, 536.

Wahl, T. (2009). WinADV Version 2.027. U.S. Bureau of Reclamation, Water Resources Research Laboratory.

van Prooijen, B., J. Battjes, and W. Uijttewaal (2005). "Momentum exchange in straight uniform compound channel flow." *J. Hydraul. Eng.*, 131(3), 177– 185.

White, B. L., and Nepf, H. M. (2008). "A vortex-based model of velocity and shear stress in a partially vegetated shallow channel." *Water Res. Research*, 44(W01412), 15.

Wilkerson, G. V. (2007). "Flow through trapezoidal and rectangular channels with rigid cylinders." *Journal of Hydraulic Engineering*, 133(5), 521-533.

Wilson, C. A. M. E., Stoesser, T., Bates, P. D., and Batemann Pinzen, A. (2003). "Open channel flow through different forms of submerged flexible vegetation." *J. Hydr. Engr.*, 129(11), 847-853.

Wilson, C. A. M. E., Yagci, O., Rauch, H.-P., and Stoesser, T. (2006a). "Application of the drag force approach to model the flow-interaction of natural vegetation." *Int. J. River Basin Mgmt.*, 4(2), 137-146.

Wilson, C. A. M. E., Yagci, O., Rauch, H.-P., and Olsen, N. R. B. (2006b). "3D numerical modelling of a willow vegetated river/floodplain system." *Journal of Hydrology*, 327, 13-21.

Wormleaton, P.R. (1996). "Floodplain secondary circulation as a mechanism for flow and shear stress redistribution in straight compound channels." Coherent Flow Structures in Open Channels, P.J. Ashworth, S.J. Bennett, J.L. Best, and S.J. McClelland, eds., Wiley, Chichester, 581-608.

Yang, K., Cao, S., and Knight, D. W. (2007). "Flow patterns in compound channels with vegetated floodplains." *Journal of Hydraulic Engineering*, 133(2), 148-159.
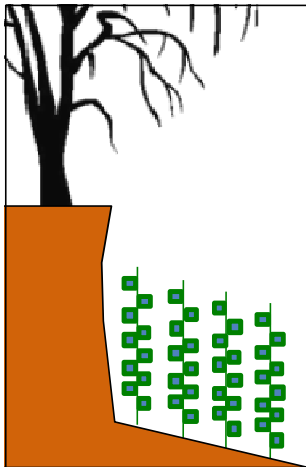
Figure 2.1. Example of a compound bank. Artificial vegetation is on the bank-toe.
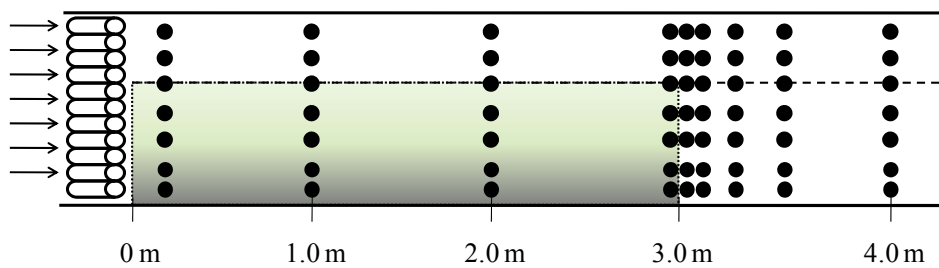
Figure 2.2. Planform view of flume; arrows indicate direction of flow, shaded region shows location of vegetation array. Circles represent velocity sampling locations. Not drawn to scale.
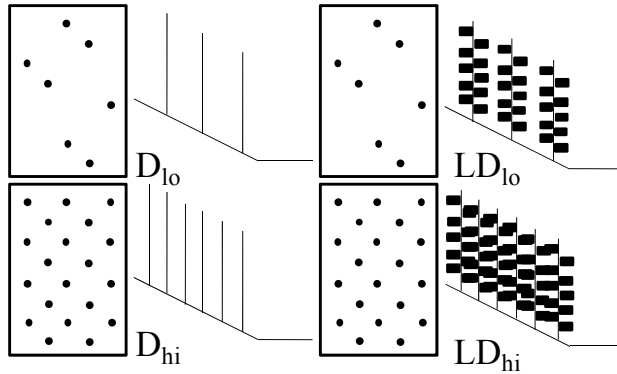
Figure 2.3. Experimental design. D_{lo} is low density, no leaves; D_{hi} is high density, no leaves; LD_{lo} is low density, with leaves; and LD_{hi} is high density, with leaves.

Table 2.1. Experimental runs. D_{lo} is low density, no leaves; D_{hi} is high density, no leaves; LD_{lo} is low density, with leaves; and LD_{hi} is high density, with leaves.

Run	Case	Q (m^{3}s^{-1})
1	noveg	0.015
2	noveg	0.03
3	noveg	0.05
4	D_{lo}	0.015
5	D_{lo}	0.03
6	D_{lo}	0.05
7	D_{hi}	0.015
8	D_{hi}	0.03
9	D_{hi}	0.05
10	LD_{lo}	0.015
11	LD_{lo}	0.03
12	LD_{lo}	0.05
13	LD_{hi}	0.015
14	LD_{hi}	0.03
15	LD_{hi}	0.05

Table 2.2. Blockage ratios (m^2/m^2) for each run with vegetation at the 2.95 m cross-section near the end of the vegetated patch. "Margin" refers to the interface between the bank-toe and main channel. Q_{lo}, Q_{med}, and Q_{hi} are 0.015 m^3/s, 0.03 m^3/s, and 0.05 m^3/s, respectively. D_{lo}, D_{hi}, LD_{lo} and LD_{hi} are defined in Figure 2.3.

Case		30° Bank-toe	Margin	15° Bank-toe	Margin
Q_{lo}	D_{lo}	0.029	0.027	0.027	0.024
Q_{lo}	D_{hi}	0.103	0.052	0.086	0.024
Q_{lo}	LD_{lo}	0.192	0.096	0.162	0.045
Q_{lo}	LD_{hi}	0.586	0.290	0.490	0.134
Q_{med}	D_{lo}	0.029	0.026	0.027	0.025
Q_{med}	D_{hi}	0.101	0.052	0.085	0.025
Q_{med}	LD_{lo}	0.185	0.091	0.159	0.046
Q_{med}	LD_{hi}	0.582	0.282	0.479	0.138
Q_{hi}	D_{lo}	0.029	0.027	0.027	0.024
Q_{hi}	D_{hi}	0.101	0.052	0.085	0.025
Q_{hi}	LD_{lo}	0.190	0.094	0.155	0.044
Q_{hi}	LD_{hi}	0.574	0.282	0.468	0.132
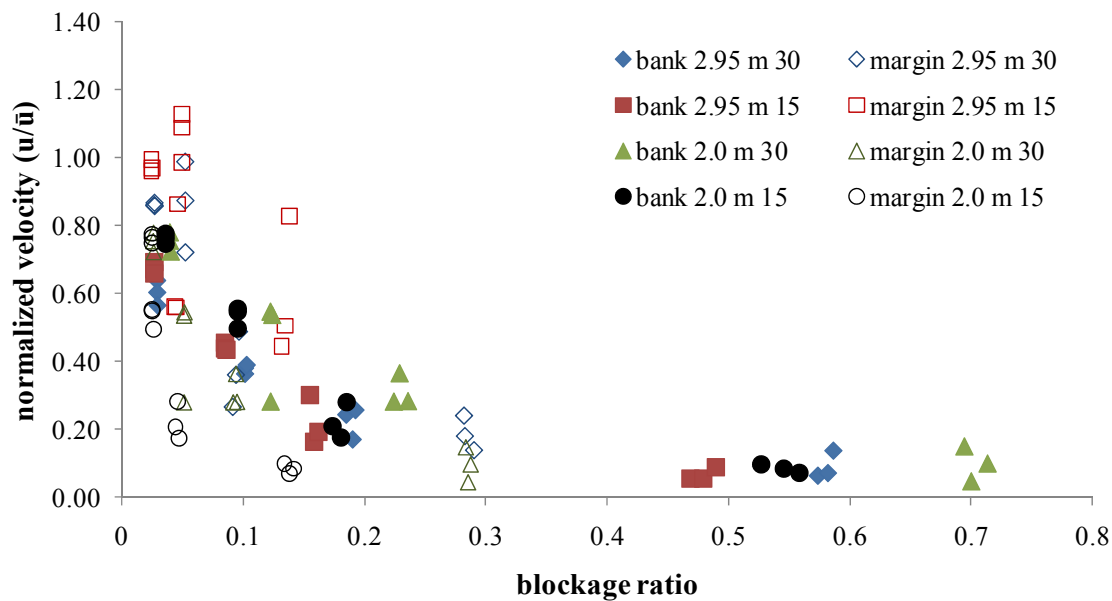
Figure 2.4. Relationship between blockage ratio and normalized velocity (u/ū) along the vegetated bank-toe (solid markers) and margin (hollow markers) for the 15° and 30° bank-toe angles. Data points represent all experimental runs at two cross-sections: 2.0 m and 2.95 m down from the beginning of the vegetation. D_{lo}, D_{hi}, LD_{lo} and LD_{hi} are defined in Figure 2.3.
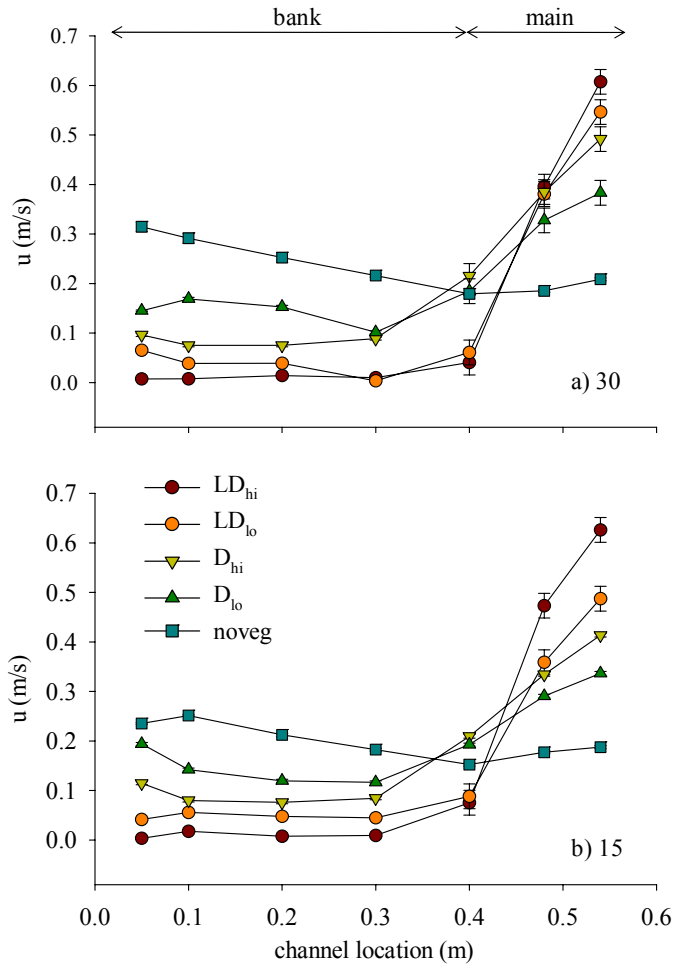
Figure 2.5. Streamwise velocity at 3 m cross-section under high discharge for: a) 30° bank-toe and b) 15° bank-toe. Bank-toe and main channel are delineated at the top of the figure. D_{lo}, D_{hi}, LD_{lo} and LD_{hi} are defined in Figure 2.3.
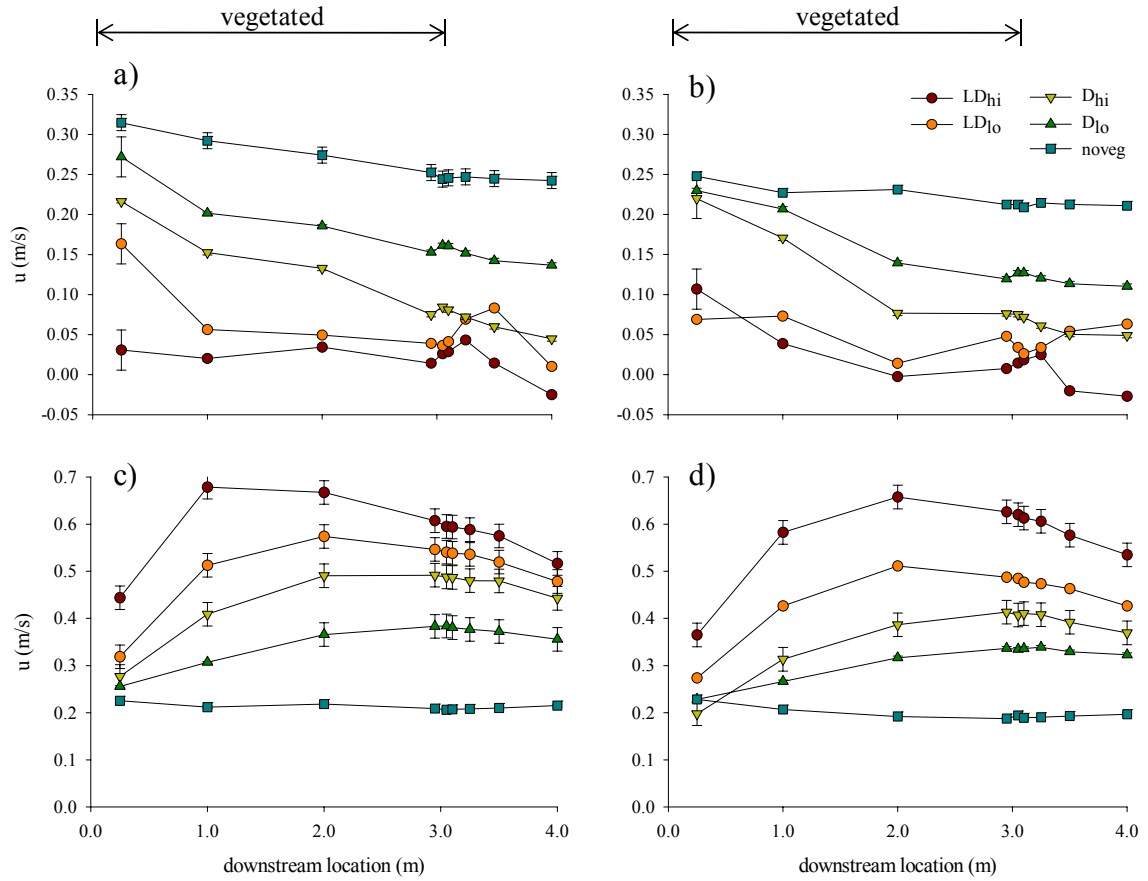
Figure 2.6. Streamwise velocity over channel length at high discharge. Velocity along the middle of the bank-toe at a) 30° and b) 15° and in main channel at c) 30° and d) 15°. The vegetated bank-toe runs from 0 to 3 m. D_{lo}, D_{hi}, LD_{lo} and LD_{hi} are defined in Figure 2.3.
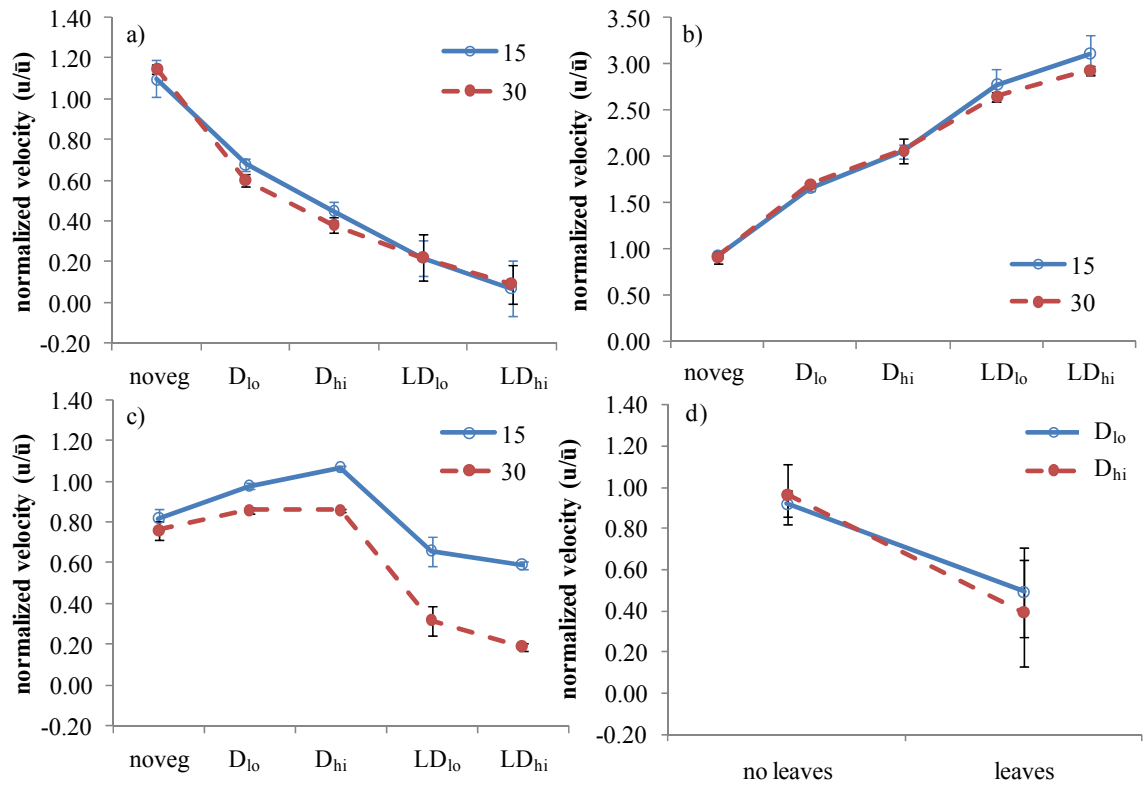
Figure 2.7. Two- way interaction plots of normalized velocity (u/ū) for select results: a-c) show interactions between blockage and bank-toe angle for a) bank-toe, b) main channel, and c) margin; d) show interactions between leaves and stem density for all runs with vegetation along the margin. Error bars represent one standard deviation. D_{lo}, D_{hi}, LD_{lo} and LD_{hi} are defined in Figure 2.3.
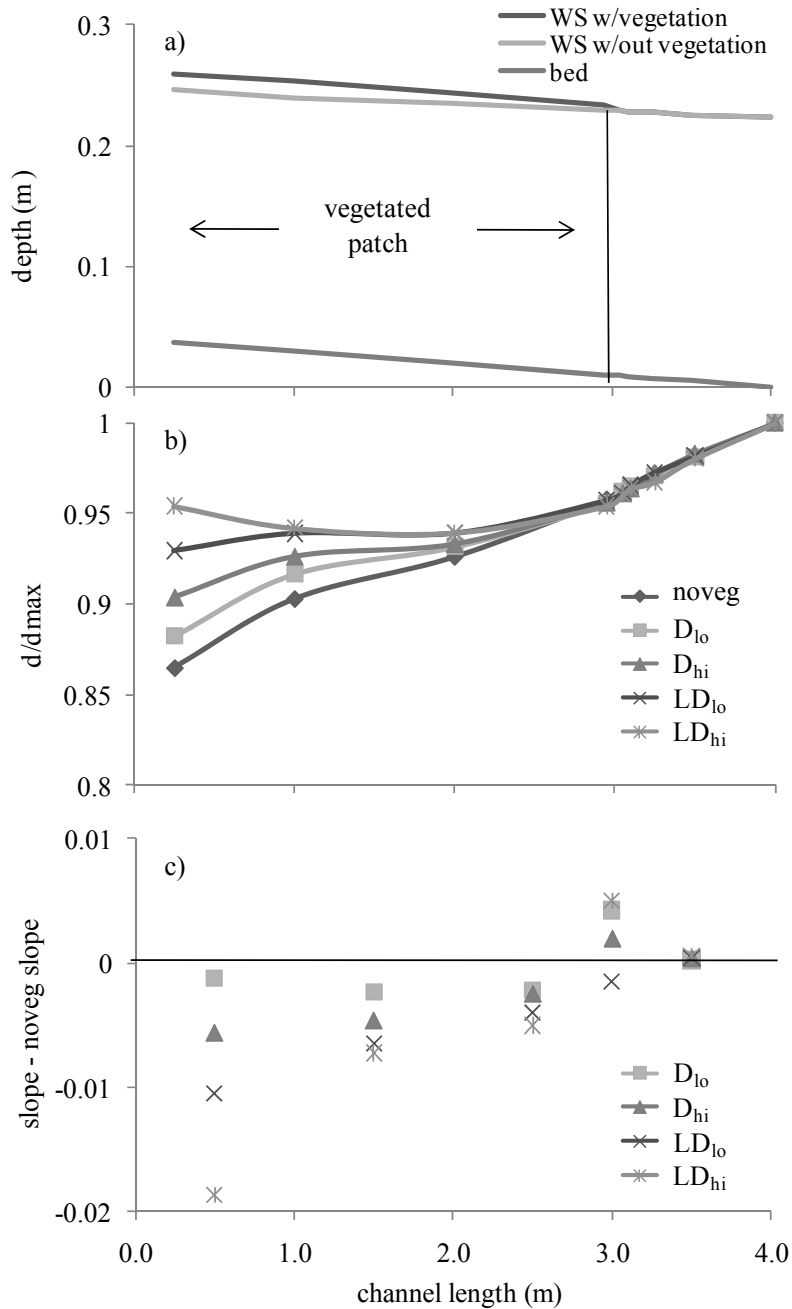
Figure 2.8. Comparison of channel depth and water surface slope for the high discharge, 30° bank-toe. Vegetation runs from 0 to 3 m. a) Hypothetical channel profile depicting backwatering effect. b) Normalized depth vs. channel length. c) Difference between slope and the unvegetated slope for 1 m increments within the vegetation and downstream of the vegetation, as well as the 0.1 m increment immediately downstream of the vegetation. D_{lo}, D_{hi}, LD_{lo} and LD_{hi} are defined in Figure 2.3.
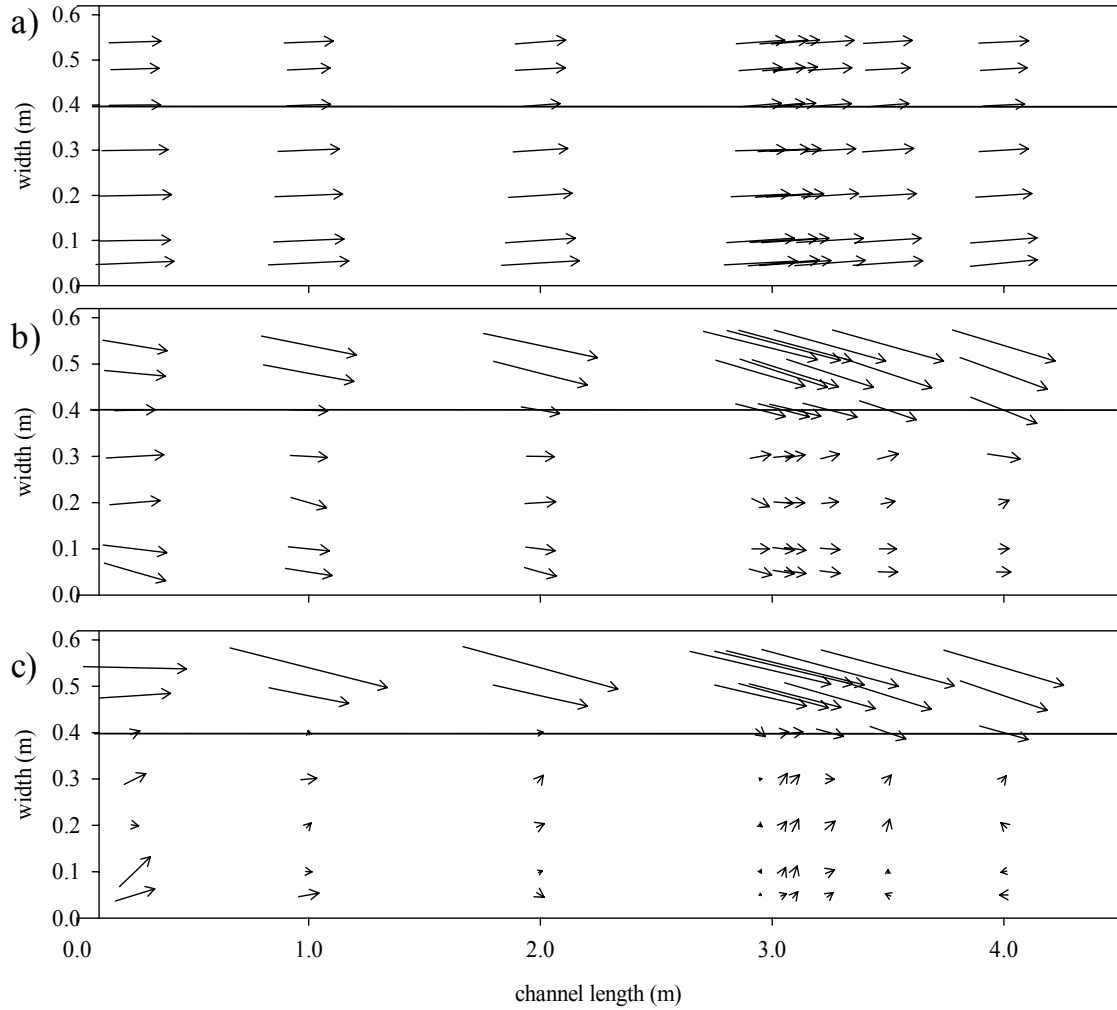
Figure 2.9. Velocity vectors computed from streamwise and lateral at high discharge. a) No vegetation. b) High density vegetation without leaves. c) High density vegetation with leaves.
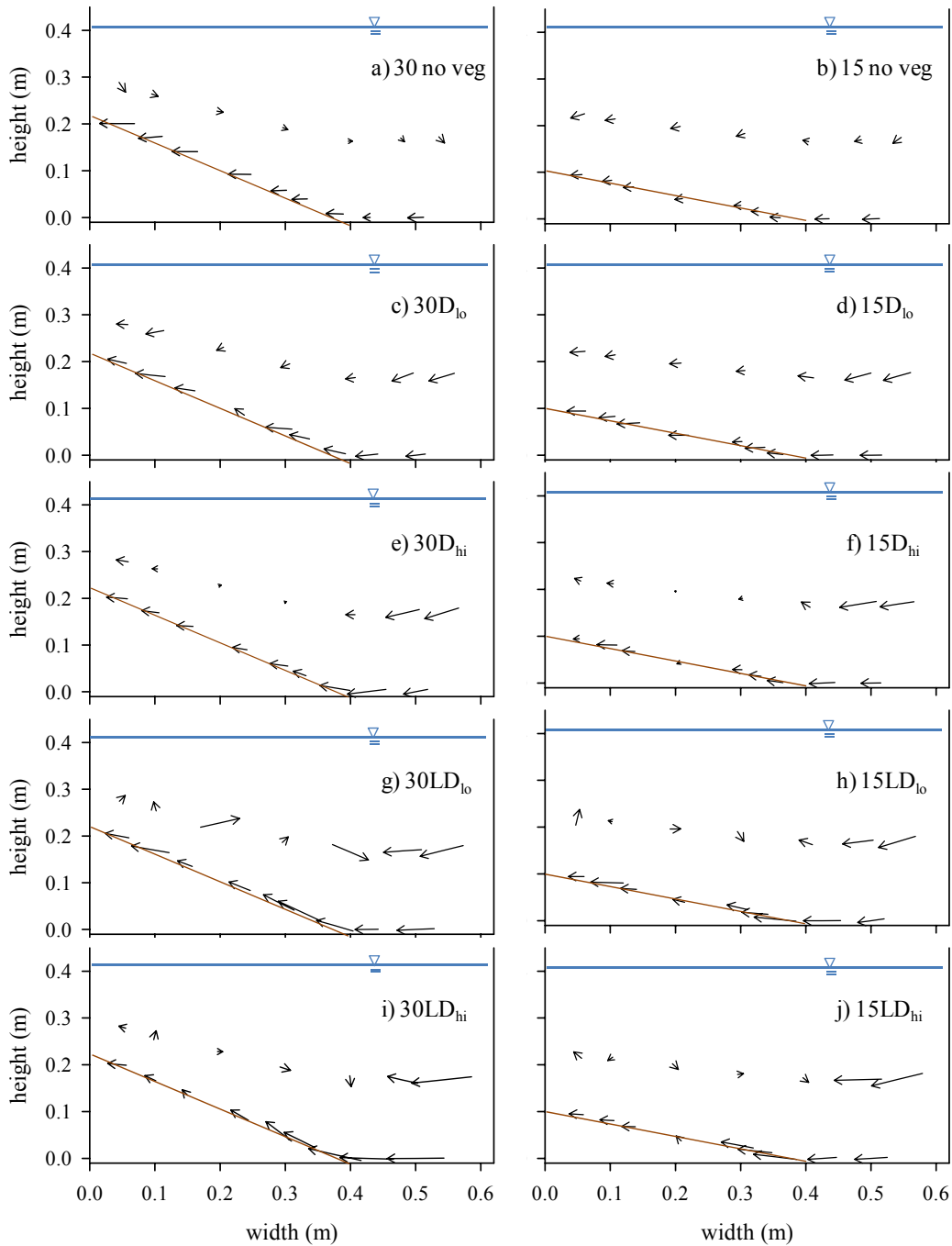
Figure 2.10. Velocity vectors computed from lateral and vertical at high discharge. The first column represents the 30° bank-toe and the second column the 15° bank-toe. Vegetation densities are: a) and b) no vegetation; c) and d) low density, no leaves; e) and f) high density, no leaves; g) and h) low density, with leaves; and i) and j) high density, with leaves.

CHAPTER 3. RESISTANCE OF VARYING VEGETATION DENSITIES ON STREAMBANKS

Nicole M. Czarnomski and Desireé Tullos

To be submitted for publication

Abstract

Streambank vegetation exerts an important, but difficult to estimate, influence on conveyance of flows in channels. The objective of this study is thus to evaluate how resistance changes with vegetation density on a vegetated streambank. Five flume experiments were conducted varying vegetation stem density (number of plants/horizontal area) and frontal area (number of leaves/vertical area) on a 30° and 15° vegetated bank-toe at three discharge rates. Average channel velocities were measured within the vegetated patch using an ADV. For each experiment, vegetation was characterized by three different vegetation density parameters: frontal area per unit volume (A_d), dimensionless A_d, and solid volume fraction. Resistance parameters C_d (drag coefficient) and Manning's n were estimated. Overall, we find a trend of increasing C_d with increasing vegetation density, related to low stem Reynolds number (Re_d). Estimates of C_d and thus Manning's n were high in comparison to most literature cited values, especially when vegetation density was high and leaves were present. Results of this study demonstrate the strong influence of vegetation density on channel velocity and estimation of resistance. Results also suggest a need to further explore appropriate mathematical representations of resistance in dense canopies, where velocity and thus Re_d is low.

Introduction

When modeling river and stream hydraulics, estimating the influence of instream vegetation on flow resistance and structure is challenging. Vegetation alters flow characteristics, reducing velocity (Kadlec 1990; Fathi-Moghadam and Kouwen 1997; Freeman et al. 2000; Järvelä 2002a, 2004; Wilson et al. 2003), introducing turbulence (Nepf 1999; Righetti and Armanini 2002; Hopkinson and Wynn 2009) and changing flow structures (Nepf 1999). Assumptions regarding hydraulic parameters and variability in assessing vegetation across existing models further complicate the representation of the influence of vegetation on hydraulics (Kadlec 1990; Nikora and Nikora 2007; Nikora et al. 2008). Large margins of error in modeling results may be due in part to the unique physical characteristics of each plant community, variation in vegetation density with depth, and variation in stem density (Wilson et al. 2006a).

Vegetation influences flow characteristics both by redirecting flow and by providing resistance against the flow. For the purposes of this study, we define resistance as the measure of flow obstruction by a vegetative element. Forces related to emergent vegetation resistance include the cumulative effects of physical interception by vegetation, viscous dissipation among the stems, skin drag, wake production (pressure drag) and surface deformation (wave drag) (Lee et al. 2004). Vegetation acts as resistance against the force of the water and responds by either remaining erect, oscillating with the pulses of current as flow is redirected around the stem, bending under the force of the water, or some combination of these effects (Fathi-Mogahadam and Kouwen 1997).

Estimating the resistance to flow provided by vegetation is challenging due to the variability in the vegetation density. In a dense canopy, the drag experienced by vegetation upstream is higher than the drag on vegetation downstream due to the wake of the upstream vegetation (Petryk 1969; Zdravkovich and Pridden 1977; Bokaian and Geoola 1984; Blevins 1994, 2005; Luo et al. 1996). Vegetation in a wake experiences a "sheltering" effect (Raupach 1992) – a lower impact velocity and increased turbulence compared to upstream vegetation, which results in a lower pressure differential around the plant (Zukauskas 1987; Luo et al. 1996). To characterize resistance where multiple

plants interact, bulk vegetation C_d estimates have been developed (Nepf 1999; Garcia et al. 2004; Harvey et al. 2009).

The presence of dense emergent vegetation reduces velocity substantially (Kadlec 1990; Freeman et al. 2000; Järvelä 2002a, 2004; Czarnomski et al. in prep). As velocity is reduced, stem Reynolds number (Re_d) also decreases, which can lead to a situation where flow is transitional between laminar and turbulent. Manning's equation was developed for fully turbulent flow and does not apply when flow is transitional between laminar and turbulent (Kadlec 1990).

A number of model limitations create challenges in developing a universal understanding of the influence of vegetation on channel hydraulics. Resistance equations were originally developed for unvegetated channels; therefore, existing equations had to be modified to include vegetation. Modifications have not necessarily met all the assumptions of the original equations (Kadlec 1990). For example, the Manning's equation is generally accepted as a representation of flow resistance, yet it may not apply when vegetation is present. The Manning's equation is based on the assumption that boundary shear is the dominant form of resistance (James et al. 2004); however, it is generally accepted that the drag on vegetation is much greater than bed shear (Kadlec 1990; Fathi-Mogohadam and Kouwen 1997). An estimated Manning's n value for a given area is based on a constant relationship with depth, slope and velocity, all of which are not expected to remain constant when vegetation is present or even without the presence of vegetation. Thus, accurate modeling efforts should include multiple estimates of n over depth. Plant morphology varies by depth (Wilson et al. 2006a; Harvey et al. 2009) and resistance can change by depth as plants streamline themselves with flow (Petryk and Bosmajian 1975; Fathi-Moghadam and Kouwen 1997; Wu et al. 1999). Water surface slope can become less steep as backwatering occurs within vegetation (Kadlec 1990), and slope breaks may form as vegetation density changes or flow conditions within the vegetated patch become more uniform (Czarnomski et al. in prep).

Further, variability exists in how models are applied. For example, the most common method is the force-balance method, where drag force (F_d) is related to plant

and flow parameters by: $F_d = \frac{1}{2} \rho\, C_d\, A_p\, U^2$, where ρ is the density of water (1 kg/m^3), C_d is the drag coefficient, A_p is the plant projected area (m^2), and U is the average velocity (m/s). However, a number of variations of A_p have been used to define the density of vegetation, usually to characterize it as a frontal area per unit volume (Petryk and Bosmajian 1975; Fischenich and Dudley 1999; Nepf 1999; Fischenich 2000; Freeman et al. 2000; James et al. 2008), per unit length of channel (Wu et al. 1999), or per unit area of bed (Stone and Shen 2002). Alternatively, plant diameter or a characteristic plant width has also been substituted for A_p and density defined as the unit width per unit area of bed (Garcia et al. 2004; James et al. 2004; Tanino and Nepf 2008).

Estimates of C_d have been developed through experimental studies for individual plant species based on the relationship between velocity and parameters such as plant width, height and flexibility (Fathi-Moghadam and Kouwen 1997; Freeman et al. 2000; Järvelä 2002b; Wilson et al. 2006a,b). However, measures of site-averaged physical parameters of vegetation density can be reliable (Nikora et al. 2008), a better representative of a plant community, and easier to obtain in the field (Dudley et al. 1998). A_p can also be characterized by the presence and absence of leaves, and estimates of C_d have been made for plants with and without leaves (Fischenich and Dudley 1999; Freeman et al. 2000; Järvelä 2004).

Finally, estimating C_d is also challenging because it differs by both vegetation characteristics, as described above, and how those characteristics relate to flow properties. C_d has a strong dependency on stem Reynolds number (Re_d) since $Re_d = Uw/\nu$, where w is the average plant width and ν is the kinematic viscosity. Previous studies have shown that when $Re_d < 10^3$, as Re_d decreases, C_d increases (Järvelä 2002a, James et al. 2004; Tanino and Nepf 2008, Harvey et al. 2009). When vegetation is dense, this can lead to low Re_d and estimations of C_d that are substantially higher than those reported in the literature when $Re_d \geq 1000$ (James et al. 2004; Harvey et al. 2009).

Given these challenges in understanding and modeling the role of streambank vegetation in influencing channel hydraulics, the objective of this study was to a) compare differences in resistance for streambank vegetation with and without leaves at

varying densities, discharge and bank-toe angles, and b) evaluate methods for calculating resistance on densely vegetated streambanks. We used a flume study and flexible artificial vegetation to explore the relationship between C_d and density when $100 < Re_d < 1000$.

Methods

Experimental design

Experiments were conducted in a $6.0 \times 0.6 \times 0.6$ m recirculating flume set at a fixed slope of 0.01 m/m (Figure 3.1). At the inlet, water passed through a rock-filled baffle box and then a baffle box composed of 0.30 m long, 0.02 m diameter tubes (flow straighteners), in order to dampen turbulence and provide uniform flow. To simulate a bank-toe, an insert was installed along one side of the flume immediately downstream of the flow straighteners. Two 4.88 m long inclined inserts were used alternately to simulate a 30° bank-toe (0.45 m wide) and 15° bank-toe (0.41 wide). Vegetation was installed in two patterns: low stem density (D_{lo}) of 202 plants per m^2 and high stem density (D_{hi}) of 615 plants per m^2, which scale to 8 and 24 plants per m^2, respectively. Plants were in two forms: leaves (LD_{lo}, LD_{hi}) and no leaves (D_{lo}, D_{hi}), where leaves have a total frontal area of 875 mm^2 (Figure 3.2). For a description of plant design, see Czarnomski et al. (in prep). For each vegetation condition, measurements were collected for three different discharges: 0.015 (Q_{lo}), 0.03 (Q_{med}) and 0.05 (Q_{hi}) m^3/s.

To characterize the depth-averaged velocity without vegetation present, it was assumed that the von Kàrmàn-Prandtl law of the wall was valid and hence velocity was measured at ~0.6 × the flow depth (0.6d) at 2.0 m downstream from the beginning of the vegetated patch (Figure 3.1). Velocities within vegetation have been demonstrated to be nearly uniform with depth (White and Nepf 2008), hence measures within vegetation also were made at 0.6d. The law of the wall assumption was tested with several vertical velocity profiles. In the unobstructed channel, and velocity at 0.6d velocity was within 10% of depth-averaged velocity. Within and downstream of the vegetation, velocities were very low and 0.6d estimates were generally within an order of magnitude of the

depth-averaged velocity. Four velocity measurements were collected along the bank-toe, from 0 to 0.35 m across the channel. Velocities were measured over five minutes at 25 Hz with a 10 MHz Nortek acoustic Doppler velocimeter (ADV). Data were filtered and processed using the WinADV software Version 2.027 (Wahl 2009).

Analysis

Five methods for estimating C_d were identified:

a) Assumed values of 1.0 for stems only and 1.5 for leafy plants (Järvelä 2002b).

b) Values derived from stem Reynolds number (Re_d) vs. C_d empirical curve (Figure 3.38 in White 1991).

c) Fischenich (2000) that is also demonstrated by James et al. (2008):

$$C_d = \frac{2gS_o}{A_d u^2} \qquad [1]$$

where g is the gravitational constant, S_o is bed slope, A_d is the vegetation density per unit channel length (L^{-1}) ($\sum A_i / A\sum x$), and u is the depth-averaged velocity (m/s). A_d was measured for the bank-toe (Table 3.1). Cross-sectionally averaged velocity was used for the depth-averaged velocity. It was calculated using the continuity equation for the sum of discharges for the four subsections along the bank-toe cross-section. This equation assumes steady, uniform conditions.

d) Nepf (1999) that was determined for a range of $0.008 < ad < 0.07$ vegetation density:

$$(1 - ad)C_B u^2 + \frac{1}{2}C_d ad \left(\frac{h}{d}\right) u = gh\frac{\partial h}{\partial x} \qquad [2]$$

where *ad* is a dimensionless population density that represents a fractional volume of the flow domain occupied by plants, $C_B = 0.001$ and is the bed drag coefficient (e.g. Munson et al. 1990, p. 673), h is the flow depth that is represented by R (hydraulic radius), and $\partial h/\partial x$ is the surface slope where x is channel length. The parameter $ad = A_d * d$, where d is represented by the average plant width (m) (Table 3.1). This equation is recommended for use when porosity is close to one, thus when vegetation density is low.

e) Tanino and Nepf (2008) that was determined for a range of $0.091 < \Phi < 0.35$ vegetation density:

$$\frac{C_d u^2}{2} md = -(1 - \Phi)g\frac{d\eta}{dx} \qquad [3]$$

where m is the number of stems per unit area (L^{-1}), $\Phi = m\pi d^2/4$, m is number of plants per unit horizontal area (number / m^2) (Table 3.1), and dη/dx is the difference between the control surface slope and the vegetated surface slope and where η is the temporally and spatially averaged displacement of the free surface from the still water level calculated based on surface elevation data collected by point gages. In this equation, u is assumed to be equivalent to the depth-averaged velocity. This equation was developed to estimate C_d for dense vegetation at low Re_d.

Two methods were compared for estimating Manning's n based on vegetation parameters. A relationship between vegetation and Manning's n was given by Fischenich (2000):

$$n = R^{2/3}\left[\frac{C_d A_d}{2g}\right]^{1/2} \qquad [4]$$

where R is the hydraulic radius (m). Tanino and Nepf (2008) related vegetation and Manning's n by:

$$n = \frac{R^{2/3}}{(1-\Phi)^{3/2}}\sqrt{\frac{C_d}{2g}md} \qquad [5]$$

In our study, resistance-based estimation of velocity for comparison with measured velocity was calculated for cross-section 2.0m (Figure 3.) using values of Manning's n from the above equations and by:

$$v = \frac{K_n}{n}R^{2/3}S^{1/2} \qquad [6]$$

where S is the friction slope and all other terms have been defined.

Results

C_d

As expected, we found a strong log-linear relationship between C_d and Re_d, with C_d increasing as Re_d is decreasing (Figure 3.3). Equations [1] and [2], which are based on area per unit volume representation of vegetation density, had similar resulting trends though the magnitude of C_d was different (Figure 3.3a,b). C_d was on average 51% and

19% higher for [1] than [2] on the 30° and 15° bank-toe, respectively, for a given Re_d. As density decreased, Re_d increased and C_d decreased, especially for the highest densities. However, when density was lowest (D_{lo}), Re_d was highest and there was some indication of a slight increase in C_d. When density was represented by a solid volume fraction ([3]), cases with leaves (LD_{hi} and LD_{lo}) followed a singular log-linear function. C_d for [3] was substantially lower than [1] and [2]; up to an order of magnitude lower at the highest densities and lowest discharges. For [3], cases without leaves (D_{hi} and D_{lo}) follow an opposite trend (Figure 3.3c) – where C_d increases with increasing Re_d. This may be due to the low density of the vegetation and that [3] was developed for higher density vegetation. The transition between opposing trend lines appears when $222 < Re_d < 290$ for D_{hi} and $305 < Re_d < 470$ for D_{lo}.

As velocity decreased, C_d increased, especially when leaves were present and Re_d was low ($25 < Re_d < 300$) (Figure 3.4, Table 3.2). Measured velocity for the 30° bank-toe was 10-25% higher than the 15° bank-toe for the case without leaves and 10-50% higher than the 15° bank-toe for the cases with leaves, resulting in lower calculated C_d on the 30° bank-toe for both leaf scenarios. This relationship between C_d and velocity was true for all discharges; however, the calculated value of C_d is higher when velocity is lower at lower discharges (Figure 3.5, Table 3.2). Decreased discharge led to lower measured velocities, resulting in $Re_d < 200$, where C_d increases exponentially.

As discharge decreased, estimates of C_d increased (Figure 3.5, Table 3.2). Three experimental runs led to unusually high C_d, especially for [1] and [2] – LD_{hi} for 30° bank-toe at Q_{med} and both the 30° and 15° at Q_{lo}. These three runs also had lower than expected velocities (<0.01 m/s), which may be due to measurement errors associated with sampling in turbulent flow or close proximity to dense vegetation.

Calculated values of C_d varied substantially with the equation used. Comparing the three different methods for calculating C_d, [1] was consistently the highest ($C_d = 3.6 - 107$, excluding the three highest values estimated for low velocities, as discussed above) and [3] the lowest ($C_d = 0.4 - 24$, also excluding the three highest values), except

for on the 30° bank-toe for LD_{hi}, LD_{lo}, and D_{hi}, where [2] was the lowest. On average, the lowest value of C_d was 60-100% less than the highest value of C_d.

The presence or absence of leaves strongly affected the estimation of vegetation density and thus the relationship of C_d to vegetation density. When no leaves were present (D_{hi} and D_{lo}), C_d decreased as density increased using [1] and [2] (Figure 3.6). Once leaves were introduced, C_d increased as the density increased. For all vegetation densities using the Re-based estimate of C_d and [3] (where vegetation density is based on a solid volume fraction of the vegetation), C_d increased when density increased. The trend of either increasing or decreasing C_d by vegetation density was consistent for discharges, though the magnitude of C_d was greater as discharge decreased.

Manning's n

Regardless of the equation used to calculate Manning's n or the value of C_d, Manning's n values were high in comparison to empirical estimates of n for vegetation (Figure 3.7, Table 3.3; Chow 1959; Barnes 1967). As expected, Manning's n increased with increasing density. When Manning's n was calculated for stems only (*ad* < 0.02), n values fell between 0.05 and 0.70. For literature values of C_d or Re_d-estimated C_d, n was 0.06-0.08 and within the range of empirical values considered reasonable for brush (n = 0.035-0.160 in Chow 1959). Equations [4] and [5] led to the higher resulting n values. Once leaves were introduced (*ad* > 0.1), 0.17 < n < 9.4, which was generally higher than the empirical range of 0.110-0.500, regardless of origin of the C_d estimate.

Manning's n values calculated in this study give an indication of how artificial vegetation patterns translate to a prototype channel (Table 3.3). When considering only the lower end of the range of calculated n values estimated using literature values of C_d, n fits within floodplain vegetation categories that are reasonable representations of the experimental design for the three lower vegetation density cases. For example, both cases without leaves were considered medium to dense brush, though they could also fall under other categories. The highest blockage, LD_{hi}, had a very high n value that only coincided with the category of a channel lined with vegetation.

Estimating velocity from n and C_d

The 30° bank-toe with Q_{hi} and cases LD_{hi}, LD_{lo}, and D_{hi} had different results than all the other cases when comparing calculated velocity to measured velocity (Figure 3.8). The water surface slope was notably flatter for these three cases than for any other vegetation density. When using C_d from the literature, Re_d and [2] to calculate n, the resulting error in calculated velocity using [4] was -10 – 17% and using [5] it was -37 – 25%. Error in velocity when using C_d from [1] in [5] or [3] in [4] was more than two times greater than expected based on other similar vegetation densities at different discharges. For all other cases, when C_d was a literature value or estimated based on Re_d, calculated estimates of velocity were 40-95% higher than measured velocity.

Other than the three cases described above (30° bank-toe with Q_{hi} and LD_{hi}, LD_{lo}, and D_{hi}), higher values of Manning's n yielded more accurate results of bank-toe velocity (Figure 3.8). Using the C_d from [2] was the most accurate in estimating velocity for both [4] and [5], leading to only a fraction of a percent difference with [4] and -50 to 12% error with [5]. For all C_d but [2], velocity estimates with n calculated for the 15° bank-toe using [4] tended to be 10-20% less accurate than estimates calculated for the 30° bank-toe. Relative error was fairly similar for cases with and without leaves using [4], but for [5] there was often a higher percent error for the conditions with leaves. Velocity was underestimated by up to 83% with [5] when vegetation density was high. Results by discharge were similar.

Each method of calculating C_d and n had varying levels of success in estimating streambank velocity, often depending on vegetation density (Figure 3.8). The most accurate combination of equations for determining a reasonable estimate of velocity was to calculate C_d with [2] and Manning's n with [4] (nearly 0% error for all vegetation densities). Velocity estimates with [2] and Manning's n with [5] were also accurate (-7 to 12% error without LD_{hi}). However, using [2] and [5] to estimate velocity for the highest density vegetation (LD_{hi}) was 36-52% too low. C_d from [1] and the Manning's n with [5] had similar results as C_d from [2]; therefore it appears that [5] does not accurately

estimate n at higher vegetation densities. The combination of [3] for C_d and [4] for Manning's n was 57% too high (32-83%), after removing the 30° bank-toe estimates with Q_{hi} and LD_{hi}, LD_{lo}, and D_{hi}, which were too low.

Discussion

C_d by vegetation density

The general trend of C_d increasing with increasing vegetation density at $Re_d <$ 1000 has been observed in previous studies (Koch and Ladd 1997; Lee et al. 2004; Tanino and Nepf 2008; Harvey et al. 2009). As flow transitions from laminar to turbulent flow, there may be a shift to a trend of C_d decreasing with increasing vegetation density (Nepf 1999). In this study, depending on the method used for calculating C_d, there was some indication of an inverse relationship between C_d and density when no leaves were present (Figure 3.6). The decrease in C_d when density increases may be occurring because Re_d is transitioning to turbulent flow, although for all densities: $250 < Re_d < 850$. Note that although estimates of C_d based on Re_d were given in this study, using an approximation of C_d based upon Re_d did not improve estimates of velocity.

Our results reflect the need for a better understanding of the trend between different vegetation densities and the threshold at which we begin to see increasing or decreasing C_d. It may be necessary to use separate equations for woody plants when there are leaves and no leaves (e.g. Jarvela 2004), which substantially changes vegetation density, Re_d, and velocity within the vegetated patch (Czarnomski et al. in prep). Additional studies exploring the relationship between C_d and Re_d may be especially important when vegetation density is lower and Re_d is transitional between laminar and turbulent flow.

Our results also demonstrate the need to better understand how estimating vegetation density can influence the relationship between density and C_d. Differences in values of C_d by density between equations [1] and [2] and equation [3] may be related, in part, to how vegetation density is derived. Estimates of A_p that are based on number of

stems per unit area may result in different relationships than estimates of whole plant area per unit volume. [1] and [2] use the vegetation parameter, A_d, or a dimensionless version of A_d, which is a commonly used estimate for vegetation density that accounts for the area of a cross-section occupied by plant material compiled over a length of channel. The units of vegetation density used for [3] are not depth dependent or dimensionless, and rely on an average plant width or stem diameter.

Choosing a representative density parameter may be important in characterizing the resistance of a vegetation community. For example, in this study A_d is not very different for the case with high density stems without leaves (D_{hi}) and the low density stems with leaves (LD_{lo}). Yet *ad*, a dimensionless parameter based on stem width, shows much greater difference between the two cases. Lee et al. (2004) suggested the need to retain spacing and width in density estimates to distinguish between plant populations with varying morphologies. It is not clear how this can also account for the difference between leafy and non-leaved vegetation, but there is some indication of a need to account for plant width rather than simply stem diameter when calculating resistance (Tanino and Nepf 2008).

Estimation of resistance

Often the goal of estimating resistance is to determine channel conveyance and estimate discharge for a reach or flow depth for flood events. Estimates of resistance are considered reasonable if they can successfully estimate the parameters of interest. Generally, empirical values of C_d or n are assumed when making conveyance estimations, but in this study that considers dense vegetation, empirical estimates were frequently much lower than estimated values. This suggests that estimates of channel flows using empirical C_d and n are likely to overestimate velocities and discharge in scenarios with dense vegetation, particularly when velocities are low.

Estimated values of C_d from this study were generally higher than those recommended by empirical estimates and those found in the literature, but when vegetation density and Re_d are similar, results from this study are not substantially

different from previously reported results (Harvey et al. 2009). Highest values of C_d were calculated when vegetation density was highest and velocities low, which was exacerbated by low discharge. It is possible that when velocities were very low, form drag had less of an effect than viscous drag, making the force-balance method of calculating resistance inappropriate (Nikora and Nikora 2007).

There were marked differences in C_d by bank-toe angle, which is likely due to differences in velocity within the vegetated patch. The higher velocity for the 30° bank-toe is likely due to the conservation of momentum, since the cross-sectional area is lower than for the 15° bank-toe while discharge remains the same. Discharge was the same for both bank-toe angles; therefore, more water had to move through a smaller cross-sectional area. Vegetation density was also different for the two bank-toe angles, though they were similar enough that if all else were equal, it might be expected that the values of C_d would also be more similar.

Higher values of C_d led to higher estimates of Manning's n than the expected empirical estimates and more accurate estimates of velocity. Studies have shown that vegetation can result in an order of magnitude of difference in Manning's n (Cowan 1956; Petryk and Bosmijian 1975; Hickin 1984), which could reduce flow velocities by up to 84% (Huang and Nanson 1997). In our analyses, values of C_d that were closer to the literature recommended values of 1.0 and 1.5 resulted in Manning's n values that were closer to what was expected from the empirical estimates, but these values greatly overestimated the velocities within the vegetated patch.

It could be that for streambank vegetation, using channel-based empirical estimates of Manning's n is not appropriate. Empirical estimates of Manning's n were derived for an entire channel cross-section and not just the bank (Barnes 1967) and were developed from longer channel lengths, where plant densities and communities can be more diverse and patchy. It might be assumed that the most appropriate empirical estimates of vegetation on a bank-toe would be more similar to what is described as a "vegetated channel lining" (n = 0.03 - 0.50), which varies by an order of magnitude

(Table 3.3). Regardless, the range for "vegetated channel lining" is broad, making it difficult to accurately estimate n.

Determining the accuracy of individual equations used to calculate C_d and Manning's n is outside the scope of this study. Not enough is known about the range of C_d, Manning's n and velocities within a vegetated patch. Furthermore, few methods for estimating appropriate vegetation density for use in resistance equations are easily applied in the field (Dudley et al. 1998). The equations in this study were chosen due to their ability to incorporate enough detail about the vegetation to provide a more accurate estimate of a given plant community and their adaptability to field application.

Conceptualizing resistance in a vegetated patch

When trying to characterize resistance for a vegetated patch, it is important to consider how to scale up our estimates of resistance. Several parameters will vary through the patch, including vegetation density, velocity, and Re_d. It is possible that assumptions we make to use current resistance relationships are no longer valid at a patch-scale.

Since resistance is known to vary by Re_d (White 1991; Koch and Ladd 1997; Tanino and Nepf 2008; Harvey et al. 2009), it may be important to consider where within the vegetated patch that resistance is calculated. For example, for D_{hi} when Q_{hi} and 30° bank-toe, the velocity changed from 0.22 to 0.13 m/s within 2.0 m of vegetated bank-toe, even though hydraulic radius and density of vegetation were nearly the same (Czarnomski et al. in prep). Velocity could also be higher at the vegetation-main channel interface of the vegetated patch. This suggests that C_d would differ depending on lateral and longitudinal position within a vegetated patch. Drag on the upstream end of the vegetated patch and the margin would be operating under Re_d conditions that were higher than at other positions within the patch and also may follow a different relationship between C_d and vegetation density (i.e. Nepf 1999).

Re_d is likely to be low within heavily vegetated banks, even if discharge is high; therefore, it is necessary to understand resistance forces and to know whether form drag

is dominant at very low Re_d when vegetation density is high. Studies of forces at low Re_d demonstrate that viscous forces are important at low Re (Bridge 2003, Fig 3.3; Nikora and Nikora 2007). Nikora and Nikora (2007) suggest that for aquatic plants, form drag can be neglected and that resistance is a function of the plant surface area over which viscous drag acts. Vegetation bends and stems and leaves reorient themselves with flow (Petryk and Bosmajian 1975; Fathi-Mogohadam and Kouwen 1997; Freeman et al. 2000; Järvelä 2002a), thus eliminating form drag (Nikora and Nikora 2007).

Resistance equations have been built upon theories of the generation of eddy scale flow in the wake of vegetation stems (Nepf 1999; Tanino and Nepf 2008; Harvey et al. 2009). With leafy vegetation, more turbulence is generated and it is possible that theory based on eddy scaling of flow does not apply (Laurel Larsen, personal communication). Resistance relationships built upon this theory may not pertain to vegetation situations with leaves or more complicated vegetation morphology.

Vegetated patches are naturally variable by length, width and height due to plant morphology, growth patterns and environmental site conditions. Because of this, depth-averaged equations for calculating resistance may not be appropriate. This is especially true when canopies are vertically variable and water depth also varies.

Further, several assumptions are made when collecting empirically-based values of C_d that may not apply within a vegetated patch. Most estimates of C_d are based on single cylinders or cylinders at low densities. Vegetation communities tend to be more complex and streambank vegetation is often very dense. In addition, studies have demonstrated that biomechanical properties such as flexing of the stem, reorientation of leaves, and lifting of leaves can alter estimates of density by depth, resulting in a strong relationship of resistance by depth (Fathi-Mogohadam and Kouwen 1997; Freeman et al. 2000; Järvelä 2002a,b: Wilson et al. 2006a,b).

Finally, obtaining accurate measures of velocity within a densely vegetated canopy or one with leaves may be challenging. As velocity slows and turbulence within the canopy increases, many velocity sampling devices may not operate accurately. Velocity may vary by depth, becoming negative for a large part of the flow depth when

plants are rough, and creating error with depth-averaged velocities (Liu et al. 2008). Location of the sampling device may also be critical. Velocity increases at the approach of a stem and a wake downstream of the stem may reduce velocity or reverse flow direction (Nepf 1999; Liu et al. 2008).

Conclusions

As we seek to find accurate estimates of resistance to calculate conveyance through a channel, it is important to find methods for estimating resistance caused by vegetation. This study illustrates the complexity in accurately characterizing resistance for vegetated streambanks. Common empirical estimates of channel resistance may not adequately apply on subsections of a channel cross-section dominated by vegetation. It is possible that at a higher density, vegetation has altered flow conditions within the vegetated patch so that commonly used methods for calculating resistance no longer apply. Conditions may vary within the vegetated patch, where the upstream and vegetation-main channel interface experience the greatest velocities and thus have different resistance coefficients. A better understanding is needed to identify which fluid theories apply under the conditions created by dense vegetation. Further studies should be conducted to explore velocities within vegetated patches of varying densities, the relationship between low Re_d and vegetation density, and how biomechanical properties of plants such as flexibility, morphology, and leaves, affect vegetation densities.

Acknowledgements

References

Barnes, H. H. (1967). "Roughness characteristics of natural channels." US Geological Survey Water-Supply Paper 1849, Denver, CO.

Blevins, R. (1994). Flow-Induced Vibration, Krieger, Malabar, Fla.

Blevins, R. D. (2005). "Forces on and stability of a cylinder in a wake." *J. Offshore Mech. Arct. Eng.*, 127(1), 39–45.

Bokaian, A., and Geoola, F. (1984). "Wake-induced galloping of two interfering circular cylinders." *J. Fluid Mech.,* 146, 383–415.

Bridge, J.S. (2003). Rivers and floodplains: forms, processes, and sedimentary record. Blackwell Science, Ltd. 551 pp.

Chow, V. T. 1959. Open Channel Hydraulics. McGraw-Hill, Inc.

Cowan, W.L. (1956). "Estimating hydraulic roughness coefficients." *Agric. Eng.*, 37, 473-475.

Czarnomski, N.M., Tullos, D., Thomas, R.E. and Simon, A. (in prep). "Streambank velocity and flow patterns when influenced by vegetation density."

Dudley, S. J., Bonham, C. D., Abt, S. R., and Fischenich, J. C. (1998). "Comparison of methods for measuring woody riparian vegetation density." *Journal of Arid Environments*, 38, 77-86.

Fathi-Moghadam, M., and Kouwen, N. (1997). "Nonrigid, nonsubmerged, vegetative roughness on floodplains." *J. Hydr. Engr.*, 123(1), 51-57.

Fischenich, J. C. (2000). "Resistance due to vegetation." USAE Waterways Experiment Station, Vicksburg, MS.

Fischenich, J. C., and Dudley, S. (1999). "Determining drag coefficients and area for vegetation." U.S. Army Engineer Research and Development Center, Vicksburg, MS.

Freeman, G. E., Rahmeyer, W. H., and Copeland, R. R. (2000). "Determination of resistance due to shrubs and woody vegetation." ERDC/CHL TR-00-25, U.S.ACE.

García, M.H., López, F., Dunn, C. and Alonso, C.V. (2004). "Flow, turbulence, and resistance in a flume with simulated vegetation." Riparian Vegetation and Fluvial Geomorphology, S.J Bennett and A. Simon, eds., American Geophysical Union, 11-28.

Harvey, J. W., Schaffranek, R. W., Noe, G. B., Larsen, L. G., Nowacki, D. J., and O'Connor, B. L. (2009). "Hydroecological factors governing surface water flow on a low-gradient floodplain." *Water Resources Research*, 45(W0342), 20.

Hickin, E.J. (1984). "Vegetation and river channel dynamics." *Can. Geogr.*, 28, 111-126.

Hopkinson, L., and Wynn, T. (2009). "Vegetation impacts on near bank flow." *Ecohydrology*, online, 1-15.

Huang, H. Q., and Nanson, G. C. (1997). "Vegetation and channel variation; a case study of four small streams in southeastern Australia." *Geomorphology,* 18(3-4), 237-249.

James, C. S., Birkhead, A. L., Jordanova, A. A., and O'Sullivan, J. J. (2004). "Flow resistance of emergent vegetation." *Journal of Hydraulic Research*, 42(4), 390-398.

James, C. S., Goldbeck, U. K., Patini, A., and Jordanova, A. A. (2008). "Influence of foliage on flow resistance of emergent vegetation." *Journal of Hydraulic Research*, 46(4), 536–542.

Järvelä, J. (2002a). "Flow resistance of flexible and stiff vegetation: a flume study with natural plants." *J. Hydr.*, 269, 44-54.

Jarvela, J. (2002b). "Determination of flow resistance of vegetated channel banks and floodplains." River Flow, D. Bousmar and Y. Zech, eds., Swets & Zeitlinger, Lisse, 311-318.

Järvelä, J. (2004). "Determination of flow resistance caused by non-submerged woody vegetation." *Int. J. River Basin Mgmt.*, 2(1), 61-70.

Kadlec, R. H. (1990). "Overland flow in wetlands: vegetation resistance." *Journal of Hydraulic Engineering*, 116(5), 691-706.

Koch, D. L., and Ladd, A. J. C. (1997). "Moderate Reynolds number flows through periodic and random arrays of aligned cylinders." *Journal of Fluid Mechanics*, 349, 31-66.

Lee, J. K., Roig, L. C., Jenter, H. L., and Visser, H. M. (2004). "Drag coefficients for modeling flow through emergent vegetation in the Florida Everglades." *Ecological Engineering*, 22, 237-248.

Liu, D., Diplas, P., Fairbanks, J. D., and Hodges, C. C. (2008). "An experimental study of flow through rigid vegetation." *Journal of Geophysical Research*, 113(F04015), 16.

Luo, S., Gan, T. and Chew, Y. (1996). "Uniform flow past one (or two in tandem) finite length circular cylinder(s)." *J. Wind Eng. Ind. Aerodyn.*, 59, 69–93.

Munson, B., Young, D. and Okiishi, T. (1990). Fundamentals of Fluid Mechanics, John Wiley, New York.

Nepf, H. M. (1999). "Drag, turbulence, and diffusion in flow through emergent vegetation." *Water Res. Research.*, 35(2), 479-489.

Nikora, N., and Nikora, V. (2007). "A viscous drag concept for flow resistance in vegetated channels." *International Association of Hydraulic Research*, Venice, Italy, 9.

Nikora, V., Larned, S., Nikora, N., Debnath, K., Cooper, G., and Reid, M. (2008). "Hydraulic resistance due to aquatic vegetation in small streams: field study." *Journal of Hydraulic Engineering*, 134(9), 1326-1332.

Petryk, S. (1969). Drag on cylinders in open channel flow, Ph.D. thesis, Colo. State Univ., Fort Collins.

Petryk, S., and Bosmajian, G. (1975). "Analysis of flow through vegetation." *J. Hydr. Div., Proc., ASCE*, 101(HY7), 871-884.

Raupach, M. R. (1992). "Drag and drag partition on rough surfaces." *Boundary-Layer Meterology,* 60(4), 375-395.

Righetti, M., and Armanini, A. (2002). "Flow resistance in open channel flows with sparsely distributed bushes." *Journal of Hydrology*, 269, 55–64.

Stone, B. M., and Shen, H. T. (2002). "Hydraulic resistance of flow in channels with cylindrical roughness." *Journal of Hydraulic Engineering*, 128(5), 500-506.

Tanino, Y., and Nepf, H. M. (2008). "Laboratory investigation of mean drag in a random array of rigid, emergent cylinders." *Journal of Hydraulic Engineering*, 134(1), 1-34.

Wahl, T. (2009). WinADV Version 2.027. U.S. Bureau of Reclamation, Water Resources Research Laboratory.

White, F.M. (1991). "Viscous Fluid Flow – Second Edition." McGraw-Hill Series in Mechanical Engineering. McGraw-Hill, Inc., New York. 614.

White, B. L., and Nepf, H. M. (2008). "A vortex-based model of velocity and shear stress in a partially vegetated shallow channel." *Water Resources Research*, 44(W01412), 15.

Wilson, C. A. M. E., Stoesser, T., Bates, P. D., and Batemann Pinzen, A. (2003). "Open channel flow through different forms of submerged flexible vegetation." *J. Hydr. Engr.*, 129(11), 847-853.

Wilson, C. A. M. E., Yagci, O., Rauch, H.-P., and Stoesser, T. (2006a). "Application of the drag force approach to model the flow-interaction of natural vegetation." *Int. J. River Basin Mgmt.*, 4(2), 137-146.

Wilson, C. A. M. E., Yagci, O., Rauch, H.-P., and Olsen, N. R. B. (2006b). "3D numerical modelling of a willow vegetated river/floodplain system." *Journal of Hydrology*, 327, 13-21.

Wu, F.-C., Shen, H. W., and Chou, Y.-J. (1999). "Variation of roughness coefficients for unsubmerged and submerged vegetation." *Journal of Hydraulic Engineering*, 125(9), 934-942.

Zdravkovich, M. M., and Pridden, D. L. (1977). "Interference between two circular cylinders; series of unexpected discontinuities." *J. Industrial Aerodynamics*, 2, 255–270.

Zukauskas, A. (1987). "Heat transfer from tubes in cross-flow." *Adv. Heat Trans.,* 18, 87–159.
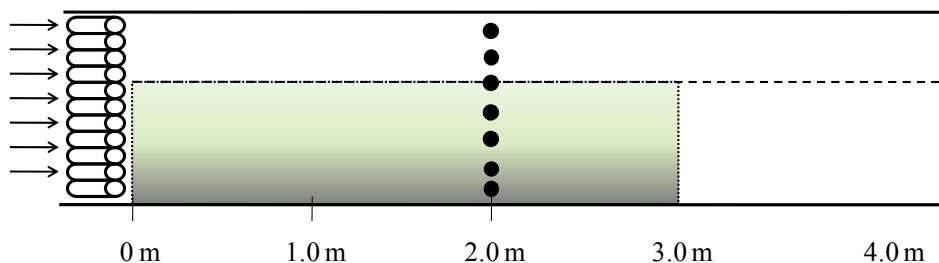
Figure 3.1. Planform view of flume; arrows indicate direction of flow, shaded region shows location of vegetation array. Circles represent velocity sampling locations. Not drawn to scale.
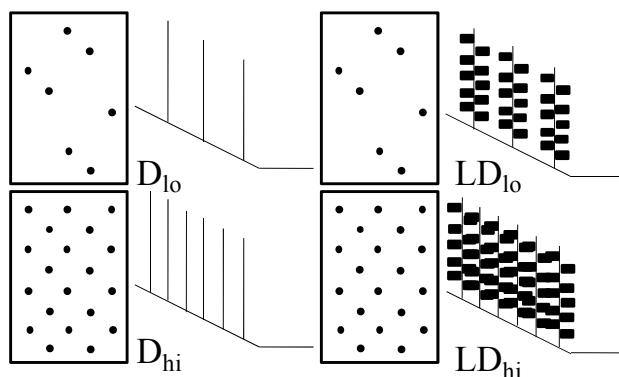
Figure 3.2. Experimental design. D_{lo} is low density, no leaves; D_{hi} is high density, no leaves; LD_{lo} is low density, with leaves; and LD_{hi} is high density, with leaves.

Table 3.1. Vegetation density for this study. The low end of the range represents the 30° bank-toe and the high end represents the 15° bank-toe. D_{lo}, D_{hi}, LD_{lo} and LD_{hi} are defined in Figure 3.2.

Parameter	D_{lo}	D_{hi}	LD_{lo}	LD_{hi}
A_d	$1.0 - 1.1$	$3.1 - 3.7$	$5.6 - 7.0$	$17.0 - 21.3$
ad	$0.004 - 0.005$	$0.014 - 0.016$	$0.13 - 0.16$	$0.4 - 0.5$
Φ	0.003	0.010	0.073	0.223
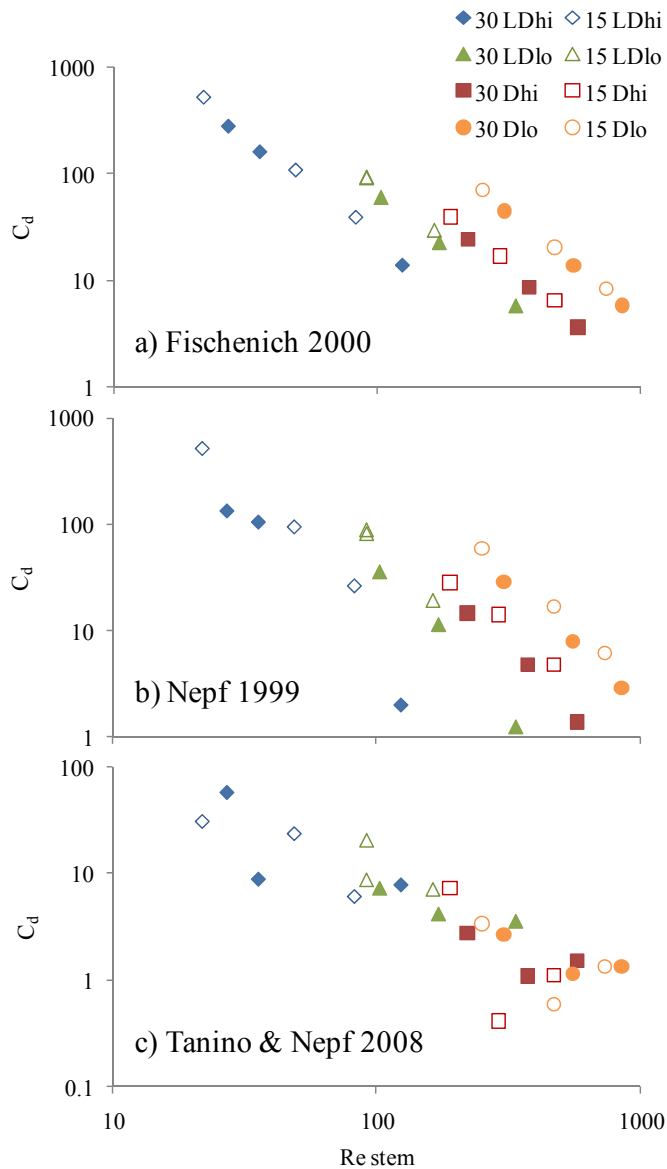
Figure 3.3. Drag coefficient (C_d) by stem Reynolds number (Re_d) for all discharges. 30°
and 15° bank-toe angles are indicated. Method used to calculate results is a) [1], b) [2],
and c) [3]. Symbols represent different vegetation densities. D_{lo}, D_{hi}, LD_{lo} and LD_{hi} are
defined in Figure 3.2.

Table 3.2. Re_d and C_d calculated from equations [1], [2], and [3] by density, discharge, and bank-toe angle. Q_{lo}, Q_{med}, and Q_{hi} are 0.015 m³/s, 0.03 m³/s, and 0.05 m³/s, respectively. D_{lo}, D_{hi}, LD_{lo} and LD_{hi} are defined in Figure 3.2.

			Re_d	C_d		
				[1]	[2]	[3]
LD_{hi}	Q_{hi}	15°	82.3	38.5	26.6	6.0
		30°	124.0	13.8	2.0	7.9
	Q_{med}	15°	48.8	107.0	94.4	23.6
		30°	27.2	284.2	131.9	57.6
	Q_{lo}	15°	21.9	518.1	509.2	30.8
		30°	35.8	162.9	103.8	8.9
LD_{lo}	Q_{hi}	15°	163.9	29.4	19.2	7.0
		30°	336.3	5.7	1.2	3.5
	Q_{med}	15°	91.4	92.0	81.2	20.6
		30°	172.1	22.3	11.4	4.1
	Q_{lo}	15°	91.2	90.4	88.0	8.6
		30°	103.4	59.4	35.7	7.3
D_{hi}	Q_{hi}	15°	471.0	6.5	4.7	1.1
		30°	577.5	3.6	1.4	1.5
	Q_{med}	15°	291.2	16.9	14.2	0.4
		30°	376.3	8.5	4.8	1.1
	Q_{lo}	15°	190.2	39.3	28.2	7.3
		30°	221.5	24.2	14.5	2.8
D_{lo}	Q_{hi}	15°	736.5	8.3	6.1	1.3
		30°	853.4	5.8	2.9	1.3
	Q_{med}	15°	470.8	20.4	16.9	0.6
		30°	555.7	13.6	7.9	1.1
	Q_{lo}	15°	251.7	71.3	59.7	3.4
		30°	304.6	44.9	28.6	2.7
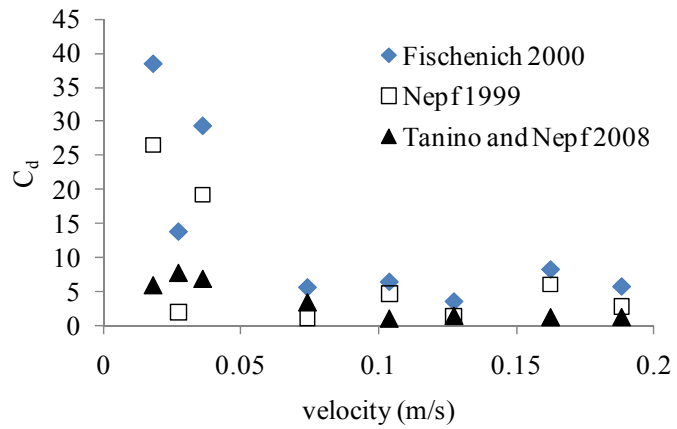
Figure 3.4. Comparison of drag coefficient (C_d) by average bank-toe velocity when Q_{hi} (0.05 m³/s).
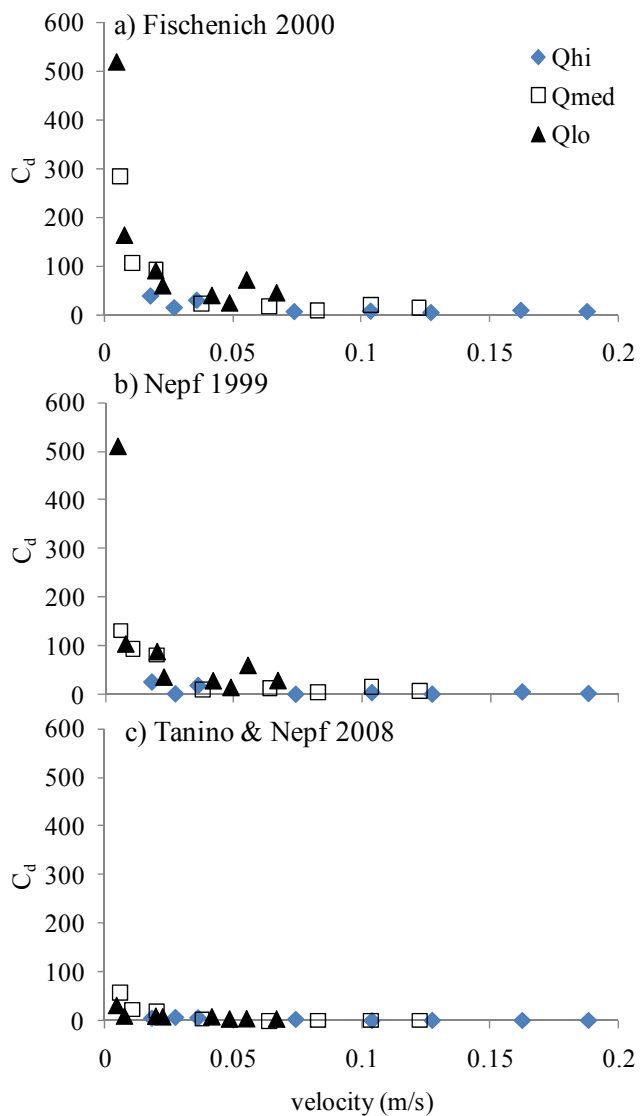
Figure 3.5. Comparison of drag coefficient (C_d) by average bank-toe velocity using equations [1], b) [2], and c) [3]. For all three discharges: Q_{hi} (0.05 m^3/s), Q_{med} (0.03 m^3/s), and Q_{lo} (0.015 m^3/s).
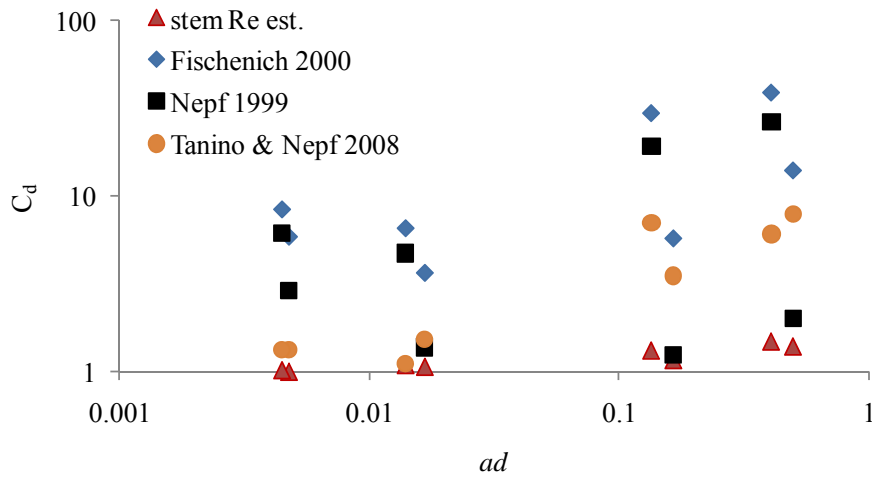
Figure 3.6. Drag coefficient (C_d) versus *ad* (vegetation density) when Q_{hi} (0.05 m^3/s). Stem Re est. is derived from an empirical curve, other values of C_d are based on equations [1], [2], and [3].
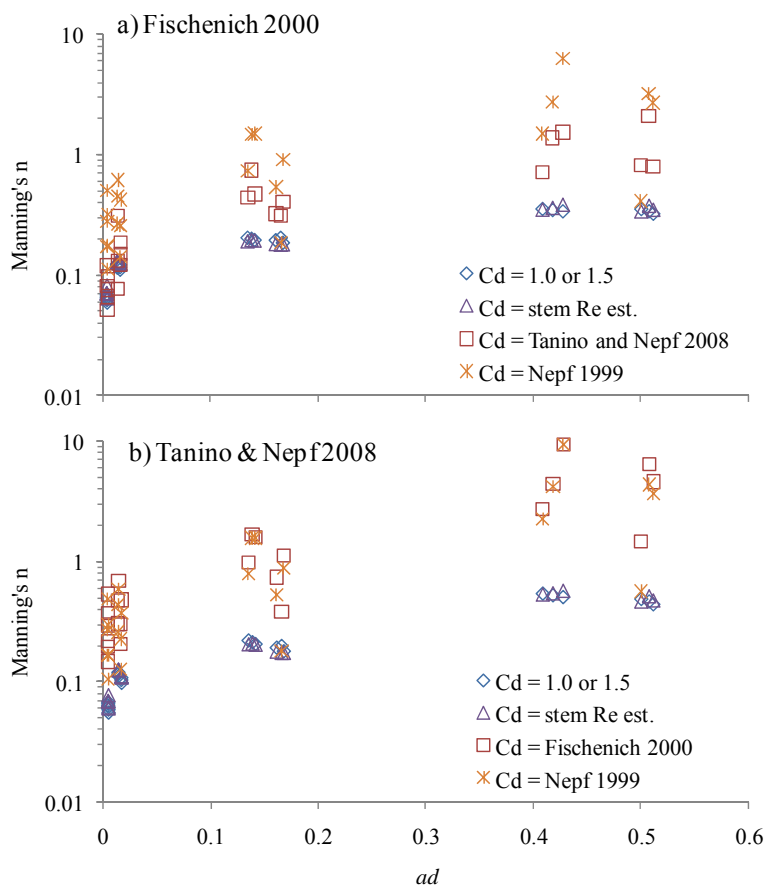
Figure 3.7. Manning's n by vegetation density (*ad*) for all discharges using equations [4] and [5].

Table 3.3. Range of Manning's n values using the combination of equations [2] and [4], literature values of 1.0 or 1.5, empirical estimates, and a description of the empirical estimate from Manning's n for Channels (Chow 1959) that is most similar to the vegetation case. D_{lo}, D_{hi}, LD_{lo} and LD_{hi} are defined in Figure 3.2.

Case	Manning's n ([2] & [4])	Manning's n (1.0 or 1.5)	Manning's n (Chow 1959)	Description of Manning's n
D_{lo}	0.1 – 0.5	0.06-0.07	0.045-0.110	medium to dense brush in winter
D_{hi}	0.1 – 0.6	0.11-0.12	0.070-0.160	medium to dense brush in summer
LD_{lo}	0.5 – 1.5	0.18-0.21	0.110-0.200	dense willows, summer, straight
LD_{hi}	0.4 – 6.3	0.32-0.36	0.030-0.500	vegetal lining of channels
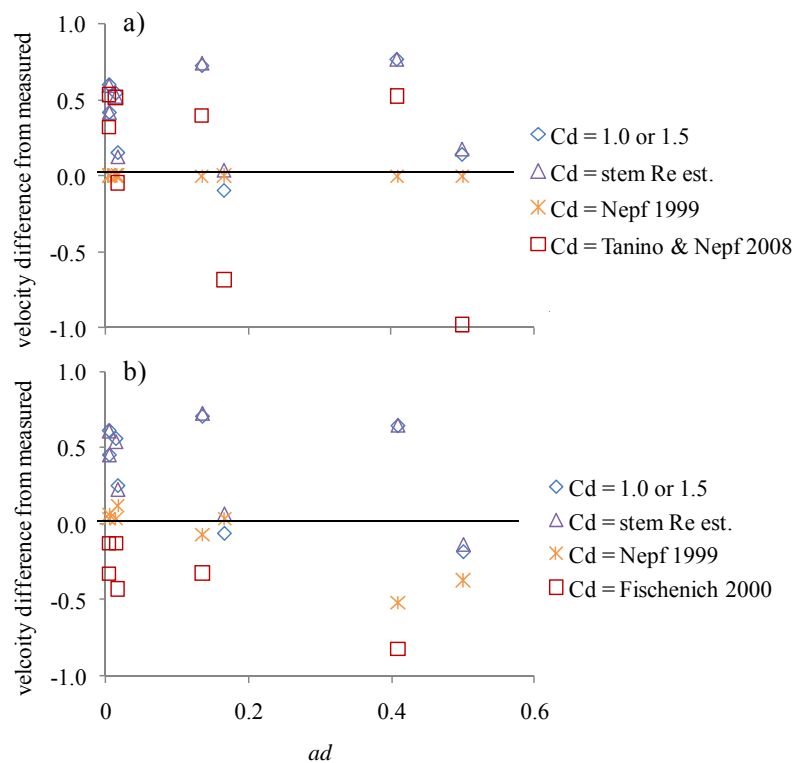
Figure 3.8. Ratio of the difference in calculated velocity and measured velocity when velocity is calculated using equation [6] and n values from a) [4] and b) [5]. For each equation used, four different values of C_d were tested. Results are presented for Q_{hi} (0.05 m^3/s).

CHAPTER 4. SHEAR STRESS AND TURBULENCE ALONG A STREAMBANK DUE TO CHANGES IN VEGETATION CANOPY DENSITY AND BANK ANGLE

Nicole M. Czarnomski, Desireé Tullos, Robert E. Thomas, Andrew Simon, Jonathan Palacios, and Eugene Zhang

Abstract

Vegetation along the toe of a streambank can alter the forces applied to the bank surface and can protect banks against erosion, though efforts are still needed to better understand the influence of vegetation on streambank hydraulics. In this study, we investigate the role of vegetation density and bank-toe angle on turbulence and shear stress on the bank-toe. Five flume experiments were used to explore how changes in vegetation density (plant frontal area per unit cross-sectional area) influence boundary shear stress on a 30° and 15° vegetated bank-toe at three discharge rates. Velocity profiles were measured to explore flow patterns around and under the canopy. Turbulent stress measures based on turbulent kinetic energy and Reynolds stress were used to evaluate boundary shear stress. Tensor fields were visualized to further our understanding of vorticity and hydraulics near the boundary. Results indicate that, with increasing vegetation density, turbulence and shear stress decreased along the majority of the bank-toe and increased at the bottom of the bank-toe, thus a greater opportunity for erosion exists at sensitive locations along the bottom of the bank-toe and in the main channel. Reynolds stresses increased under the canopy, resulting in higher shearing forces along the bank-toe, especially on the 30° slope. Generally, we find that while vegetation may reduce shear stress along the bank-toe due to a decrease in velocity, turbulence induced by vegetation may increase erosion at the interface between the main channel and vegetated bank-toe.

Introduction

Planting vegetation has become a common streambank bioengineering practice to protect banks from being eroded by the sheering forces of water. When planning a streambank bioengineering project, many questions arise in regards to how to effectively plant the bank for minimizing erosion (Allen and Leech 1997, Bentrup and Hoag 1998). To develop an adequate planting design, it is important to know the density of plantings and the location of plantings that will produce the desired reduction in erosion (Bentrup and Hoag 1998). It is also important to recognize whether these results depend on specific site conditions such as bank angle.

Riparian vegetation is known to influence erosion and deposition patterns on streambanks (Francis 2006). Vegetation along the toe of a streambank can reduce water velocities and deflect flow away from banks (Bertram 1984; McBride et al. 2007; Yang et al. 2007; White and Nepf 2008; Hopkinson and Wynn 2009), altering the forces applied to the bank and protecting banks against erosion. Vegetation also introduces turbulence, roughening flow and introducing localized scour, often along the floodplain-main channel interface (McBride et al. 2007; White and Nepf 2008; Hopkinson and Wynn 2009). Vegetation has been known to activate turbulence at the interface between the canopy and the free-stream (Yang et al. 2007; White and Nepf 2008; Hopkinson and Wynn 2009; Zong and Nepf 2010). Flow structures such as vortices and eddies form at the interface (Nepf 1999, White and Nepf 2008; Zong and Nepf 2010) and downstream of vegetated patches (Czarnomski et al. in prep). Turbulence and associated flow structures can lead to erosion (Lavelle and Mofjeld 1987; Diplas et al. 2008). Thus, it is unsurprising that shear stresses along the bed are influenced by vegetation density (Thompson et al. 2004; Bennett et al. 2002; White and Nepf 2008).

Hydraulic response to the density of vegetation can lead to varying erosional and depositional patterns. Individual plant stems may be scoured around the base similar to that found with bridge piers, where scour is due to locally formed vortices, inciting erosion to the point where the plant could be eroded from the ground (Bendix and Hupp 2000; Freeman et al. 2000). Plants can also cause wakes, resulting in low velocities and

shear stresses immediately downstream of the stem (Nepf 1999; Thompson et al. 2004; Liu et al. 2008), resulting in deposition within and immediately downstream of vegetated patches (Bennett et al. 2002; Zong and Nepf 2010).

Hydraulic streambank erosion is often quantified using an excess shear stress equation: $$E = K_d (\tau - \tau_c)^a$$ where E is erosion rate (m/s), K is the erodibility coefficient (m^3/N-s), τ is applied shear stress (Pa), τ_c is the critical shear stress (Pa), and a is an exponent assumed to equal 1.0. Generally this equation utilizes a bulk estimate of the applied shear stress: $\tau = \rho g R S$, where ρ is the density of water (assumed constant and equal to 1000 kg/m^3), g is the gravitational acceleration constant (9.81 m/s^2), R is the hydraulic radius (m), and S is the surface slope. Applied shear equations account for vegetation by averaging the effects over a reach, but this does not sufficiently describe the potential for erosion at locations of interest (e.g. interface between the main channel and vegetated bank-toe) within the channel reach (Kean and Smith 2004; Hopkinson 2009).

For vegetated streambanks, hydraulic erosion is especially of interest on the bank-toe. Studies of turbulence and shear stress due to vegetation density on sparsely treed floodplains have found an increase in turbulence within the vegetated patch (Nepf 1999; McBride et al. 2007). On an inclined streambank, turbulence for a sparsely vegetated bank was found to remain similar to the unvegetated streambank (Hopkinson and Wynn 2009). The addition of more dense vegetation types has increased turbulence at the bottom of the bank-toe and the vegetation-main channel interface, introducing a narrow band of higher shear stress at the vegetation-main channel interface (Yang et al. 2007; White and Nepf 2008; Gorrick 2009; Hopkinson and Wynn 2009). Complex canopy structure can also increase turbulence within a vegetated patch that propagates throughout the water column (Liu and Diplas 2010). This study was conducted to further understand how vegetation with varying canopy complexity and varying density influences erosion on and adjacent to an inclined streambank.

Our study objective was to evaluate vulnerability of the streambank toe to erosion by measuring stresses representing turbulent fluctuations along the bank-toe and bed at

varying levels of vegetation density and for different bank-toe angles and discharges. To identify vulnerability of the bank-toe associated with varying densities of vegetation, we used a scaled flume experiment to determine the magnitude of change in applied forces (shear stress and turbulence) due to differences in density of vegetation and bank-toe angle. We anticipated that, although a higher density of vegetation reduces flow velocities, it also introduces additional turbulence into the flow structure, promoting erosion at sensitive locations on the bank-toe. In addition, we applied visualization of tensor fields with the objective of understanding how vegetation influenced hydraulics along the bank-toe and in the open channel.

Methods

Experiment 1 – Near-bed measurements

Experiments were conducted in a $6.0 \times 0.6 \times 0.6$ m recirculating flume set at a fixed slope of 0.01 m/m (Figure 4.1). At the inlet, water passed through a rock-filled baffle box and then a baffle box composed of 0.30 m long, 0.02 m diameter tubes (flow straighteners), in order to dampen turbulence and provide uniform flow. To simulate a bank-toe, an insert was installed along one side of the flume immediately downstream of the flow straighteners. Two 4.88 m long inclined inserts were used alternately to simulate a 30° and 15° toe of a compound streambank, scaled by an average Froude scaling factor of 4.35 and 4.88, respectively, from an average prototype stream of a 3rd-4th order channel. The three different discharges (0.015, 0.030, and 0.050 m^3/s^1) correspond to 0.6, 1.2, and 2.0 m^3/s^1 in the prototype stream. Near-boundary velocity was measured at 7 or 9 cross-stream locations within 7 cross-sections (Figure 4.1a). Velocities were measured over five minutes at 25 Hz with a 10 MHz Nortek acoustic Doppler velocimeter (ADV). Sampling volume was 9 mm. Data were filtered and processed using the WinADV software Version 2.027 (Wahl 2009).

Artificial plants were used to represent natural plants, with scaled flexibility and "leaved" and "leafless" conditions. The vegetation array was 3 m long, beginning immediately downstream of the flow straighteners (Figure 4.1a). Vegetation was installed

in two patterns: low stem density (D_{lo}) of 202 stems per m^2 and high stem density (D_{hi}) of 615 stems per m^2, which scale to 8 and 24 stems per m^2, respectively (Figure 4.2). Eight stems per square meter can be considered a fairly normal stand of mature willow or cottonwood saplings, whereas twenty-four stems per square meter can be considered a very dense stand. Plants were made of 450 mm long, 4.54 mm diameter acrylic rods, scaled down from 2 m tall, 20 mm diameter woody vegetation. Artificial plants represent small riparian trees and shrubs with a similar range of flexibility, such as willow and ash. Plants were in two forms: leaves (designated with an "L" – LD_{lo}, LD_{hi}) and no leaves (D_{lo}, D_{hi}). Leaved plants consisted of the same acrylic rods affixed with ten 28-gauge wire "branches" and ten 25×35 mm "leaves" made of contact paper (875 mm^2 total) spaced to reflect a pattern of frontal area found by Wilson et al. (2006). Vegetation density was calculated as the ratio of frontal area to flow area for each plant pattern and form and is given in Table 4.1.

Experiment 2 – Velocity profiles

Velocity profiles were collected using the same flume and the vegetation array from LD_{hi} and removing the upstream 1 m of vegetation (Figure 4.1b). Six measurements were collected in the first 10.0 cm from the bed: 0.2, 1.0, 2.5, 5.0, 7.5 and 10.0 cm. After 10.0 cm, measurements were collected as follows: 13.5, 16.5, 20.0, 23.5, 26.5, and so forth until measurements could no longer be taken. A maximum of 10 measurements were collected per profile on the 30° bank-toe, 11 measurements on the 15° bank-toe, and 13 measurements at all other locations within the channel for both bank-toe slopes. Sampling volume was 3 mm, sampled over a three minute interval. The top 7 cm of each profile were not measured due to limitations of the ADV.

Analysis

We used two estimates of boundary shear stress and an estimate of turbulence to determine the shearing forces at specific locations within the channel. Estimates of turbulent kinetic energy (TKE) and Reynolds shear stress are adequate substitutions for

applied shear stress (Biron et al. 2004; Daniels and Rhodes 2004; Pope et al. 2006; Hopkinson 2009) and are better representations of shear stress at a point than the bulk estimate (Hopkinson 2009).

Shear stress based on TKE was quantified by the following equation:

$$\tau_{TKE} = C_1[0.5\rho(RMS_u^2 + RMS_v^2 + RMS_w^2)]$$

where C_1 is a proportionality constant assumed to be 0.21 (Daniels and Rhodes 2004), and RMS is the root mean square differences between instantaneous velocities in the streamwise (u), lateral (v), and vertical (w) directions and their corresponding time-averaged velocities (Clifford and French 1993), given by:

$$RMS_u = \sqrt{((\textstyle\sum u'^2)/N)}, \; u' = U-u$$
$$RMS_v = \sqrt{((\textstyle\sum v'^2)/N)}, \; v' = V-v$$
$$RMS_w = \sqrt{((\textstyle\sum w'^2)/N)}, \; w' = W-w$$

TKE represents competition between reduced velocity within the vegetation and increased turbulence from vegetation (Hopkinson and Wynn 2009) and has been shown to represent three-dimensional stress (Kim et al. 2000; Daniels and Rhodes 2004; Hopkinson 2009). RMS represents turbulence intensity and can be considered a measure of the magnitude of turbulent flux. Turbulence intensity can indicate where shear stresses are highest and where we might expect bed and bank erosion to occur.

Reynolds shear stress was quantified for the lateral and vertical directions using:

$$\tau_{uv} = -\rho<u'v'>$$
$$\tau_{uw} = -\rho<u'w'>$$

Reynolds shear stress represents stresses due to the turbulent fluctuations that represent momentum exchange across a plane (Robert 2003). These parameters represent the directionality of the stress. Quadrant analysis of u' and w' provides a more detailed description of turbulence structure and has been related to sediment transport (Bennett and Best 1995; Buffin-Belanger and Roy 1998). When τ_{uw} is positive (Quadrants II and IV), it is related to ejection (u'<0, w'>0) and sweep (u'>0, w'<0) events. Quadrants I (u'>0, w'>0) and III (u'<0, w'<0), are described as outward interactions and inward interactions, respectively.

Tensor field visualizations

Tensor field visualizations are based on flow kinematics, where the gradient of the velocity vector field is an asymmetric tensor that can be used to infer the behavior of the velocity field and 3D flow can be projected onto a 2D manifold (Zhang et al. 2009). With the development of eigenvalue and eigenvector manifolds, tensor analysis can be related to rotation, angular deformation, and dilation in fluid mechanics. Spatial distortion of the flow field is measured by the coefficient of isotropic scaling (γ_d), the coefficient of rotation (γ_r), and the coefficient of anisotropic stretching (γ_s). The coefficients are defined for a given asymmetric tensor field *T*, which contains the spatial derivatives of the velocity field gradient with every point, **p**, on a manifold surface a second-order tensor field:

$$T(\mathbf{p}) = \begin{pmatrix} T_{uu}(\mathbf{p}) & T_{uv}(\mathbf{p}) \\ T_{vu}(\mathbf{p}) & T_{vv}(\mathbf{p}) \end{pmatrix}$$

and,

$$\gamma_d(\mathbf{p}) = \frac{T_{uu}(\mathbf{p}) + T_{vv}(\mathbf{p})}{2}$$

$$\gamma_r(\mathbf{p}) = \frac{T_{vu}(\mathbf{p}) - T_{uv}(\mathbf{p})}{2}$$

$$\gamma_s(\mathbf{p}) = \frac{\sqrt{(T_{uu}(\mathbf{p}) - T_{vv}(\mathbf{p}))^2 + (T_{uv}(\mathbf{p}) + T_{vu}(\mathbf{p}))^2}}{2}$$

where $\gamma_d(\mathbf{p})$ measures expansion and contraction at the particle scale, $\gamma_r(\mathbf{p})$ measures particle rotation and $\gamma_s(\mathbf{p})$ measures anisotropic stretching or elongation due to motion. The u-v velocities are primarily addressed and w velocity ignored because coefficients are based on this second-order tensor field.

Visualizations can be interpreted by colors and streamlines and are projected based on all measures, represented as a continuous color variation and by dominant measures, where colors are binned and discrete so that boundaries can be more easily interpreted. Red represents positive vortices and counterclockwise flow along a plane parallel to the main channel boundary. Green represents negative vortices and clockwise flow. Blue shows negative scaling, where there is a contraction of fluid elements and

flow particles are leaving the flow plane in a vertical direction. The opposite is represented by yellow, which shows the expansion of fluid elements and flow particles entering from other flow planes. White shows particle stretching, representing 1) a faster mixing rate due to the larger surface area of the particle for the same volume of particle, and 2) energy dissipation because of work done to stretch the particle. Tensor magnitudes are plotted with a color scheme that goes blue to green to yellow to red with rising intensity (e.g. the field is turning/stretching/diverging/speeding up/slowing down the most in the yellow and red regions). Magnitude can be also be detected in the deformation of the tensor field. When eigenvectors are real numbers, stretching dominates (hyperstreamlines) and when a complex number, rotation dominates (glyphs).

Results

In evaluating the potential for hydraulic erosion on a streambank, an initial assessment of τ indicates that channel shear decreases with an increase in vegetation density. However, measures of shear stresses and turbulence along the boundary suggest that, though shear stresses decrease on the bank-toe, the sensitive interface between bank-toe and main channel and the main channel have increased shear stresses.

Bulk shear stress

An assessment of τ scaled to the prototype channel shows that as expected, τ decreased by 15 – 33 Pa and 7 – 12 Pa with the introduction of vegetation for the 30° bank-toe and 15° bank-toe, respectively (Figure 4.3). For the 30° bank-toe, τ decreased as vegetation density increased. Though vegetation also reduced τ for the 15° bank-toe, an apparent threshold was reached at about 70 Pa where τ varied minimally.

Flow through the vegetated patch

Flow approaching a vegetated patch with emergent vegetation was directed both around the vegetation and under the canopy. On average, flow velocities on the bank-toe were 90% lower within and downstream of vegetation than upstream of the vegetation,

but velocity was not uniform by depth (Figure 4.4). Flow velocities under the canopy (i.e. near-boundary) within and downstream of the vegetation experienced a sharp 6-fold and 5-fold increase (30° bank-toe and 15° bank-toe, respectively) compared to upstream of the vegetation. At approximately 0.05 m from the bed, the obstruction caused by the canopy rapidly decreased velocities within and downstream of the vegetation to just 5-20% of the upstream velocity mid-bank on the 30° bank-toe. Though similar results were observed for the 30° and 15° bank-toes, velocity below the canopy fluctuated more sharply and with greater magnitude for the 30° bank-toe.

Increased flow along the boundary of the bank-toe led to increased boundary velocities at the interface and main channel (Figure 4.4). The lower half of main channel velocity profiles within and downstream of the vegetated patch were > 2 times that of the upstream velocity profiles. The observed reversal in main channel velocity upstream of the vegetation when there was a 15° bank-toe could be due to an abnormally high velocity measured near the bed or a sampling problem related to that near-bed measurement. Main channel velocities were similar nearer to the surface of the water. Elevated velocities within and downstream of the vegetated patch were also observed at the interface and decreased with increasing distance from the bed. Thus, velocities within and downstream of the vegetated patch were lower than those upstream after 1/3 of flow depth.

Changes in velocity along the bed may indicate the presence of a mixing layer, similar to what would develop above a submerged canopy. τ_{uw} below the canopy was 2-5 times greater than upstream on the 15° bank-toe, but τ_{uw} below the canopy was substantially lower than upstream on the 30° bank-toe (Figure 4.5). On the 30° bank-toe, τ_{uw} had stresses up to 82 Pa when upstream of the vegetation and was < 1 Pa within and downstream of the vegetation. On both bank-toes, τ_{uw} was generally < 1 Pa, fluctuating between sediment transport (positive) and inward and outward interactions (negative). High τ_{uw} results were likely observed because velocity was averaged over a very small flow depth. Though the high τ_{uw} may not be an accurate estimate of applied shear stress, it may assist in identifying where in the water column spiking may occur.

At the interface and in the main channel, τ_{uw} fluctuations increased throughout the velocity profile when vegetation was adjacent or upstream (Figure 4.5). This suggests greater mixing is occurring even after water has emerged downstream of the vegetated patch. Additionally, larger increases in τ_{uw} were observed near the boundary than the rest of the profile, despite elevated velocities throughout all or substantial parts of the velocity profile (Figure 4.4). Increases in the magnitude of τ_{uw} at the boundary in the main channel and the interface may result in increased shearing forces on the bed adjacent to and downstream of a vegetated patch.

Flow on the bed

Counterclockwise flow rotation formed longitudinally along the bank-toe boundary when no vegetation was present, but once vegetation was introduced, clockwise rotation formed along the bottom of the bank-toe and more flow moved in and out of the near-boundary flow plane across the bank-toe boundary (Figure 4.6a). In the main channel, flow reversed direction from counter-clockwise to clockwise flow, with less flux of flow in and out of the boundary plane. At the top of the bank-toe, flow moved into the plane, which is especially evident when looking at the dominant tensors (Figure 4.6b). The dominant presence of white across the entire channel cross-section, with and without vegetation, indicates that mixing and energy dissipation was a dominant action across the entire boundary.

Without vegetation, counterclockwise flow was faster on the bank-toe than the mixing that was occurring in the main channel (Figure 4.6c). With vegetation, clockwise flow along the bottom of the bank-toe and in the main channel were the most intense flow features. Though some indication of counterclockwise flow on the bank-toe remained when no leaves were present, the two vegetation densities had fairly similar boundary velocity patterns. Mixing that occurred on the unvegetated bank-toe was less extensive than on the vegetated bank-toe.

Turbulence intensity in the channel

Turbulence intensity (RMS), which indicates erosion potential, increased along the bottom of the bank-toe when vegetation was present on the bank-toe. On the bottom of the bank-toe, the area most sensitive to erosion, RMS increased up to 5 times over the unvegetated case when leafy vegetation was present on the bank-toe and discharge was high (Figure 4.7). On the top half of the bank-toe when vegetation was present, RMS generally decreased by 0-40% from the unvegetated case, but also increased by 100-140% at specific locations for LD_{lo}, LD_{hi} and D_{hi}.

Results are similar for other discharges, though the magnitude of RMS values was less. At lower discharge and with LD_{hi}, the peak of $RMS_{u,v,w}$ shifted from the main channel-bank-toe interface to the bottom of the bank-toe, within the vegetation. RMS for LD_{hi} in the main channel remained elevated, though was not as high as LD_{lo}.

Overall, downstream turbulence intensity (RMS_u) was 0.8 less up to 2.1 times greater than lateral turbulence intensity (RMS_v), and 2.2 to 5.1 times greater than vertical turbulence intensity (RMS_w). This indicates the strength of downstream flow velocities on the boundary is greater in comparison to the lateral and vertical velocities. RMS results were fairly similar for the 30° and 15° bank-toes, except for that the magnitude for the 15° bank-toe of turbulence intensity was up to 30% lower along the interface.

Turbulence intensity was higher for vegetation with leaves than for vegetation without leaves. Over the unvegetated case, RMS_u, RMS_v, and RMS_w increased 400 – 500% along the interface of the 30° bank-toe when leaves were present and 75 – 200% without leaves. A similar result was true for the 15° bank-toe, where RMS increased 130 – 310% with leaves and 70 – 140% without leaves. Thus, leaves may introduce more potential for erosion.

Shearing forces in the channel

Examination of three-dimension stresses, τ_{TKE}, demonstrated that with an increase in vegetation there was an increase in shear stress along the bottom of the bank-toe. Without vegetation, τ_{TKE} was fairly uniform along the bank-toe and bed of the

unvegetated channel, ranging from 0.08-0.16 Pa for the 15° bank-toe and 0.06 to 0.20 Pa for the 30° bank-toe (Figure 4.8). As vegetation density increased on the bank-toe, τ_{TKE} increased 5-10 times the unvegetated case along the bottom 25% of the bank-toe. In the interface, turbulent shear increased 10-fold and 5-fold over the unvegetated case with the presence of the 30° and 15° bank-toe, respectively. For example, τ_{TKE} increased from 0.12 Pa for the unvegetated case to 2.49 Pa when LD_{hi} along the interface when discharge was high. Additionally, with vegetation, τ_{TKE} increased by 2-4 times on the 30° bank-toe and was slightly lower than the unvegetated case on the 15° bank-toe. The same results were observed at lower discharges, though τ_{TKE} was nearly an order of magnitude lower.

With the presence of leaves (i.e. LD_{lo} and LD_{hi}), turbulent stress increased by the greatest magnitude, especially on the 30° bank-toe (Figure 4.8). The leafy vegetation increased τ_{TKE} by 10-20 times the unvegetated case on the 30° bank-toe, when discharge was high, whereas on the 15° bank-toe τ_{TKE} increased by 3-8 times. When no leaves were present the magnitude of τ_{TKE} was lower, but still greater than the unvegetated case for the 30° bank-toe.

When vegetation was present on the 30° bank-toe, vertical stress (τ_{uw}) dominated on the bank-toe and lateral stress (τ_{uv}) dominated in the main channel outside of the vegetated patch. Within the vegetated bank-toe, when Q_{hi}, τ_{uw} for LD_{hi} was 45% higher than τ_{uv}, and 75% higher along the interface within the vegetation. Just outside of the vegetation τ_{uv} was 70% higher than τ_{uw} in the interface. Without vegetation, τ_{uv} dominated along the entire cross-section, approximately 75% higher than τ_{uw}. This suggests lateral momentum exchange occurred between the main channel and bank-toe when vegetation was present, and vertical stresses associated with sediment transport were dominant on the bank-toe, especially along the interface.

Results on the 15° bank-toe were not consistent with those found on the 30° bank-toe. Though τ_{uv} was also approximately 95% higher than τ_{uw} just outside of the vegetated patch in the main channel, τ_{uv} was also dominant at the bottom of the bank-toe and intermittently on the bank-toe. Also τ_{uw} was just as significant on the unvegetated bank-toe as it was with vegetation present (35-75% and 30-70% greater than τ_{uv}, respectively).

Vertical stress analysis indicates decreased potential for sediment transport on the bank-toe and increased sediment transport in the main channel with the introduction of vegetation (Figure 4.9). Without vegetation, τ_{uw} was generally positive (0-0.05 Pa) on both the bank-toe and in the main channel. Once vegetation was introduced, τ_{uw} was negative on the bank-toe, with an increase in intensity at the bottom of the bank-toe dependent on vegetation density. In the main channel, positive τ_{uw} increased with increasing vegetation density. Some small pockets of higher positive τ_{uw} were observed on the bank-toe regardless of vegetation density. Positive τ_{uw} in the main channel and on pockets on the bank-toe suggest the occurrence of ejection and sweep events along the boundary. Results from both bank-toe angles were similar except that, compared to the 30° bank-toe, the 15° bank-toe had a lower magnitude of increase in stress with increasing vegetation density. Results were also similar by discharge, just of a lower magnitude.

Quadrant analysis was used to explore the frequency of possible sediment transport opportunities and directionality of stresses. Overall, flow was directed downward 50% of the time and upward 50% of the time. When τ_{uw} was positive, approximately 30% of the time u'w' was correlated with sweep events and 30% of the time with ejection events. The remaining 40% of the time, u'w' was correlated with outward and inward interactions. When τ_{uw} was negative, the opposite relationship was observed. This suggests that when vegetation is present, a larger proportion of the sediment transport events occur in the main channel, but that sediment transport may still occur within the vegetated bank-toe. There are a higher proportion of sediment transport events on the bank-toe when it is unvegetated.

Discussion

Resulting boundary shear stress values supported bulk shear estimations that overall shear stress decreased, but also show that turbulence and stress increased at sensitive locations along the interface between the bank-toe and main channel. It is likely that the bulk estimates of shear stress indicated a decrease in shear stress in vegetated

channels because of the large percentage of the channel covered in vegetation, where stresses decreased. Even though the localized stresses on the bank-toe boundary largely decreased, shear stress did increase in the interface and main channel due to increased turbulence and velocity around the vegetated patch.

Erosion potential on or near bank

Erosion is related to the development of turbulence structures (Lavelle and Mofjeld 1987; Diplas et al. 2008) which can be created by vegetation. In this study, flow approaching the vegetated bank-toe was directed into the interstitial spaces between the leaves, inducing mixing and creating a turbulent structure within and surrounding the vegetation. Turbulence propagated into the interface between the vegetated bank-toe and the main channel, and when a canopy was present, was also directed beneath the canopy.

For the leafy vegetation cases, turbulence introduced by water entering and exiting the canopy created a flow structure below the canopy similar what develops above a submerged canopy (e.g. Nikora 2009). Because flow was highly turbulent and higher velocity, there was an increased magnitude of forces at the bottom of and underneath the canopy along the boundary (Figure 4.5). This increase in velocity has been observed in other studies (Freeman et al. 2000; Yang et al. 2007; Liu et al. 2008; Hopkinson and Wynn 2009) and may cause scour around the base of plants (Bendix and Hupp 2000; Freeman et al. 2000). The velocity increase below the canopy may be partly attributed to velocity spiking caused by a horseshoe or junction vortex at the base of the stem (Liu et al. 2008), though the effect of velocity spiking was likely either masked or magnified by the presence of the canopy.

Results from tensor visualization indicate that regardless of the presence of a canopy, the introduction of vegetation altered the directionality of flow structures, possibly reducing sediment transport potential (Figure 4.6). Counterclockwise flow may be caused by instabilities associated with the inflection point above a velocity spike, creating instabilities in flow, causing it to fold and create coherent structures (Liu et al. 2008). Without vegetation, on the bank-toe and in the transition to the main channel,

there was an increase in velocity followed by a decrease in velocity within the lower 0.1 m of flow depth. Higher velocity may have mixed with the lower velocity flow above, creating counterclockwise vortices that rolled and pushed the high velocity further away from the bed (Liu et al. 2008). In combination with results showing higher shear stress on the unvegetated bank-toe than the vegetated bank-toe, this suggests that flow moving away from the bank-toe boundary could entrain and transport sediment. Once vegetation was introduced, boundary flow patterns were interrupted and counterclockwise vorticity was reduced, suggesting a decrease in erosion potential.

Observed increases in shear stress adjacent to the vegetated patch are supported by previous findings (Thornton et al. 2000; Gorrick 2009; Hopkinson and Wynn 2009). In this study, we found that not only did the area adjacent to the vegetated patch have increased shear, but the interface between the main channel and vegetated patch also experienced higher turbulence and increased velocities, inducing higher τ_{TKE}. The shear layer just outside of the vegetated patch was especially turbulent, as found in previous studies (White and Nepf 2008; Hopkinson and Wynn 2009). Visualization of clockwise flow in the main channel could indicate flow separation downstream of stems and a potential source of the increased turbulence. Turbulent shear stress and turbulence intensity also increased along the interface and main channel, especially when a canopy was present to encourage more turbulent flow.

Sweep events (u'>0, w'<0) are associated with erosion (Buffin-Belanger and Roy 1998) and in this study were primarily found in the main channel. Considering that turbulence creates instantaneous forces that are greater than time-averaged values (Lavelle and Mofjeld 1987; Nelson et al. 1993; McLean et al. 1994; Roy et al. 1999) and due to the directionality of velocities attributed to Quadrant III events (u'<0, w'<0), we suspect critical entrainment could occur with Quadrant III events if the events are significantly greater than average positive τ_{uw} events or if the events are of sufficient duration in time to accomplish dislodgement (Diplas et al. 2008). Quadrant III events observed on the bottom of the bank-toe when vegetation densities were highest were

double that of positive τ_{uw} events. Further experimentation would be necessary to confirm this theory.

Sediment eroded from the bank-toe-main channel interface may be deposited on the bank-toe. Zong and Nepf (2010) found sediment depositing on a flat vegetated bank along the length of the vegetated patch in a wedge that grew in proportion to the length of the vegetated patch. Sediment may be deposited on to the vegetated bank due to the activity in the turbulent shear layer (White and Nepf 2008; Zong and Nepf 2010), and in this study the turbulent interface increased in turbulence intensity with increasing vegetation density. The increase in turbulence intensity is due in part to the high velocity in the main channel being directed back to the vegetated bank-toe. Evidence of the directionality of flow from main channel into the vegetated patch supports the possibility that sediment could be entrained in the flow due to high shear stresses and positive τ_{uw} in the main channel and deposited on the bank-toe where velocities decrease substantially and flow is directed into the bank-toe. Unmeasured observations of deposition downstream of stems support the theory that deposition can occur on the bank-toe.

Role of vegetation density and blockage area

Vegetation density may be the most important parameter in characterizing turbulent stresses in the channel. In our study, increases in vegetation density promoted increases in turbulence and stress, especially along the bottom of the bank-toe. Though previous studies have shown that small increases in density may increase turbulence within the vegetated patch (Nepf 1999), we observed reductions in turbulence within the vegetation. This is likely due to the increase in competition between reduced velocity and increased turbulence leading to small changes in turbulence on the bank (Nepf 1999). Therefore, after a certain threshold of vegetation density, turbulence within the vegetation decreases. This study illustrated that although turbulence decreased on the bank-toe with increasing vegetation density due to decreasing velocities, turbulence increased at the interface and in the main channel due to increased mixing.

Presence of additional roughness due to leaves and plant canopy are important influences on turbulent stress. Turbulence, and thus stresses due to turbulence, increased most when a canopy was present generating more turbulent flow. Though it is difficult to discern differences in total vegetation density and the effect of leaves, differences in turbulence intensity and turbulent shear stress between vegetated cases of high density/no leaves (D_{hi}) and low density/no leaves (LD_{lo}) were larger than would be expected based on differences in vegetation density.

Since higher turbulence may increase erosion, results from this study suggest the risk of erosion along the bank-toe-channel interface and in the main channel may increase if plants leaf out prior to a high flow event. For example, increased erosion may occur in a channel where flow is regulated and high flow events happen later in the year, after leaf out and new plants have been established lower on the bank. Patterns of scour on the bank-toe may also change after leaf out occurs. Scour may increase if the high velocities below the canopy are not reduced by some additional increase in boundary roughness. Boundary roughness would also help protect the bank-toe from the increase in turbulence and vertical shear stress observed below the canopy, especially along the bottom of the bank-toe. It is important to note that deposition may also occur due to decreases in velocity, as described above.

The importance of including leaves or other canopy roughness in ecohydraulic experiments is demonstrated in this study. In the field, much of the streambank vegetation consists of small trees, shrubs or grasses (Bendix and Hupp 2000). In studies where vegetation is replicated by rigid dowels, although the stem density may increase, total density would not increase at the same magnitude as if leaves were present. This additional density cannot be replicated by increasing dowel stem density, but instead must replicate elements of natural morphology (e.g. Yang et al. 2007; Hopkinson and Wynn 2009). Studies by individual species may not be necessary, because site-averaged physical parameters may be sufficient measures of plants as resistance elements (Nikora et al. 2008).

Role of bank angle

A key difference between bank-toe angles is the finding that the magnitude of turbulence and stress was always considerably higher for the 30° bank-toe. The difference in magnitude was not observed within the vegetation or on the bank-toe, but at the bottom of the bank-toe and in the main channel, where velocity was higher.

Velocity, thus turbulence and stress, may be greater for the 30° bank-toe because there is greater flow displacement due to the smaller overall cross-section. As the vegetated patch redirects flow around the vegetation and into the main channel, more water is displaced, increasing the velocity in the main channel. This could be enhanced by the design of the flume, where water is instantly diverted from the flow straighteners around the bank-toe insert, both over the surface of the bank-toe (especially lower down the bank-toe) and into the main channel. This could account for the velocity spikes along the bed upstream of the vegetation (Figure 4.4). On the 15° bank-toe, the vegetation may be doing a larger proportion of the work moving water from bank-toe to main channel, because less water is diverted around the bank-toe insert.

Conclusions

Results from this study show that, with an increase in vegetation density, there was an increase in turbulence and turbulent stress observed at the bottom of the bank-toe and in the main channel. Increases in turbulent stresses are related to increased sediment erosion and deposition in these locations. The presence of leaves increased the turbulent mixing and shear stresses, emphasizing the need to conduct experiments with natural vegetation or artificial vegetation that mimics an increase in canopy roughness. These findings suggest the need to consider vegetation morphology and timing of flood events when planting streambank vegetation to reduce erosion.

Additional research is necessary to track sediment scour and deposition dependent on increases in vegetation density. While beyond the scope of this study, consideration of soil type and the role of vegetation root strength, how they influence critical shear stress on the bank, will be important in better understanding erosion potential and streambank

failure. Insights from tensor visualization analysis could be useful in understanding flow around roughness elements. It is a new tool and more research is necessary to fully understand the implications of tensor visualization results.

Acknowledgements

References

Allen, H. H., and Leech, J. R. (1997). "Bioengineering for Streambank Erosion Control; TR EL-97-8." US Army Corps of Engineers, Vicksburg, MS.

Bendix, J., and Hupp, C. R. (2000). "Hydrological and geomorphological impacts on riparian plant communities." *Hydrological Processes*, 14, 2977-2990.

Bennett, S. J., Pirim, T., and Barkdoll, B. D. (2002). "Using simulated emergent vegetation to alter stream flow direction within a straight experimental channel." *Geomorphology*, 44, 115-126.

Bennett, S. J., and Best, J. L. (1995). "Mean flow and turbulence structure over fixed, two-dimensional dunes: implications for sediment transport and bedform stability." *Sedimentology*, 42, 491-513.

Bentrup, G. and Hoag, J.C. (1998). The Practical Streambank Bioengineering Guide. USDA Natural Resources Conservation Service, Plant Materials Center, Aberdeen, Idaho.

Bertram, V. H.-U. (1984). "Uber die hydraulische Berechnung von Gerinnen mit Uferbewuchs." *Z.f. Kulturtechnik und Flurbereinigung*, 25, 77-86.

Biron, P. M., Robson, C., Lapointe, M. F., and Gaskin, S. J. (2004). "Comparing different methods of bed shear stress estimates in simple and complex flow fields." *Earth Surface Processes and Landforms*, 29, 1403-1415.

Buffin-Belanger, T., and Roy, A. G. (1998). "Effects of a pebble cluster on the turbulent structure of a depth-limited flow in a gravel-bed river." *Geomorphology*, 25, 249-267.

Clifford, N.J., and French, J.R. (1993). "Monitoring and modeling turbulent flows: historical and contemporary perspectives." *Turbulence: Perspectives on Flow and Sediment Transport,* N.J. Clifford, J.R. French, and J. Hardisty, eds., Wiley, Chichester, 1-34.

Czarnomski, N.M., Tullos, D., Thomas, R.E. and Simon, A. (in prep). "Streambank velocity and flow patterns when influenced by vegetation density."

Daniels, M.D. and Rhodes, B.L. (2004). "Spatial pattern of turbulence kinetic energy and shear stress in a meander bend with large woody debris." Riparian Vegetation and Fluvial Geomorphology, S.J Bennett and A. Simon, eds., American Geophysical Union, 87-98.

Diplas, P., Dancey, C. L., Celik, A. O., Valyrakis, M., Greer, K., and Akar, T. (2008). "The role of impulse on the initiation of particle movement under turbulent flow conditions." *Science*, 322, 717-720.

Francis, R. A. (2006). "Allogenic and autogenic influences upon riparian vegetation dynamics." *Area*, 38(4), 453-464.

Freeman, G. E., Rahmeyer, W. H., and Copeland, R. R. (2000). "Determination of resistance due to shrubs and woody vegetation." ERDC/CHL TR-00-25, U.S.ACE.

Gorrick, S. "Field and laboratory investigations on the effects of riparian vegetation on stream flow and sediment dynamics." *33rd International Association of Hydraulic Engineering & Research (IAHR) Biennial Congress*, Vancouver, B.C., 8.

Hopkinson, L. (2009). "Chapter 5 - Determining field methods to measure boundary shear stress along hydraulically rough streambanks," Virginia Tech, Blacksburg, VA.

Hopkinson, L., and Wynn, T. (2009). "Vegetation impacts on near bank flow." *Ecohydrology*, online, 1-15.

Kean, J.W. and Smith, J.D. (2004). "Flow and boundary shear stress in channels with woody bank vegetation." Riparian Vegetation and Fluvial Geomorphology, S.J Bennett and A. Simon, eds., American Geophysical Union, 237-252.

Kim, S.-C., Friedrichs, C. T., Maa, J. P.-Y., and Wright, L. D. (2000). "Estimating bottom stress in tidal boundary layer from acoustic doppler velocimeter data." *Journal of Hydraulic Engineering*, 126(6), 399-406.

Lavelle, J. W., and Mofjeld, H. O. (1987). "Do critical stresses for incipient motion and erosion really exist?" *Journal of Hydraulic Engineering*, 113(3), 370-393.

Liu, D., Diplas, P., Fairbanks, J. D., and Hodges, C. C. (2008). "An experimental study of flow through rigid vegetation." *Journal of Geophysical Research*, 113(F04015), 16.

Liu, D., Diplas, P., Hodges, C.C., Fairbanks, J.D. (2010). "Hydrodynamics of flow through double layer rigid vegetation." *Geomorphology*, 116(3-4), 286-296.

McBride, M., Hession, W. C., Rizzo, D. M., and Thompson, D. M. (2007). "The influence of riparian vegetation on near-bank turbulence: a flume experiment." *Earth Surf. Proc. Landf.*, 32(13), 2019-2037.

McLean, S. R., Nelson, J. M., and Wolfe, S. R. (1994). "Turbulence structure over two-dimensional bed forms: implications for sediment transport." *Journal of Geophysical Research*, 99(C6), 12729-12747.

Nelson, J. M., McLean, S. R., and Wolfe, S. R. (1993). "Mean flow and turbulence fields over two-dimensional bed forms." *Water Resources Research*, 29(12), 3935-3953.

Nepf, H. M. (1999). "Drag, turbulence, and diffusion in flow through emergent vegetation." *Water Res. Research.*, 35(2), 479-489.

Nikora, V., Larned, S., Nikora, N., Debnath, K., Cooper, G., and Reid, M. (2008). "Hydraulic resistance due to aquatic vegetation in small streams: field study." *Journal of Hydraulic Engineering*, 134(9), 1326-1332.

Nikora, V. (2009). "Hydrodynamics of aquatic ecosystems: an interface between ecology, biomechanics and environmental fluid mechanics." *River Research and Applications*, online, 18.

Pope, N. D., Widdows, J., and Brinsley, M. D. (2006). "Estimation of bed shear stress using the turbulent kinetic energy approach – a comparison of annular flume and field data." *Continental Shelf Research*, 26, 959-970.

Robert, A. (2003). River Processes: An Introduction to Fluvial Dynamics. Oxford University Press, New York.

Roy, A. G., Biron, P. M., Buffin-Belanger, T., and Levasseur, M. (1999). "Combined visual and quantitative techniques in the study of natural turbulent flows." *Water Resources Research*, 35(3), 871-877.

Thompson, A. M., Wilson, B. N., and Hansen, B. J. (2004). "Shear stress partitioning for idealized vegetated surfaces." *Transactions of the American Society of Agricultural Engineers*, 47(3), 701-709.

Thornton, C. I., Abt, S. R., Morris, C. E., and Fischenich, J. C. (2000). "Calculating shear stress at channel-overbank interfaces in straight channels with vegetated floodplains." *Journal of Hydraulic Engineering*, 126(12), 929-936.

Wahl, T. (2009). WinADV Version 2.027. U.S. Bureau of Reclamation, Water Resources Research Laboratory.

White, B. L., and Nepf, H. M. (2008). "A vortex-based model of velocity and shear stress in a partially vegetated shallow channel." *Water Resources Research*, 44(W01412), 15.

Wilson, C. A. M. E., Yagci, O., Rauch, H.-P., and Stoesser, T. (2006). "Application of the drag force approach to model the flow-interaction of natural vegetation." *Int. J. River Basin Mgmt.*, 4(2), 137-146.

Yang, K., Cao, S., and Knight, D. W. (2007). "Flow patterns in compound channels with vegetated floodplains." *Journal of Hydraulic Engineering*, 133(2), 148-159.

Zhang, E., Yeh, H., Lin, Z., and Laramee, R. S. (2009). "Asymmetric tensor analysis for flow visualization." *IEEE Transactions on Visualization and Computer Graphics*, 15(1), 106-122.

Zong, L., and Nepf, H. M. (2010). "Flow and deposition in and around a finite patch of vegetation." *Geomorphology*, 116(3-4), 363-372.
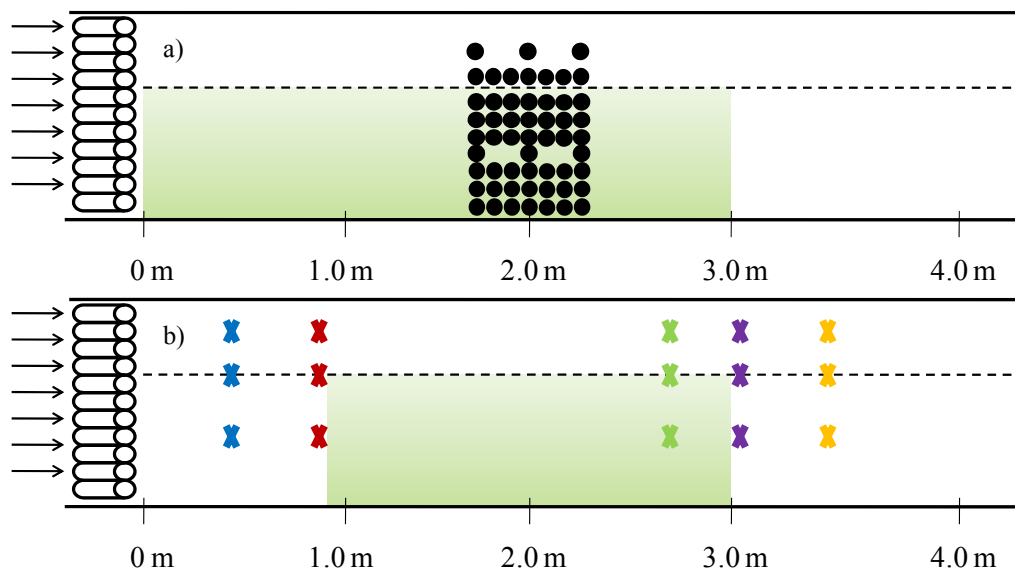
Figure 4.1. Planform view of flume; arrows indicate direction of flow, shaded region shows location of vegetation array. a) O's represent locations of boundary measurements. b) X's represent locations of velocity profiles measured on 30° bank-toe when vegetation pattern LD_{hi} and $Q = 0.05$ m^3/s; colors correspond to Figure 4.4 and Figure 4.5. Flume not drawn to scale.
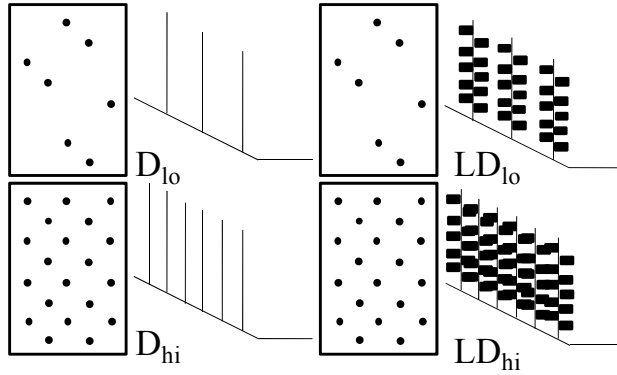
Figure 4.2. Experimental design. D_{lo} is low density, no leaves; D_{hi} is high density, no leaves; LD_{lo} is low density, with leaves; and LD_{hi} is high density, with leaves.

Table 4.1. Vegetation density (m^2/m^2) for each run with vegetation at the 2.0 m cross-section. D_{lo}, D_{hi}, LD_{lo} and LD_{hi} are defined in Figure 4.2.

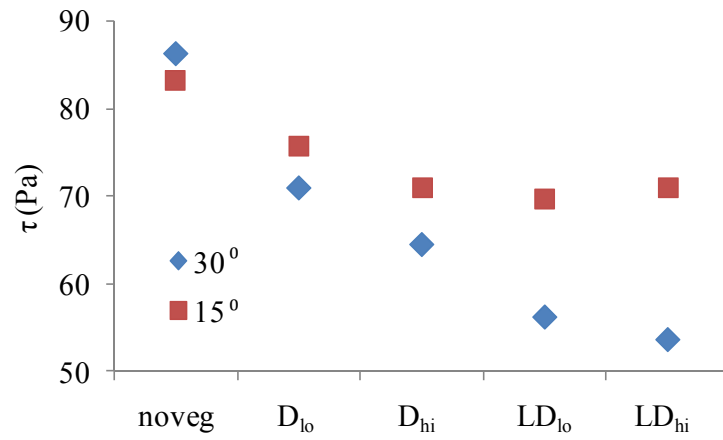| Case		30° Bank-toe	15° Bank-toe
Q_{lo}	D_{lo}	0.041	0.036
Q_{lo}	D_{hi}	0.124	0.096
Q_{lo}	LD_{lo}	0.236	0.185
Q_{lo}	LD_{hi}	0.714	0.559
Q_{med}	D_{lo}	0.040	0.036
Q_{med}	D_{hi}	0.122	0.095
Q_{med}	LD_{lo}	0.224	0.181
Q_{med}	LD_{hi}	0.701	0.546
Q_{hi}	D_{lo}	0.040	0.036
Q_{hi}	D_{hi}	0.123	0.095
Q_{hi}	LD_{lo}	0.229	0.174
Q_{hi}	LD_{hi}	0.695	0.527

Figure 4.3. Bulk shear stress estimates scaled to prototype channel when Q_{hi} (0.05 m^3 s^{-1}). D_{lo}, D_{hi}, LD_{lo} and LD_{hi} are defined in Figure 4.2.
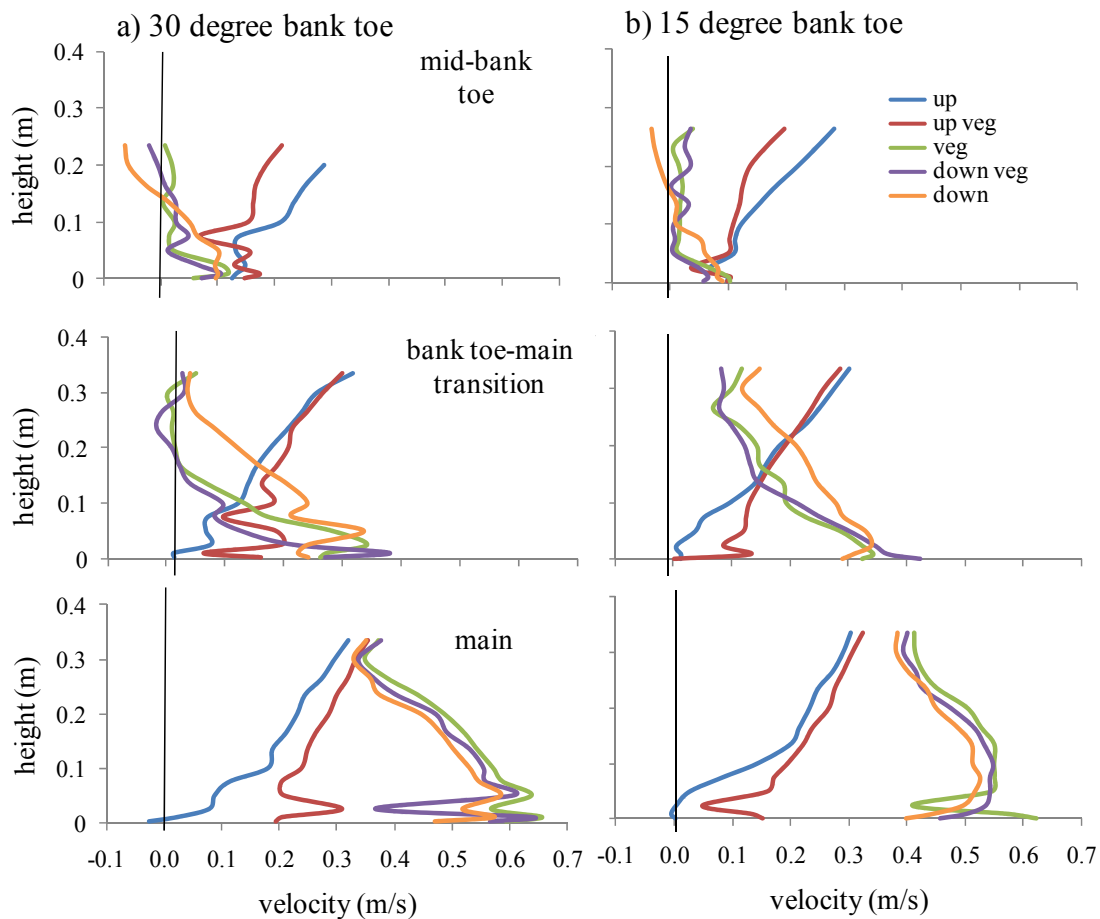
Figure 4.4. Velocity profiles. Legend refers to sampling locations along the length of the channel in reference to the vegetated patch. See Figure 4.1b for a description of sampling locations.

Figure 4.5. τ_{uw} profiles. Legend refers to sampling locations along the length of the channel in reference to the vegetated patch. See Figure 4.1b for a description of sampling locations.
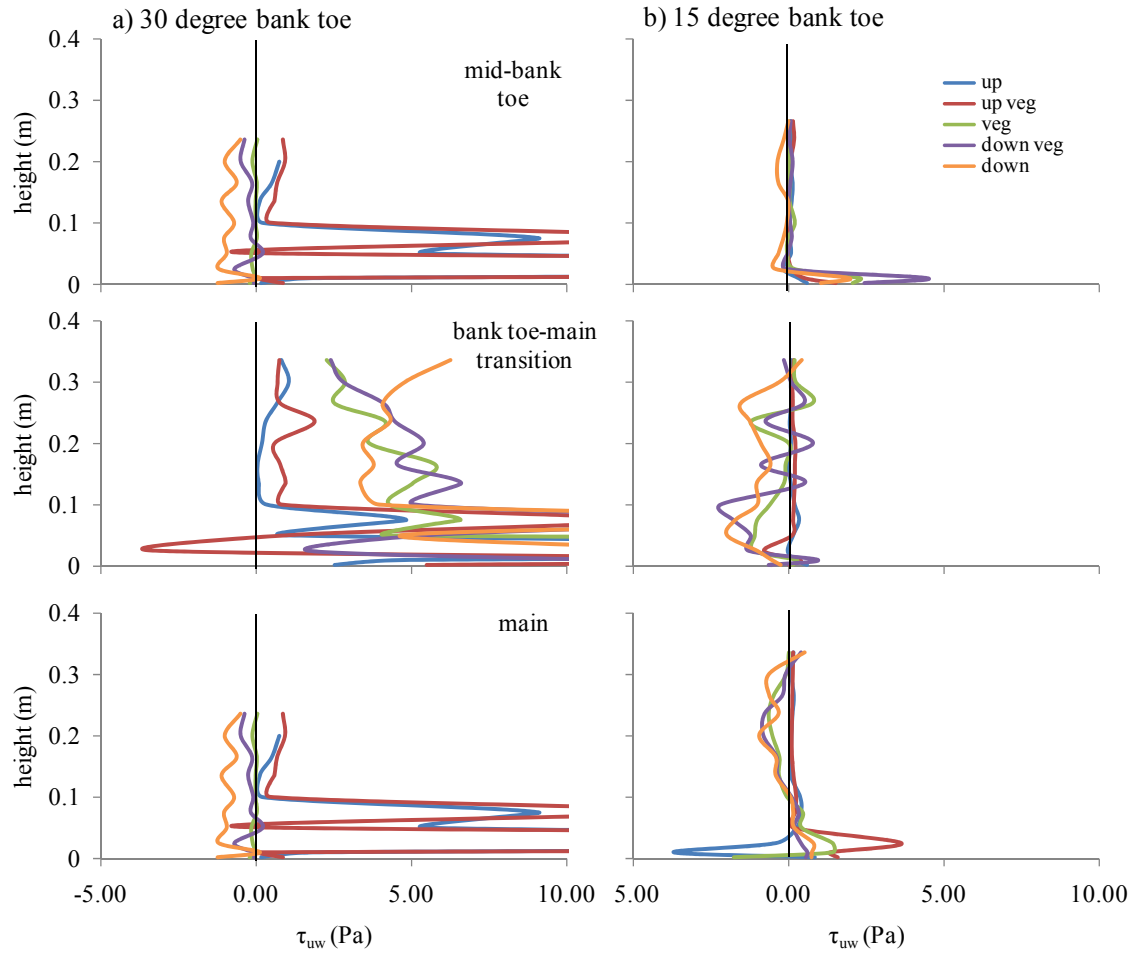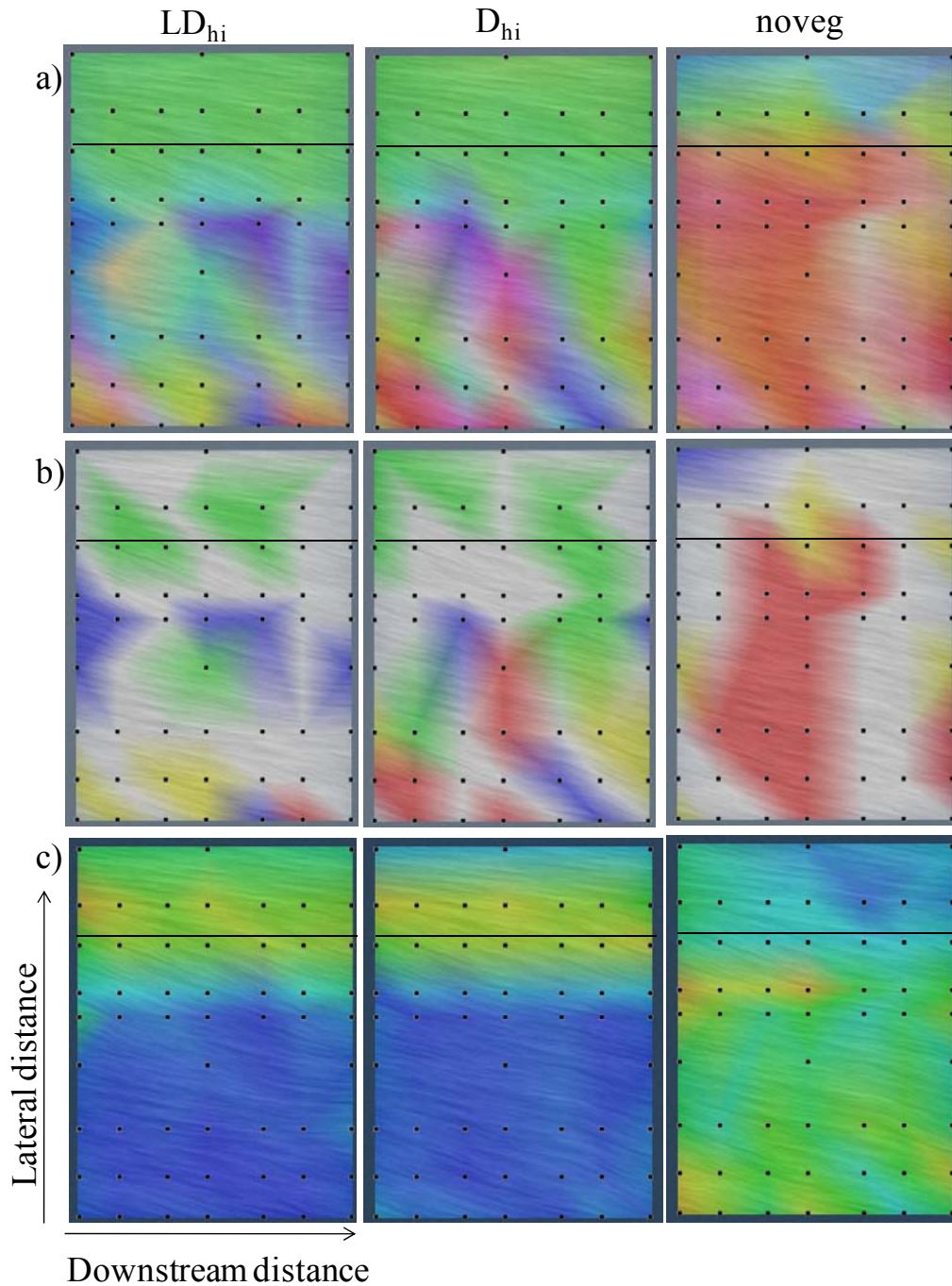
Figure 4.6. Near-boundary velocity tensor visualizations showing vorticity and flow directionality. Plots represent a channel cross-section from 1.8 m to 2.3 m for the 30° bank-toe at Q_{hi}, where the line represents the interface between the bank-toe and main channel. a) all, b) dominant, and c) magnitude. See methods for explanation of color designations. D_{hi} and LD_{hi} are defined in Figure 4.2.
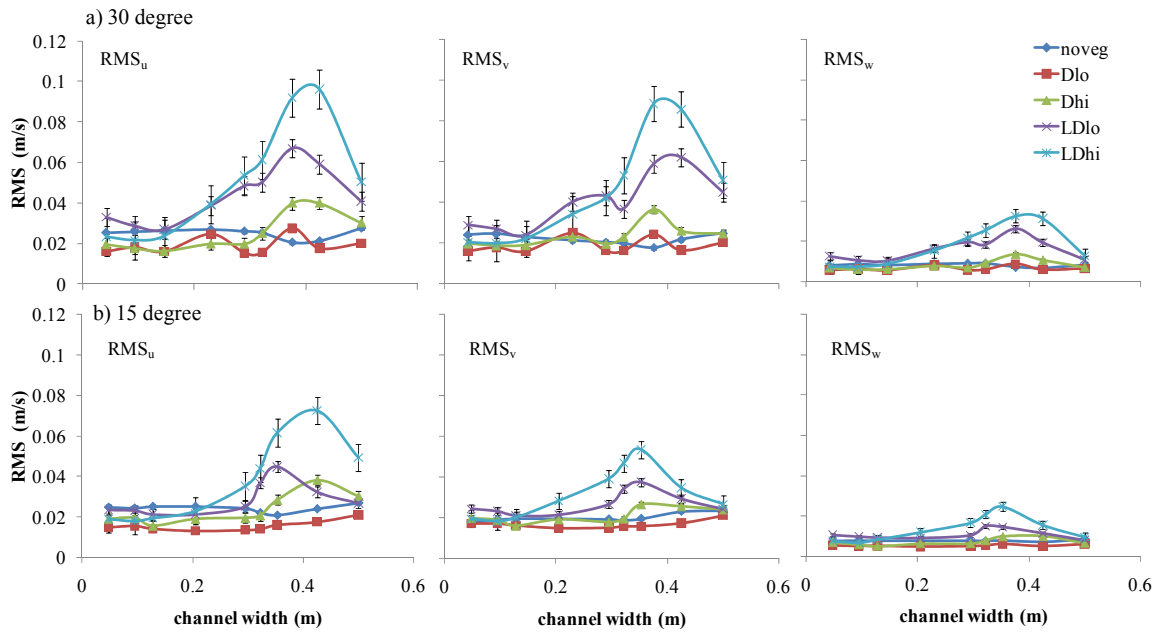
Figure 4.7. RMS in the u, v, and w directions along a cross-section when Q_{hi} for the a) 30° and b) 15° bank-toes. D_{lo}, D_{hi}, LD_{lo} and LD_{hi} are defined in Figure 4.2.
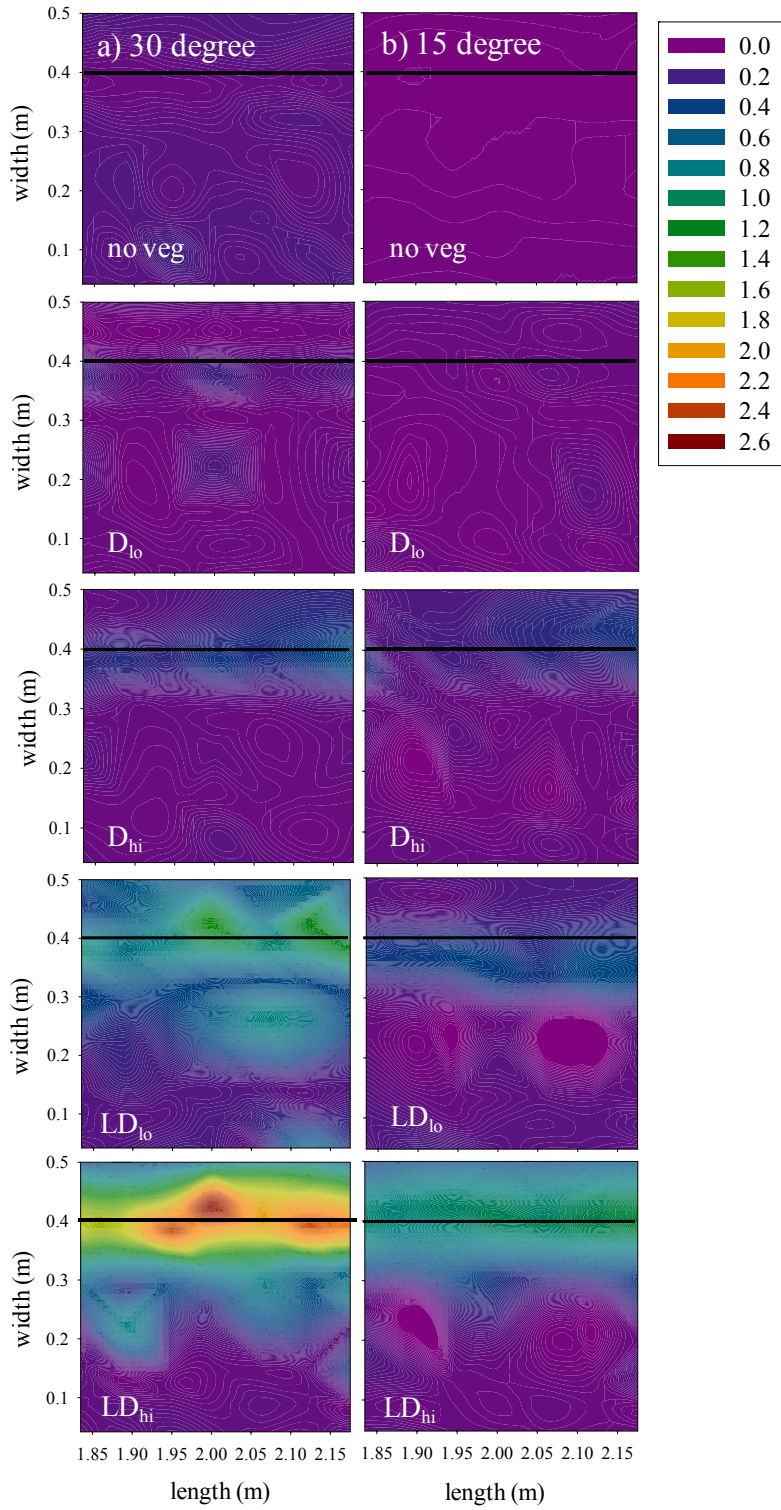
Figure 4.8. τ_{TKE} for cross-sectional channel area for the a) 30° and b) 15° bank-toes. D_{lo}, D_{hi}, LD_{lo} and LD_{hi} are defined in Figure 4.2.
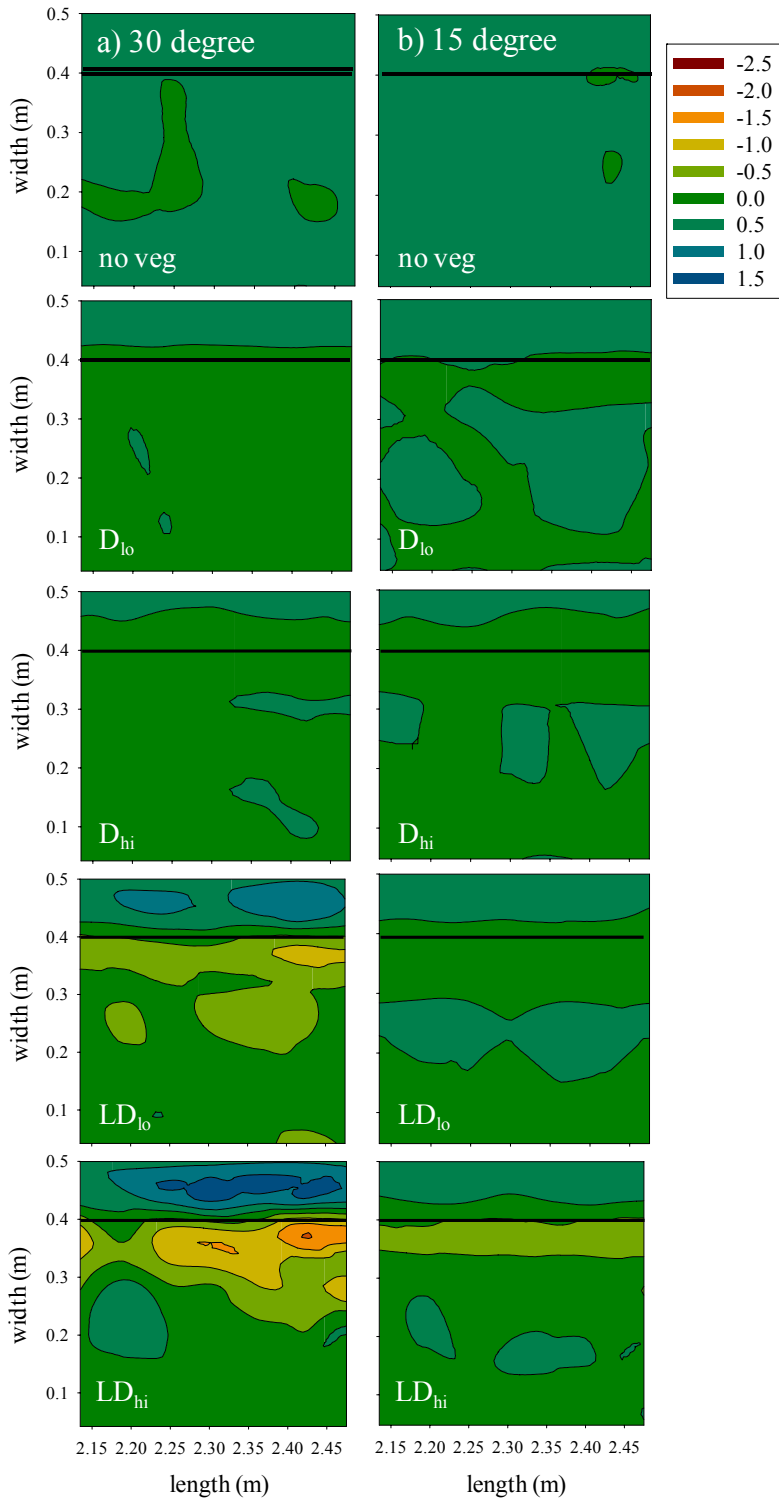
Figure 4.9. τ_{uw} for Q_{hi} for the a) 30° and b) 15° bank-toes. D_{lo}, D_{hi}, LD_{lo} and LD_{hi} are defined in Figure 4.2.

CHAPTER 5. CONCLUSIONS

Understanding the role of vegetation on streambank hydraulics is important in modeling flow dynamics, flood conditions, and characterizing the influence of restoration activities. This research has demonstrated that when vegetation is present on a bank-toe, velocity and forces are reduced on the majority of the bank-toe because of the increase in resistance. High velocity and forces on the bank-toe are shifted into the interface between vegetation and the open channel and into the open channel.

Increases in vegetation density led to significant reductions in bank-toe velocity, increases in main channel velocity, increases in drag, and increases in turbulence and shear stress along the interface between the vegetation and main channel. Water surface elevations within the vegetated patch also increased with increasing density. When vegetation density was very high, a large-scale eddy formed downstream of the vegetated patch. Although the changes in channel hydraulics can be assessed based on vegetation density, canopy structure (i.e. the presence or absence of leaves) may also be influential.

The importance of canopy structure was most evident when calculating resistance coefficients and in the development of turbulence within and around the vegetated patch. It is possible that at a higher densities, which is often observed when leaves are present, vegetation alters flow conditions within the vegetated patch to such an extent that commonly used methods for calculating resistance no longer apply. In this study, the presence of leaves increased the turbulent mixing and shear stresses, emphasizing the need to conduct experiments with natural vegetation or artificial vegetation that mimics an increase in canopy roughness. These findings suggest the need to consider vegetation morphology and timing of flood events when planting streambank vegetation to reduce erosion.

Blockage of flow by vegetation was more influential than bank-toe angle. Flow patterns and locations of turbulence and higher shear stress were roughly similar regardless of bank-toe angle. Although vegetation density was the primary factor in

changing channel velocity and forces, for a given vegetation density, the magnitude of the resulting velocities and forces frequently differed by bank-toe angle.

Additional research could improve understanding of how vegetation density influences streambank hydraulics. There are several key areas where we should focus attention:

1) Calculation of resistance coefficients – It was clear that with dense vegetation, velocity and stem Reynolds number were low, and resistance coefficients were difficult to estimate. Further studies should be conducted to explore velocities within vegetated patches of varying densities, the relationship between low Re_d and vegetation density, and how biomechanical properties of plants such as flexibility, morphology, and leaves, affect vegetation densities.

2) Turbulence, shear stress, and sediment transport – Turbulent flow and shear stress increased with increasing vegetation density along the interface of vegetation and the open channel. More study is necessary to understand where sediment is being eroded from, how far it is transported, and where it is being deposited in relation to individual stems within the vegetated patch. To characterize erosion potential at the scale of a vegetated patch, consideration must be made for soil type and the role of vegetation root strength and how they influence critical shear stress on the bank.

3) New analysis tools – The relationship between vegetation and hydraulics is complicated to observe. Insights from visualization analysis could be useful in understanding flow around vegetation elements and through vegetated patches.

4) Natural vegetation and plant community structure – In future studies, it is important to include a broader spectrum of vegetation and plant community types, such as leafy canopies, random stem patterns and mixed plant morphologies. A better characterization of vegetation from the perspective of a fluid particle may assist in arriving at more accurate estimations of vegetation density and blockage.

5) Field studies – Development and refinement of field methods for obtaining vegetation density data and inclusion of more field studies are important steps to building a stronger framework for characterizing vegetation in river and stream hydraulics.

BIBLIOGRAPHY

Allen, H. H., and Leech, J. R. (1997). "Bioengineering for Streambank Erosion Control; TR EL-97-8." US Army Corps of Engineers, Vicksburg, MS.

Barnes, H. H. (1967). "Roughness characteristics of natural channels." US Geological Survey Water-Supply Paper 1849, Denver, CO.

Bendix, J., and Hupp, C. R. (2000). "Hydrological and geomorphological impacts on riparian plant communities." *Hydrological Processes*, 14, 2977-2990.

Bennett, S. J., and Best, J. L. (1995). "Mean flow and turbulence structure over fixed, two-dimensional dunes: implications for sediment transport and bedform stability." *Sedimentology*, 42, 491-513.

Bennett, S. J., Bridge, J. S., and Best, J. L. (1998). "The fluid and sediment dynamics of upper-stage plane beds." *Journal of Geophysical Research*, 103(C1), 1239-1274.

Bennett, S. J., Pirim, T., and Barkdoll, B. D. (2002). "Using simulated emergent vegetation to alter stream flow direction within a straight experimental channel." *Geomorphology*, 44, 115-126.

Bentrup, G. and Hoag, J.C. (1998). The Practical Streambank Bioengineering Guide. USDA Natural Resources Conservation Service, Plant Materials Center, Aberdeen, Idaho.

Bertram, V. H.-U. (1984). "Uber die hydraulische Berechnung von Gerinnen mit Uferbewuchs." *Z.f. Kulturtechnik und Flurbereinigung*, 25, 77-86.

Biron, P. M., Robson, C., Lapointe, M. F., and Gaskin, S. J. (2004). "Comparing different methods of bed shear stress estimates in simple and complex flow fields." *Earth Surface Processes and Landforms*, 29, 1403-1415.

Blevins, R. (1994). Flow-Induced Vibration, Krieger, Malabar, Fla.

Blevins, R. D. (2005). "Forces on and stability of a cylinder in a wake." *J. Offshore Mech. Arct. Eng.*, 127(1), 39–45.

Bokaian, A., and Geoola, F. (1984). "Wake-induced galloping of two interfering circular cylinders." *J. Fluid Mech.,* 146, 383–415.

Bridge, J.S. (2003). Rivers and floodplains: forms, processes, and sedimentary record. Blackwell Science, Ltd. 551 pp.

Buffin-Belanger, T., and Roy, A. G. (1998). "Effects of a pebble cluster on the turbulent structure of a depth-limited flow in a gravel-bed river." *Geomorphology*, 25, 249-267.

Chow, V. T. 1959. Open Channel Hydraulics. McGraw-Hill, Inc.

Clifford, N.J., and French, J.R. (1993). "Monitoring and modeling turbulent flows: historical and contemporary perspectives." *Turbulence: Perspectives on Flow and Sediment Transport,* N.J. Clifford, J.R. French, and J. Hardisty, eds., Wiley, Chichester, 1-34.

Corenblit, D., Steiger, J., Gurnell, A. M., Tabacchi, E., and Roques, L. (2009). "Control of sediment dynamics by vegetation as a key function driving biogeomorphic succession within fluvial corridors." *Earth Surface Processes and Landforms*, 34, 1790-1810.

Cowan, W.L. (1956). "Estimating hydraulic roughness coefficients." *Agric. Eng.*, 37, 473-475.

Czarnomski, N.M., Tullos, D., Thomas, R.E. and Simon, A. (in prep). "Streambank velocity and flow patterns when influenced by vegetation density."

Czarnomski, N.M. (in prep). Influence of Vegetation on Streambank Hydraulics. PhD dissertation, Oregon State University, Corvallis.

Czarnomski, N.M., Tullos, D., Thomas, R.E., Simon A., Palacios, J. and Zhang E. (in prep). "Shear stress and turbulence along a streambank due to changes in vegetation canopy density and bank angle."

Daniels, M.D. and Rhodes, B.L. (2004). "Spatial pattern of turbulence kinetic energy and shear stress in a meander bend with large woody debris." Riparian Vegetation and Fluvial Geomorphology, S.J Bennett and A. Simon, eds., American Geophysical Union, 87-98.

Diplas, P., Dancey, C. L., Celik, A. O., Valyrakis, M., Greer, K., and Akar, T. (2008). "The role of impulse on the initiation of particle movement under turbulent flow conditions." *Science*, 322, 717-720.

Dudley, S. J., Bonham, C. D., Abt, S. R., and Fischenich, J. C. (1998). "Comparison of methods for measuring woody riparian vegetation density." *Journal of Arid Environments*, 38, 77-86.

Fathi-Moghadam, M., and Kouwen, N. (1997). "Nonrigid, nonsubmerged, vegetative roughness on floodplains." *J. Hydr. Engr.*, 123(1), 51-57.

Fischenich, J. C. (2000). "Resistance due to vegetation." USAE Waterways Experiment Station, Vicksburg, MS.

Fischenich, J. C., and Dudley, S. (1999). "Determining drag coefficients and area for vegetation." U.S. Army Engineer Research and Development Center, Vicksburg, MS.

Francis, R. A. (2006). "Allogenic and autogenic influences upon riparian vegetation dynamics." *Area*, 38(4), 453-464.

Freeman, G. E., Rahmeyer, W. H., and Copeland, R. R. (2000). "Determination of resistance due to shrubs and woody vegetation." ERDC/CHL TR-00-25, U.S.ACE.

García, M.H., López, F., Dunn, C. and Alonso, C.V. (2004). "Flow, turbulence, and resistance in a flume with simulated vegetation." Riparian Vegetation and Fluvial Geomorphology, S.J Bennett and A. Simon, eds., American Geophysical Union, 11-28.

Gartner, B. L. (1991). "Structural staability and architecture of vines vs. shrubs of poison oak, Toxicodendron diversilobum." *Ecology*, 72(6), 2005-2015.

Gorrick, S. "Field and laboratory investigations on the effects of riparian vegetation on stream flow and sediment dynamics." *33rd International Association of Hydraulic Engineering & Research (IAHR) Biennial Congress*, Vancouver, B.C., 8.

Gurnell, A. M., and Petts, G. (2006). "Trees as riparian engineers: The Tagliamento River, Italy." *Earth Surface Processes and Landforms*, 31, 1558-1574.

Harvey, J. W., Schaffranek, R. W., Noe, G. B., Larsen, L. G., Nowacki, D. J., and O'Connor, B. L. (2009). "Hydroecological factors governing surface water flow on a low-gradient floodplain." *Water Resources Research*, 45(W0342), 20.

Hickin, E.J. (1984). "Vegetation and river channel dynamics." *Can. Geogr.*, 28, 111-126.

Hopkinson, L. (2009). "Chapter 5 - Determining field methods to measure boundary shear stress along hydraulically rough streambanks," Virginia Tech, Blacksburg, VA.

Hopkinson, L., and Wynn, T. (2009). "Vegetation impacts on near bank flow." *Ecohydrology*, online, 1-15.

Huang, H. Q., and Nanson, G. C. (1997). "Vegetation and channel variation; a case study of four small streams in southeastern Australia." *Geomorphology,* 18(3-4), 237-249.

James, C. S., Birkhead, A. L., Jordanova, A. A., and O'Sullivan, J. J. (2004). "Flow resistance of emergent vegetation." *Journal of Hydraulic Research*, 42(4), 390-398.

James, C. S., Goldbeck, U. K., Patini, A., and Jordanova, A. A. (2008). "Influence of foliage on flow resistance of emergent vegetation." *Journal of Hydraulic Research*, 46(4), 536–542.

Järvelä, J. (2002). "Flow resistance of flexible and stiff vegetation: a flume study with natural plants." *J. Hydr.*, 269, 44-54.

Jarvela, J. (2002b). "Determination of flow resistance of vegetated channel banks and floodplains." River Flow, D. Bousmar and Y. Zech, eds., Swets & Zeitlinger, Lisse, 311-318.

Järvelä, J. (2004). "Determination of flow resistance caused by non-submerged woody vegetation." *Int. J. River Basin Mgmt.*, 2(1), 61-70.

Kadlec, R. H. (1990). "Overland flow in wetlands: vegetation resistance." *Journal of Hydraulic Engineering*, 116(5), 691-706.

Kean, J.W. and Smith, J.D. (2004). "Flow and boundary shear stress in channels with woody bank vegetation." Riparian Vegetation and Fluvial Geomorphology, S.J Bennett and A. Simon, eds., American Geophysical Union, 237-252.

Kim, S.-C., Friedrichs, C. T., Maa, J. P.-Y., and Wright, L. D. (2000). "Estimating bottom stress in tidal boundary layer from acoustic doppler velocimeter data." *Journal of Hydraulic Engineering*, 126(6), 399-406.

Knight, D. W., Omran, M., and Tang, X. (2007). "Modeling depth-averaged velocity and boundary shear in trapezoidal channels with secondary flows." *Journal of Hydraulic Engineering*, 133(1), 39-47.

Koch, D. L., and Ladd, A. J. C. (1997). "Moderate Reynolds number flows through periodic and random arrays of aligned cylinders." *Journal of Fluid Mechanics*, 349, 31-66.

Lavelle, J. W., and Mofjeld, H. O. (1987). "Do critical stresses for incipient motion and erosion really exist?" *Journal of Hydraulic Engineering*, 113(3), 370-393.

Lee, J. K., Roig, L. C., Jenter, H. L., and Visser, H. M. (2004). "Drag coefficients for modeling flow through emergent vegetation in the Florida Everglades." *Ecological Engineering*, 22, 237-248.

Li, R. M., and Shen, H. W. (1973). "Effect of tall vegetations on flow and sediment." *J. Hydr. Div., Proc., ASCE*, 99(HY5), 793-814.

Liu, D., Diplas, P., Fairbanks, J. D., and Hodges, C. C. (2008). "An experimental study of flow through rigid vegetation." *Journal of Geophysical Research*, 113(F04015), 16.

Liu, D., Diplas, P., Hodges, C.C., Fairbanks, J.D. (2010). "Hydrodynamics of flow through double layer rigid vegetation." *Geomorphology*, 116(3-4), 286-296.

Lopez, F., and Garcia, M. H. (1998). "Open-channel flow through simulated vegetation: suspended sediment transport modeling." *Water Resources Research*, 34(9), 2341-2352.

Lopez, F., and Garcia, M. H. (2001). "Mean flow and turbulence structure of open-channel flow through non-emergent vegetation." *Journal of Hydraulic Engineering*, 127(5), 392-402.

Luo, S., Gan, T. and Chew, Y. (1996). "Uniform flow past one (or two in tandem) finite length circular cylinder(s)." *J. Wind Eng. Ind. Aerodyn.*, 59, 69–93.

McBride, M., Hession, W. C., Rizzo, D. M., and Thompson, D. M. (2007). "The influence of riparian vegetation on near-bank turbulence: a flume experiment." *Earth Surf. Proc. Landf.,* 32(13), 2019-2037.

McLean, S. R., Nelson, J. M., and Wolfe, S. R. (1994). "Turbulence structure over two-dimensional bed forms: implications for sediment transport." *Journal of Geophysical Research*, 99(C6), 12729-12747.

Mueller, D. S., Abad, J. D., Garcia, C. M., Gartner, J. W., Garcia, M. H., and Oberg, K. A. (2007). "Errors in acoustic doppler profiler velocity measurements caused by flow disturbance." *Journal of Hydraulic Engineering*, 133(12), 1411-1420.

Munson, B., Young, D. and Okiishi, T. (1990). Fundamentals of Fluid Mechanics, John Wiley, New York.

Nelson, J. M., McLean, S. R., and Wolfe, S. R. (1993). "Mean flow and turbulence fields over two-dimensional bed forms." *Water Resources Research*, 29(12), 3935-3953.

Nepf, H. M. (1999). "Drag, turbulence, and diffusion in flow through emergent vegetation." *Water Res. Research.*, 35(2), 479-489.

Niklas, K.J. (1992). *Plant Biomechanics*. University of Chicago Press, Chicago, 607.

Nikora, V. (2009). "Hydrodynamics of aquatic ecosystems: an interface between ecology, biomechanics and environmental fluid mechanics." *River Research and Applications*, online, 18.

Nikora,V., Larned, S., Debnath, K., Cooper, G., Reid, M., Nikora, N. (2006). "Effects of aquatic and bank-side vegetation on hydraulic performance of small streams." *Proceedings of the International Conference on Fluvial Hydraulics River Flow 2006*, v. 1, Taylor and Francis, London, pp. 639-646.

Nikora, N., and Nikora, V. (2007). "A viscous drag concept for flow resistance in vegetated channels." *International Association of Hydraulic Research*, Venice, Italy, 9.

Nikora, V., Larned, S., Nikora, N., Debnath, K., Cooper, G., and Reid, M. (2008). "Hydraulic resistance due to aquatic vegetation in small streams: field study." *Journal of Hydraulic Engineering*, 134(9), 1326-1332.

Pasche, E., and Rouvé, G. (1985). "Overbank flow with vegetatively roughened flood plains." *J. Hydr. Engr.*, 111(9), 1262-1278.

Petryk, S. (1969). Drag on cylinders in open channel flow, Ph.D. thesis, Colo. State Univ., Fort Collins.

Petryk, S., and Bosmajian, G. (1975). "Analysis of flow through vegetation." *J. Hydr. Div., Proc., ASCE*, 101(HY7), 871-884.

Pope, N. D., Widdows, J., and Brinsley, M. D. (2006). "Estimation of bed shear stress using the turbulent kinetic energy approach – a comparison of annular flume and field data." *Continental Shelf Research*, 26, 959-970.

Raupach, M. R. (1992). "Drag and drag partition on rough surfaces." *Boundary-Layer Meterology,* 60(4), 375-395.

Righetti, M., and Armanini, A. (2002). "Flow resistance in open channel flows with sparsely distributed bushes." *Journal of Hydrology*, 269, 55–64.

Robert, A. (2003). River Processes: An Introduction to Fluvial Dynamics. Oxford University Press, New York.

Roy, A. G., Biron, P. M., Buffin-Belanger, T., and Levasseur, M. (1999). "Combined visual and quantitative techniques in the study of natural turbulent flows." *Water Resources Research*, 35(3), 871-877.

Shiono, K., and Knight, D.W. (1991). "Turbulent open-channel flows with variable depth across the cross-section." *J. Fluid Mech.*, 222, 617-646.

Smith C.R. (1996). "Coherent flow structures in smooth-wall turbulent boundary layers: facts, mechanisms, and speculation." Coherent Flow Structures in Open Channels, P.J. Ashworth, S.J. Bennett, J.L. Best, and S.J. McClelland, eds., Wiley, Chichester, 1–39.

Stone, B. M., and Shen, H. T. (2002). "Hydraulic resistance of flow in channels with cylindrical roughness." *Journal of Hydraulic Engineering*, 128(5), 500-506.

Tanino, Y., and Nepf, H. M. (2008). "Laboratory investigation of mean drag in a random array of rigid, emergent cylinders." *Journal of Hydraulic Engineering*, 134(1), 1-34.

Thomas, H., and Nisbet, T. R. (2006). "An assessment of the impact of floodplain woodland on flood flows." *Water and Environment Journal*, Journal compilation, 1-13.

Thompson, D. M. (2005). "The history of the use and effectiveness of instream structures in the United States." *Reviews in Engineering Geology*, 14, 35-50.

Thompson, A. M., Wilson, B. N., and Hansen, B. J. (2004). "Shear stress partitioning for idealized vegetated surfaces." *Transactions of the American Society of Agricultural Engineers*, 47(3), 701-709.

Thornton, C. I., Abt, S. R., Morris, C. E., and Fischenich, J. C. (2000). "Calculating shear stress at channel-overbank interfaces in straight channels with vegetated floodplains." *Journal of Hydraulic Engineering*, 126(12), 929-936.

Tominaga A., Nezu I., Ezaki K., Nakagawa H. (1989). "Turbulent structure in straight open channel flows." *Journal of Hydraulic Research*, 27(1), 149–173.

Tritton DJ. 1988. Physical Fluid Dynamics. Clarendon, Oxford, 536.

van Prooijen, B., J. Battjes, and W. Uijttewaal (2005). "Momentum exchange in straight uniform compound channel flow." *J. Hydraul. Eng.*, 131(3), 177– 185.

Wahl, T. (2009). WinADV Version 2.027. U.S. Bureau of Reclamation, Water Resources Research Laboratory.

White, F.M. (1991). "Viscous Fluid Flow – Second Edition." McGraw-Hill Series in Mechanical Engineering. McGraw-Hill, Inc., New York. 614.

White, B. L., and Nepf, H. M. (2008). "A vortex-based model of velocity and shear stress in a partially vegetated shallow channel." *Water Res. Research*, 44(W01412), 15.

Wilkerson, G. V. (2007). "Flow through trapezoidal and rectangular channels with rigid cylinders." *Journal of Hydraulic Engineering*, 133(5), 521-533.

Wilson, C. A. M. E., Stoesser, T., Bates, P. D., and Batemann Pinzen, A. (2003). "Open channel flow through different forms of submerged flexible vegetation." *J. Hydr. Engr.*, 129(11), 847-853.

Wilson, C. A. M. E., Yagci, O., Rauch, H.-P., and Stoesser, T. (2006). "Application of the drag force approach to model the flow-interaction of natural vegetation." *Int. J. River Basin Mgmt.*, 4(2), 137-146.

Wilson, C. A. M. E., Yagci, O., Rauch, H.-P., and Olsen, N. R. B. (2006). "3D numerical modelling of a willow vegetated river/floodplain system." *Journal of Hydrology*, 327, 13-21.

Wormleaton, P.R. (1996). "Floodplain secondary circulation as a mechanism for flow and shear stress redistribution in straight compound channels." Coherent Flow Structures in Open Channels, P.J. Ashworth, S.J. Bennett, J.L. Best, and S.J. McClelland, eds., Wiley, Chichester, 581-608.

Wu, F.-C., Shen, H. W., and Chou, Y.-J. (1999). "Variation of roughness coefficients for unsubmerged and submerged vegetation." *Journal of Hydraulic Engineering*, 125(9), 934-942.

Yang, K., Cao, S., and Knight, D. W. (2007). "Flow patterns in compound channels with vegetated floodplains." *Journal of Hydraulic Engineering*, 133(2), 148-159.

Zdravkovich, M. M., and Pridden, D. L. (1977). "Interference between two circular cylinders; series of unexpected discontinuities." *J. Industrial Aerodynamics*, 2, 255–270.

Zhang, E., Yeh, H., Lin, Z., and Laramee, R. S. (2009). "Asymmetric tensor analysis for flow visualization." *IEEE Transactions on Visualization and Computer Graphics*, 15(1), 106-122.

Zong, L., and Nepf, H. M. (2010). "Flow and deposition in and around a finite patch of vegetation." *Geomorphology*, 116(3-4), 363-372.

Zukauskas, A. (1987). "Heat transfer from tubes in cross-flow." *Adv. Heat Trans.,* 18, 87–159.

APPENDICIES

Appendix A. Comparison of cross-sectional channel locations.

Downstream velocity varied across the channel cross-section, depending on vegetation density. A comparison was made between the velocity measures to determine whether there was enough similarity between adjacent measures to group them and estimate an average velocity over the area. Because velocities differed by vegetation density and discharge, comparisons were made by calculating:

$$\text{normalized difference in velocity} = \frac{|\text{velocity at } y_1 - \text{velocity at } y_2|}{|y_1 - y_2|}$$

where y is the cross-sectional position, (e.g. for a given cross-section, normalized difference in velocity = |velocity at 0.05 m – velocity at 0.10 m|/|0.05-0.10|). Results are shown for all discharges, both bank-toe angles and all vegetation densities. Figure 1 shows that differences in velocity are reduced along the bank-toe (0 to 0.4 m), that some increase in velocity occurs along the bottom of the bank-toe (0.3 to 0.4 m), and main channel velocities are much larger and more variable than bank-toe velocities (0.4 to 0.54 m). Thus, measurement locations were classified according to channel location – bank-toe from 0 to 0.35 m across the channel, bank-toe-main channel margin from 0.35 to 0.44 m, and main channel from 0.44 to 0.62 m.
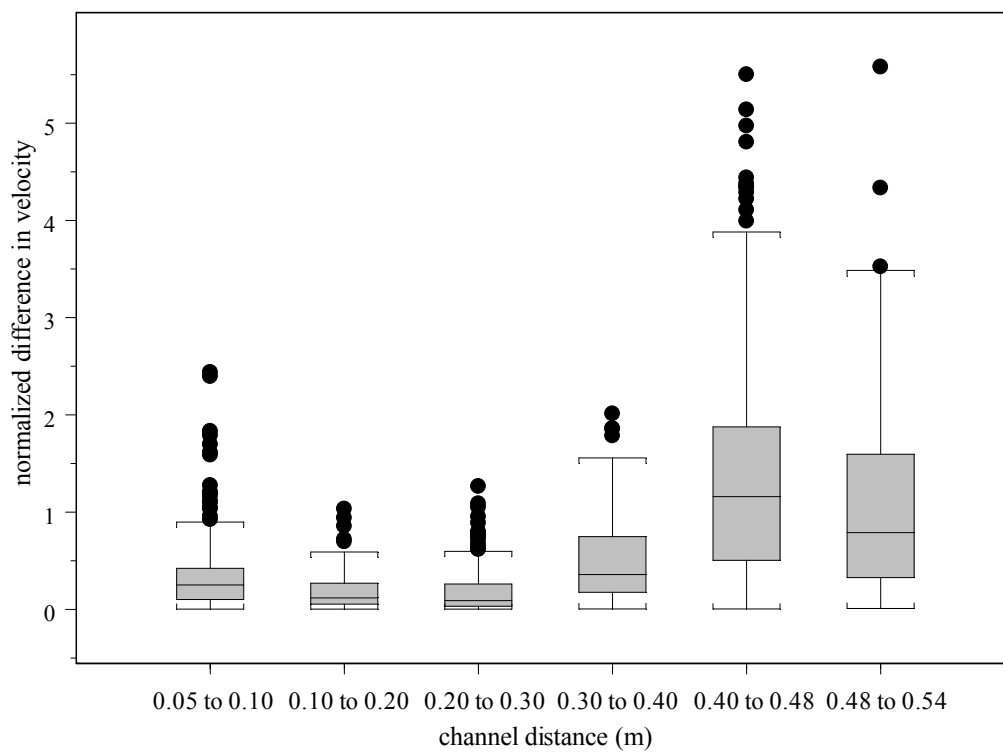
Figure 1. Boxplot of normalized differences in velocity between cross-sectional channel locations.

Appendix B. Comparison of cross-sectional data along the length of the flume.

Downstream velocity varied over the length of the flume, depending on vegetation density. A comparison was made between the velocity measures at each cross-section along a given channel width location to determine where uniform flow conditions were achieved. Because velocities differed by vegetation density and discharge, comparisons were made by calculating:

$$\text{normalized difference in velocity} = \frac{|\text{velocity at } x_1 - \text{velocity at } x_2|}{|x_1 - x_2|}$$

where x is the longitudinal distance, (e.g. for a given cross-sectional location, normalized difference in velocity = |velocity at 0.25 m – velocity at 1.0 m|/|0.25-1.0|). Uniform flow conditions were considered to be met at cross-section 2.0 or 2.95 m, which had less variation in velocity between them and the upstream and downstream transects (see Figure 1).
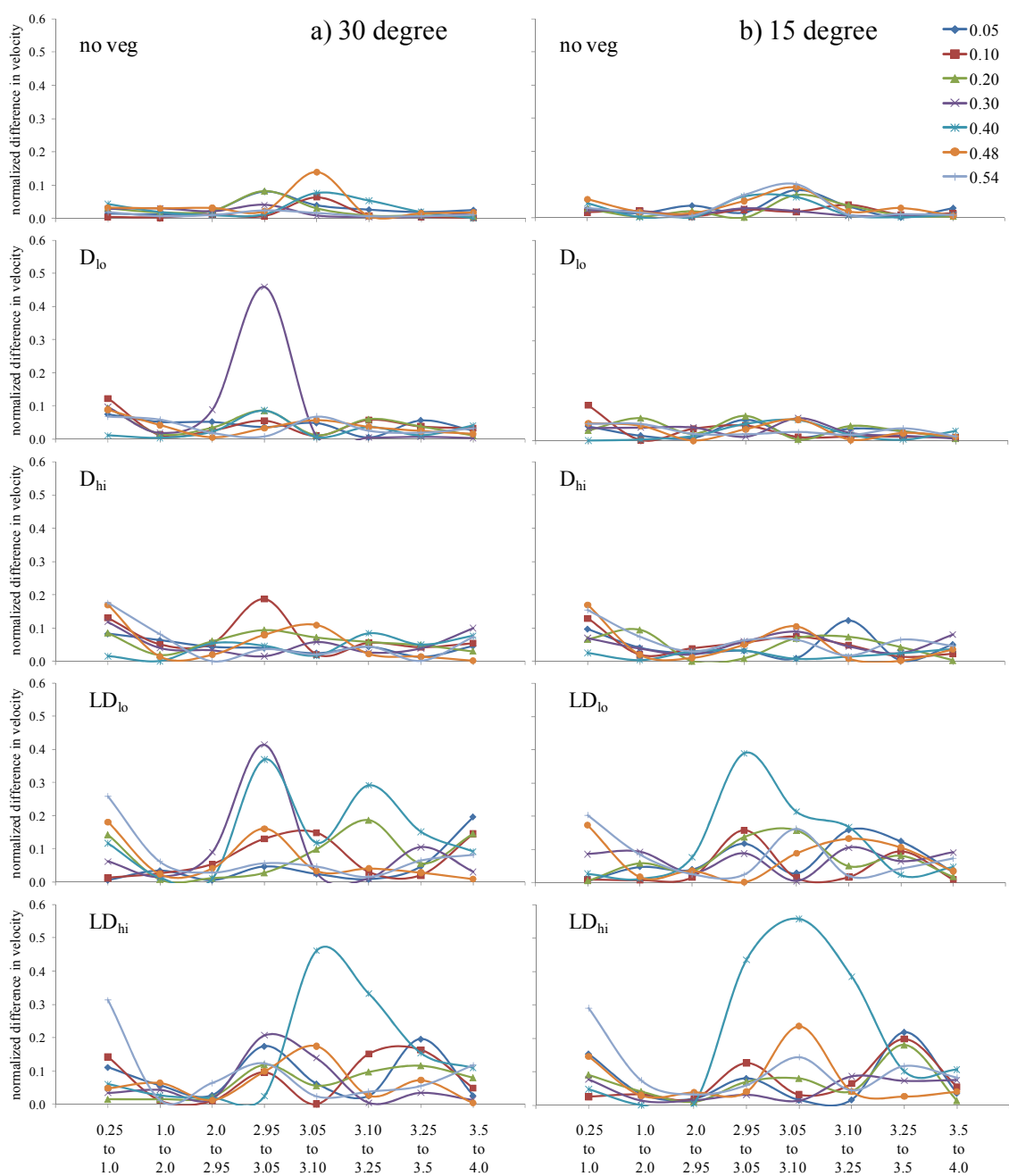
Figure 1. Normalized differences in velocity between longitudinal channel locations for a given cross-sectional location on a) the 30° bank-toe, and b) the 15° bank-toe. The x-axis displays the longitudinal distance along the flume.